THE PROCEEDINGS OF
THE PHYSICAL SOCIETY

Section A

VOL. 65, PART 3 1 March 1952 No. 387 A

Quantization of Einstein's Gravitational Field: Linear Approximation

BY SURAJ N. GUPTA
Cavendish Laboratory, Cambridge *

Communicated by L. Rosenfeld; MS. received 3rd October 1951

ABSTRACT. The approximate linear form of Einstein's gravitational field is quantized by using an indefinite metric. It is shown that only two types of gravitons can be observed, though many more can exist in virtual states in the presence of interaction. The observable gravitons are shown to be particles of spin 2. Using the interaction representation, the interaction of the gravitational field with the matter field is briefly discussed.

§1. INTRODUCTION

THE present investigation is undertaken to carry out the quantization of Einstein's gravitational field, and to investigate the interaction of gravitational quanta or 'gravitons' with other elementary particles. For simplicity we shall first quantize the approximate linear form of Einstein's field, while the exact treatment of the non-linear gravitational field will be given in a subsequent paper. Some work on the quantization of the gravitational field has been carried out in earlier days by Rosenfeld (1930), but since then very little progress has been made in this direction.

For the quantization of the approximate linear gravitational field we shall follow the same treatment as has been applied to the radiation field in an earlier paper (Gupta 1950, to be referred to as A). Thus we shall use an indefinite metric for the components of the gravitational field with a negative commutator, and then the gravitons corresponding to these components will be made unobservable by means of supplementary conditions. In this way we shall find that only two types of gravitons can be observed, though many more can exist in virtual states. Since the gravitational field has a large number of components, the present treatment is necessarily more involved than the treatment for the radiation field, but we shall not come across any new difficulty.

It must be observed that the supplementary conditions play a vital role in our treatment. For, if there were no supplementary conditions, the present theory would involve observable states with negative probabilities, which would be physically meaningless. It appears, therefore, that the role of the supplementary conditions (or the coordinate conditions) is more fundamental than was originally intended by Einstein.

* Now I.C.I. Research Fellow at the University of Manchester

§2. LINEAR APPROXIMATION FOR THE GRAVITATIONAL FIELD

The fundamental equation for Einstein's gravitational field is given by

$$R^{\mu\nu}-\tfrac{1}{2}Rg^{\mu\nu}=-\tfrac{1}{2}\kappa^2T^{\mu\nu}, \qquad \ldots\ldots(1)$$

where the symbols $g^{\mu\nu}$, $R^{\mu\nu}$, and R have the usual meaning, κ is a constant, and $T^{\mu\nu}$ is the energy momentum tensor of the 'matter' field, where matter includes everything except the gravitational field. Since the covariant divergence of the left-hand side of (1) is known to vanish, it follows that the covariant divergence of $T^{\mu\nu}$ will also vanish, whence one obtains

$$\frac{\partial\mathfrak{T}_\mu^\nu}{\partial x^\nu}-\tfrac{1}{2}\mathfrak{T}^{\alpha\beta}\frac{\partial g_{\alpha\beta}}{\partial x^\mu}=0, \qquad \ldots\ldots(2)$$

where $\mathfrak{T}^{\alpha\beta}=T^{\alpha\beta}(-g)^{1/2}$ is the energy momentum tensor density for the matter field. Also, in order to express the conservation of energy and momentum, we write

$$\frac{\partial}{\partial x^\nu}(\mathfrak{T}_\mu^\nu+\mathfrak{t}_\mu^\nu)=0; \qquad \ldots\ldots(3)$$

here $\mathfrak{t}^{\mu\nu}$ is the energy momentum pseudo-tensor density for the gravitational field, which satisfies the equation

$$\frac{\partial\mathfrak{t}_\mu^\nu}{\partial x^\nu}=-\tfrac{1}{2}\mathfrak{T}^{\alpha\beta}\frac{\partial g_{\alpha\beta}}{\partial x^\mu}. \qquad \ldots\ldots(4)$$

Following Einstein (1918), we now obtain the linear approximation for the above field equations by putting

$$g_{\mu\nu}=\epsilon_{\mu\nu}+\kappa h_{\mu\nu}, \qquad \ldots\ldots(5)$$

where $\epsilon_{\mu\nu}$ are the constant Minkowskian values for $g_{\mu\nu}$, and the second and higher powers of κ are to be neglected. Using the usual flat space–time tensor notation*, we can then write eqns. (1) and (4) as

$$\Box^2h_{\mu\nu}-\left(\frac{\partial^2h_{\mu\lambda}}{\partial x_\nu\partial x_\lambda}+\frac{\partial^2h_{\nu\lambda}}{\partial x_\mu\partial x_\lambda}\right)+\frac{\partial^2h_{\lambda\lambda}}{\partial x_\mu\partial x_\nu}+\delta_{\mu\nu}\left(\frac{\partial^2h_{\lambda\varrho}}{\partial x_\lambda\partial x_\varrho}-\Box^2h_{\lambda\lambda}\right)=\kappa T_{\mu\nu}, \qquad \ldots\ldots(6)$$

$$\frac{\partial t_{\mu\nu}}{\partial x_\nu}=\frac{\kappa}{2}\frac{\partial h_{\nu\lambda}}{\partial x_\mu}T_{\nu\lambda}. \qquad \ldots\ldots(7)$$

According to Einstein, we can also choose coordinate conditions or supplementary conditions given by

$$\frac{\partial h_{\mu\nu}}{\partial x_\nu}-\frac{1}{2}\frac{\partial h_{\lambda\lambda}}{\partial x_\mu}=0, \qquad \ldots\ldots(8)$$

so that (6) reduces to

$$\Box^2h_{\mu\nu}-\tfrac{1}{2}\delta_{\mu\nu}\Box^2h_{\lambda\lambda}=\kappa T_{\mu\nu}. \qquad \ldots\ldots(9)$$

It is convenient to put

$$h_{\mu\nu}=\gamma_{\mu\nu}-\tfrac{1}{2}\delta_{\mu\nu}\gamma_{\lambda\lambda}, \qquad \ldots\ldots(10)$$

and thus we can write (9), (8) and (7) as

$$\Box^2\gamma_{\mu\nu}=\kappa T_{\mu\nu}, \qquad \ldots\ldots(11)$$

$$\frac{\partial\gamma_{\mu\nu}}{\partial x_\nu}=0, \qquad \ldots\ldots(12)$$

$$\frac{\partial t_{\mu\nu}}{\partial x_\nu}=\frac{\kappa}{2}\frac{\partial\gamma_{\nu\lambda}}{\partial x_\mu}T_{\nu\lambda}-\frac{\kappa}{4}\frac{\partial\gamma_{\lambda\lambda}}{\partial x_\mu}T_{\nu\nu}. \qquad \ldots\ldots(13)$$

* We take the space–time coordinates as x_1, x_2, x_3, it.

It follows from the above equations that

$$t_{\mu\nu}=\frac{1}{2}\left[\frac{\partial\gamma_{\lambda\varrho}}{\partial x_\mu}\frac{\partial\gamma_{\lambda\varrho}}{\partial x_\nu}-\frac{1}{2}\frac{\partial\gamma_{\lambda\lambda}}{\partial x_\mu}\frac{\partial\gamma_{\varrho\varrho}}{\partial x_\nu}-\frac{1}{2}\delta_{\mu\nu}\left(\frac{\partial\gamma_{\lambda\varrho}}{\partial x_\sigma}\frac{\partial\gamma_{\lambda\varrho}}{\partial x_\sigma}-\frac{1}{2}\frac{\partial\gamma_{\lambda\lambda}}{\partial x_\sigma}\frac{\partial\gamma_{\varrho\varrho}}{\partial x_\sigma}\right)\right]. \quad \ldots\ldots(14)$$

In particular, we obtain for the Hamiltonian density

$$H=\frac{1}{2}\left[\frac{\partial\gamma_{\lambda\varrho}}{\partial t}\frac{\partial\gamma_{\lambda\varrho}}{\partial t}-\frac{1}{2}\frac{\partial\gamma_{\lambda\lambda}}{\partial t}\frac{\partial\gamma_{\varrho\varrho}}{\partial t}+\frac{1}{2}\left(\frac{\partial\gamma_{\lambda\varrho}}{\partial x_\sigma}\frac{\partial\gamma_{\lambda\varrho}}{\partial x_\sigma}-\frac{1}{2}\frac{\partial\gamma_{\lambda\lambda}}{\partial x_\sigma}\frac{\partial\gamma_{\varrho\varrho}}{\partial x_\sigma}\right)\right]. \quad \ldots\ldots(15)$$

The eqns. (11), (12) and (13), describing a linear gravitational field, are so simple that it may seem surprising that they have to be regarded only as an approximation to a more involved theory. It should, therefore, be noted that the supplementary conditions (12) are compatible with the field eqn. (11) only in an approximate sense, for (11) and (12) give respectively

$$\Box^2\frac{\partial\gamma_{\mu\nu}}{\partial x_\nu}=\kappa\frac{\partial T_{\mu\nu}}{\partial x_\nu} \quad \text{and} \quad \Box^2\frac{\partial\gamma_{\mu\nu}}{\partial x_\nu}=0,$$

which agree only in the first approximation. On the other hand, we shall show in the subsequent paper that for the exact non-linear gravitational field the supplementary conditions are exactly compatible with the field equations.

§ 3. QUANTIZATION OF THE GRAVITATIONAL FIELD

Lagrangian density for the linear gravitational field may be taken as

$$L=-\frac{1}{4}\left(\frac{\partial\gamma_{\mu\nu}}{\partial x_\lambda}\frac{\partial\gamma_{\mu\nu}}{\partial x_\lambda}-\frac{1}{2}\frac{\partial\gamma}{\partial x_\lambda}\frac{\partial\gamma}{\partial x_\lambda}\right), \quad \ldots\ldots(16)$$

where $\gamma_{\mu\nu}$ and γ are to be treated as independent variables. This gives in the usual way for the field equations and the Hamiltonian density

$$\Box^2\gamma_{\mu\nu}=0, \qquad \Box^2\gamma=0, \quad \ldots\ldots(17)$$

and

$$H=\frac{1}{2}\left[\frac{\partial\gamma_{\mu\nu}}{\partial t}\frac{\partial\gamma_{\mu\nu}}{\partial t}-\frac{1}{2}\frac{\partial\gamma}{\partial t}\frac{\partial\gamma}{\partial t}+\frac{1}{2}\left(\frac{\partial\gamma_{\mu\nu}}{\partial x_\lambda}\frac{\partial\gamma_{\mu\nu}}{\partial x_\lambda}-\frac{1}{2}\frac{\partial\gamma}{\partial x_\lambda}\frac{\partial\gamma}{\partial x_\lambda}\right)\right]. \quad \ldots\ldots(18)$$

In order that (18) may agree with (15), we shall ensure by means of a supplementary condition, to be discussed in the next section, that the expectation value of γ is equal to that of $\gamma_{\mu\mu}$. But for the purpose of quantization we regard γ as an independent field quantity, so that we may easily split the contributions of the various components in the Hamiltonian (18).

Now we have to obtain the commutation relations for $\gamma_{\mu\nu}$ and γ, keeping in view the fact that $\gamma_{\mu\nu}=\gamma_{\nu\mu}$. For this we note that the canonical conjugate of γ_{11} is given by

$$\pi_{11}=\frac{\partial L}{\partial(\partial\gamma_{11}/\partial t)}=\frac{1}{2}\frac{\partial\gamma_{11}}{\partial t}. \quad \ldots\ldots(19)$$

Therefore the commutation relation $[\gamma_{11}(\mathbf{r},t),\ \pi_{11}(\mathbf{r}',t)]=i\delta(\mathbf{r}-\mathbf{r}')$ gives $[\gamma_{11}(\mathbf{r},t),\ (\partial\gamma_{11}/\partial t)(\mathbf{r}',t)]=2i\delta(\mathbf{r}-\mathbf{r}')$; or, using Schwinger's notation (Schwinger 1948), we have

$$[\gamma_{11}(x),\gamma_{11}(x')]=2iD(x-x'). \quad \ldots\ldots(20)$$

On the other hand, since $\gamma_{12}=\gamma_{21}$, we get

$$\pi_{12}=\frac{\partial L}{\partial(\partial\gamma_{12}/\partial t)}=\frac{\partial\gamma_{12}}{\partial t}, \quad \ldots\ldots(21)$$

so that the commutation relation in this case is given by

$$[\gamma_{12}(x),\gamma_{12}(x')]=iD(x-x'). \quad \ldots\ldots(22)$$

According to (20) and (22), the commutation relations for $\gamma_{\mu\nu}$ may be written as

$$[\gamma_{\mu\nu}(x),\ \gamma_{\lambda\varrho}(x')]=i(\delta_{\mu\lambda}\delta_{\nu\varrho}+\delta_{\mu\varrho}\delta_{\nu\lambda})D(x-x'). \qquad \ldots\ldots(23)$$

Further, the canonical conjugate of γ is given by

$$\pi=\frac{\partial L}{\partial(\partial\gamma/dt)}=-\frac{1}{4}\frac{\partial\gamma}{\partial t},$$

and hence we obtain

$$[\gamma(x),\gamma(x')]=-4iD(x-x'). \qquad \ldots\ldots(24)$$

Following A, we now regard $\gamma_{\mu\nu}$ and γ as self-adjoint quantities, and expand them as

$$\gamma_{\mu\nu}=\sum_{\mathbf{k}}(2k)^{-1/2}\{a_{\mu\nu}(\mathbf{k})\,e^{i(\mathbf{k}.r-kt)}+a^{\dagger}_{\mu\nu}(\mathbf{k})\,e^{-i(\mathbf{k}.r-kt)}\}, \qquad \ldots\ldots(25)$$

$$\gamma=\sum_{\mathbf{k}}2(2k)^{-1/2}\{a(\mathbf{k})\,e^{i(\mathbf{k}.r-kt)}+a^{\dagger}(\mathbf{k})\,e^{-i(\mathbf{k}.r-kt)}\}, \qquad \ldots\ldots(26)$$

where a dagger denotes an adjoint. Substituting the above Fourier expansions in (23) and (24) respectively, we get

$$[a_{\mu\nu}(\mathbf{k}),\ a^{\dagger}_{\lambda\varrho}(\mathbf{k})]=\delta_{\mu\lambda}\delta_{\nu\varrho}+\delta_{\mu\varrho}\delta_{\nu\lambda} \qquad \ldots\ldots(27)$$

$$[a(\mathbf{k}),\ a^{\dagger}(\mathbf{k})]=-1. \qquad \ldots\ldots(28)$$

Again, substituting (25) and (26) in (18), using the commutation relations (27) and (28), and omitting the zero-point energy, we obtain for the Hamiltonian of the gravitational field

$$\int H dv=\sum_{\mathbf{k}}k\{\tfrac{1}{2}a^{\dagger}_{\mu\nu}(\mathbf{k})a_{\mu\nu}(\mathbf{k})-a^{\dagger}(\mathbf{k})a(\mathbf{k})\}. \qquad \ldots\ldots(29)$$

For the present purpose it is convenient to replace the operators $a_{11}(\mathbf{k})$, $a_{22}(\mathbf{k})$, $a_{33}(\mathbf{k})$ and $a_{00}(\mathbf{k})$ by $a'_{11}(\mathbf{k})$, $a'_{22}(\mathbf{k})$, $a'_{33}(\mathbf{k})$ and $a'_{00}(\mathbf{k})$, which are given by

$$\left.\begin{aligned} a'_{11}(\mathbf{k})&=\tfrac{1}{2}\{a_{11}(\mathbf{k})-a_{22}(\mathbf{k})\}, & a'_{22}(\mathbf{k})&=\tfrac{1}{2}\{a_{11}(\mathbf{k})+a_{22}(\mathbf{k})\},\\ a'_{33}(\mathbf{k})&=\frac{1}{\sqrt{2}}a_{33}(\mathbf{k}), & a'_{00}(\mathbf{k})&=\frac{1}{\sqrt{2}}a_{00}(\mathbf{k}).\end{aligned}\right\} \qquad \ldots\ldots(30)$$

According to (27) and (30), the commutation relations for the new operators are

$$\left.\begin{aligned} [a'_{11}(\mathbf{k}),\ a'^{\dagger}_{11}(\mathbf{k})]&=1, & [a'_{22}(\mathbf{k}),\ a'^{\dagger}_{22}(\mathbf{k})]&=1,\\ [a'_{33}(\mathbf{k}),\ a'^{\dagger}_{33}(\mathbf{k})]&=1, & [a_{00}(\mathbf{k}),\ a'^{\dagger}_{00}(\mathbf{k})]&=1,\end{aligned}\right\} \qquad \ldots\ldots(31)$$

and the Hamiltonian (29) may be written as

$$\begin{aligned}\int H\,dv=\sum_{\mathbf{k}}k\{&a^{\dagger}_{12}(\mathbf{k})a_{12}(\mathbf{k})+a^{\dagger}_{23}(\mathbf{k})a_{23}(\mathbf{k})+a^{\dagger}_{31}(\mathbf{k})a_{31}(\mathbf{k})\\ &-a^{\dagger}_{10}(\mathbf{k})a_{10}(\mathbf{k})-a^{\dagger}_{20}(\mathbf{k})a_{20}(\mathbf{k})-a^{\dagger}_{30}(\mathbf{k})a_{30}(\mathbf{k})\\ &+a'^{\dagger}_{11}(\mathbf{k})a'_{11}(\mathbf{k})+a'^{\dagger}_{22}(\mathbf{k})a'_{22}(\mathbf{k})+a'^{\dagger}_{33}(\mathbf{k})a'_{33}(\mathbf{k})\\ &+a'^{\dagger}_{00}(\mathbf{k})a'_{00}(\mathbf{k})-a^{\dagger}(\mathbf{k})a(\mathbf{k})\}, \qquad \ldots\ldots(32)\end{aligned}$$

where we have used the fact that $a_{\mu\nu}(\mathbf{k})=a_{\nu\mu}(\mathbf{k})$. Thus we have, in all, eleven types of gravitons corresponding to the eleven independent components of $\gamma_{\mu\nu}$ and γ. We shall refer to the gravitons corresponding to the operator $a_{12}(\mathbf{k})$ as the a_{12}-gravitons, and so on.

According to (27) and (28), the commutators involving $a_{i0}(\mathbf{k})$ and $a(\mathbf{k})$ have a negative sign. Therefore, as explained in A, we have to use an indefinite metric for the components γ_{i0} and γ of the gravitational field, while the remaining components are to be treated in the usual way. Thus, all the operators $a_{12}(\mathbf{k})$,

$a_{23}(\mathbf{k})$, $a_{31}(\mathbf{k})$, $a_{10}(\mathbf{k})$, $a_{20}(\mathbf{k})$, $a_{30}(\mathbf{k})$, $a'_{11}(\mathbf{k})$, $a'_{22}(\mathbf{k})$, $a'_{33}(\mathbf{k})$, $a'_{00}(\mathbf{k})$ and $a(\mathbf{k})$ appear as absorption operators, while their adjoints are all emission operators. It is to be noted that though now all the gravitons have positive energies, some states will occur with negative probabilities. For, due to the use of an indefinite metric, we have to normalize any state Ψ as

$$\Psi^\dagger\Psi=(-1)^{n_{10}+n_{20}+n_{30}+n} \qquad \ldots\ldots(33)$$

where n_{10}, n_{20}, n_{30} and n are the numbers of the a_{10}-, a_{20}-, a_{30}- and a-gravitons respectively in the state Ψ. This occurrence of negative probabilities, however, does not raise any difficulty of physical interpretation, for we shall show below that for all real states we have $n_{10}=n_{20}=n_{30}=n=0$.

§ 4. THE SUPPLEMENTARY CONDITIONS

In the absence of interaction the supplementary conditions for the gravitational field may be taken as

$$\frac{\partial\gamma^{(+)}_{\mu\nu}}{\partial x_\mu}\Psi=0, \qquad \ldots\ldots(34) \qquad \text{and} \qquad (\gamma^{(+)}_{\mu\mu}-\gamma^{(+)})\Psi=0, \qquad \ldots\ldots(35)$$

where $\gamma^{(+)}_{\mu\nu}$ and $\gamma^{(+)}$ are the positive frequency parts of $\gamma_{\mu\nu}$ and γ respectively. It follows from (34), (35) and their adjoint equations that $\langle\partial\gamma_{\mu\nu}/\partial x_\mu\rangle=0$, $\langle\gamma_{\mu\mu}\rangle=\langle\gamma\rangle$. Thus the supplementary conditions (34) agree with (12) in the classical limit, while (35) ensures that the Hamiltonian (18) is equivalent to (15).

Substituting the Fourier expansions (25) in (34), and choosing the x_3 axis along $\mathbf{k}$, we obtain

$$\{a_{31}(\mathbf{k})-a_{01}(\mathbf{k})\}\Psi=0, \qquad \ldots\ldots(36\,a)$$

$$\{a_{32}(\mathbf{k})-a_{02}(\mathbf{k})\}\Psi=0, \qquad \ldots\ldots(36\,b)$$

$$\{a_{33}(\mathbf{k})-a_{03}(\mathbf{k})\}\Psi=\{\sqrt{2}a'_{33}(\mathbf{k})-a_{03}(\mathbf{k})\}\Psi=0, \qquad \ldots\ldots(36\,c)$$

$$\{a_{30}(\mathbf{k})-a_{00}(\mathbf{k})\}\Psi=\{a_{30}(\mathbf{k})-\sqrt{2}a'_{00}(\mathbf{k})\}\Psi=0. \qquad \ldots\ldots(36\,d)$$

As shown in A, a solution of (36 *a*) consists of a normalized state containing no a_{31}- and a_{01}-gravitons, and a superposition of a series of redundant states with arbitrary coefficients and zero normalization. These redundant states, however, do not contribute to any observable effect. Moreover, since the normalization is conserved in course of time, a redundant state will always remain redundant. Thus for all practical purposes we may ignore such states, and regard the a_{31}- and a_{01}-gravitons as entirely absent in a non-interacting gravitational field. Similarly, (36 *b*) implies the absence of a_{32}- and a_{02}-gravitons in the absence of interaction. The situation regarding eqns. (36 *c*) and (36 *d*) is slightly simpler, for both of these equations involve the operator $a_{03}(\mathbf{k})$. It can be easily seen that the only states satisfying (36 *c*) and (36 *d*) are those which do not contain any a_{03}-, a'_{33}- and a'_{00}-gravitons.

We now consider the supplementary condition (35). Substituting the Fourier expansions (25) and (26) in (35), we get

$$\{a_{\mu\mu}(\mathbf{k})-2a(\mathbf{k})\}\Psi=0. \qquad \ldots\ldots(37)$$

Using (30), (36 *c*) and (36 *d*), we obtain from (37)

$$\{a'_{22}(\mathbf{k})-a(\mathbf{k})\}\Psi=0. \qquad \ldots\ldots(38)$$

Again, as explained above in the case of eqn. (36 *a*), (38) implies the absence of a'_{22}- and a-gravitons in a pure gravitational field.

We have seen that the supplementary conditions (34) and (35) enable us to eliminate nine types of gravitons, so that for a pure gravitational field we may take

$$n_{23}=n_{31}=n_{01}=n_{02}=n_{03}=n'_{22}=n'_{33}=n'_{00}=n=0, \qquad \ldots\ldots(39)$$

where n_{23} is the number of a_{23}-gravitons, and so on. Therefore, in a pure gravitational field, only a_{12}- and a'_{11}-gravitons can exist. It follows that the state of vacuum for the gravitational field may be defined as that containing no a_{12}- and a'_{11}-gravitons, because the other types of gravitons will be excluded by the supplementary conditions. Moreover, since according to our treatment all the components of $\gamma^{(+)}_{\mu\nu}$ and $\gamma^{(+)}$ contain the absorption operators, the state of vacuum will satisfy the relations

$$\gamma^{(+)}_{\mu\nu}\Psi_0=0, \qquad \gamma^{(+)}\Psi_0=0. \qquad \ldots\ldots(40)$$

§ 5. SPIN OF THE GRAVITONS

In the last section it was shown that only two types of gravitons can exist in a pure gravitational field. We shall now discuss the spin of these gravitons.

From the Lagrangian density (16), one can obtain the canonical energy momentum tensor $t_{\mu\nu}$ for the gravitational field as

$$t_{\mu\nu}=-\frac{\partial\gamma_{\lambda\varrho}}{\partial x_\mu}\frac{\partial L}{\partial(\partial\gamma_{\lambda\varrho}/\partial x_\nu)}-\frac{\partial\gamma}{\partial x_\mu}\frac{\partial L}{\partial(\partial\gamma/\partial x_\nu)}+\delta_{\mu\nu}L. \qquad \ldots\ldots(41)$$

This energy momentum tensor, however, has to be modified according to the treatment of Belinfante (see Wentzel 1949). For this we consider an infinitesimal Lorentz transformation

$$\delta x_\mu=\delta\omega_{\mu\nu}x_\nu \quad \text{with} \quad \delta\omega_{\mu\nu}=-\delta\omega_{\nu\mu}, \qquad \ldots\ldots(42)$$

and find a tensor $f_{\mu\nu,\varrho}$ given by

$$\begin{aligned} f_{\mu\nu,\varrho}&=-\frac{\delta\gamma_{\lambda\eta}}{\delta\omega_{\mu\nu}}\frac{\partial L}{\partial(\partial\gamma_{\lambda\eta}/\partial x_\varrho)} \\ &=\frac{\partial\gamma_{\mu\eta}}{\partial x_\varrho}\gamma_{\nu\eta}-\frac{\partial\gamma_{\nu\eta}}{\partial x_\varrho}\gamma_{\mu\eta}. \end{aligned} \qquad \ldots\ldots(43)$$

Then the modified energy momentum tensor $\theta_{\mu\nu}$ will be

$$\theta_{\mu\nu}=t_{\mu\nu}-\frac{1}{2}\frac{\partial}{\partial x_\varrho}(f_{\mu\nu,\varrho}+f_{\varrho\mu,\nu}+f_{\varrho\nu,\mu}), \qquad \ldots\ldots(44)$$

and the angular momentum density is given by

$$\begin{aligned} M_{\mu\nu,\varrho}&=x_\mu\theta_{\nu\varrho}-x_\nu\theta_{\mu\varrho} \\ &=x_\mu t_{\nu\varrho}-x_\nu t_{\mu\varrho}+f_{\mu\nu,\varrho}. \end{aligned} \qquad \ldots\ldots(45)$$

Thus we obtain for the components of the angular momentum

$$P_{ik}=-i\int M_{ik,4}\,dv=P^0_{ik}+P'_{ik}, \qquad \ldots\ldots(46)$$

with

$$P^0_{ik}=-i\int dv\,(x_iT_{k4}-x_kT_{i4}), \qquad \ldots\ldots(47)$$

$$P'_{ik}=-i\int dv\,f_{ik,4}=i\int dv\left(\gamma_{in}\frac{\partial\gamma_{kn}}{\partial x_4}-\gamma_{kn}\frac{\partial\gamma_{in}}{\partial x_4}\right), \qquad \ldots\ldots(48)$$

where P^0_{ik} is the orbital angular momentum, and P'_{ik} is the contribution due to the spin. Substituting the Fourier expansions (25) in (48), we get

$$\begin{aligned}P'_{ik}=\sum_{\mathbf{k}}\sum_{\mathbf{k}'}\frac{i}{2}\int dv\,[&-\{a_{i\eta}(\mathbf{k})\,e^{i(\mathbf{k}\cdot\mathbf{r}-kt)}+a^\dagger_{i\eta}(\mathbf{k})\,e^{-i(\mathbf{k}\cdot\mathbf{r}-kt)}\}\\&\times\{a_{k\eta}(\mathbf{k}')\,e^{i(\mathbf{k}'\cdot\mathbf{r}-k't)}-a^\dagger_{k\eta}(\mathbf{k}')\,e^{-i(\mathbf{k}'\cdot\mathbf{r}-k't)}\}\\&+\{a_{k\eta}(\mathbf{k})\,e^{i(\mathbf{k}\cdot\mathbf{r}-kt)}+a^\dagger_{k\eta}(\mathbf{k})\,e^{-i(\mathbf{k}\cdot\mathbf{r}-kt)}\}\\&\times\{a_{i\eta}(\mathbf{k}')\,e^{i(\mathbf{k}'\cdot\mathbf{r}-k't)}-a^\dagger_{i\eta}(\mathbf{k}')\,e^{-i(\mathbf{k}'\cdot\mathbf{r}-k't)}\}]\\=\sum_{\mathbf{k}}\frac{i}{2}&[a_{i\eta}(\mathbf{k})a^\dagger_{k\eta}(\mathbf{k})-a^\dagger_{i\eta}(\mathbf{k})a_{k\eta}(\mathbf{k})-a_{k\eta}(\mathbf{k})a^\dagger_{i\eta}(\mathbf{k})+a^\dagger_{k\eta}(\mathbf{k})a_{i\eta}(\mathbf{k})]\\=\sum_{\mathbf{k}}i&[a^\dagger_{k\eta}(\mathbf{k})a_{k\eta}(\mathbf{k})-a^\dagger_{i\eta}(\mathbf{k})a_{k\eta}(\mathbf{k})]. \qquad \ldots\ldots(49)\end{aligned}$$

Since the real gravitons correspond to the operators

$$a_{12}(\mathbf{k}) \quad \text{and} \quad a'_{11}(\mathbf{k})=\tfrac{1}{2}\{a_{11}(\mathbf{k})-a_{22}(\mathbf{k})\},$$

we have to consider only that part of P'_{ik} which involves the operators $a_{12}(\mathbf{k})$, $a_{11}(\mathbf{k})$, $a_{22}(\mathbf{k})$ and their adjoints. These operators occur only in the component P'_{12}, and their contribution is given by

$$\begin{aligned}P'_{12}&=\sum_{\mathbf{k}} i[a^\dagger_{21}(\mathbf{k})a_{11}(\mathbf{k})+a^\dagger_{22}(\mathbf{k})a_{12}(\mathbf{k})-a^\dagger_{11}(\mathbf{k})a_{21}(\mathbf{k})-a^\dagger_{12}(\mathbf{k})a_{22}(\mathbf{k})]\\&=\sum_{\mathbf{k}} 2i[a^\dagger_{12}(\mathbf{k})a'_{11}(\mathbf{k})-a'^\dagger_{11}(\mathbf{k})a_{12}(\mathbf{k})]. \qquad \ldots\ldots(50)\end{aligned}$$

In order to separate the contributions of the two independent components in the above equation, we introduce the operators

$$a_+(\mathbf{k})=\frac{1}{\sqrt{2}}\{a'_{11}(\mathbf{k})-ia_{12}(\mathbf{k})\}, \qquad a_-(\mathbf{k})=\frac{1}{\sqrt{2}}\{a'_{11}(\mathbf{k})+ia_{12}(\mathbf{k})\}, \quad \ldots\ldots(51)$$

where, according to (27) and (31), we have

$$\left.\begin{aligned}[a_+(\mathbf{k}),\ a^\dagger_+(\mathbf{k})]=[a_-(\mathbf{k}),\ a^\dagger_-(\mathbf{k})]=1,\\ [a_+(\mathbf{k}),\ a^\dagger_-(\mathbf{k})]=0.\end{aligned}\right\} \qquad \ldots\ldots(52)$$

In terms of these new operators we obtain

$$\begin{aligned}P'_{12}&=\sum_{\mathbf{k}} 2[a^\dagger_+(\mathbf{k})a_+(\mathbf{k})-a^\dagger_-(\mathbf{k})a_-(\mathbf{k})]\\&=\sum_{\mathbf{k}} 2[n_+(\mathbf{k})-n_-(\mathbf{k})], \qquad \ldots\ldots(53)\end{aligned}$$

where $n_+(\mathbf{k})$ and $n_-(\mathbf{k})$ give the numbers of the gravitons corresponding to the operators $a_+(\mathbf{k})$ and $a_-(\mathbf{k})$.

This shows that the gravitons are particles of spin 2, and they have two independent spin states with the spin axis parallel or antiparallel to the direction of motion of the gravitons.

§6. TREATMENT OF INTERACTION

It is evident from (11) that the interaction of the gravitational field with the matter field may be taken into account by modifying the Lagrangian density (16) as

$$L=-\frac{1}{4}\left(\frac{\partial\gamma_{\mu\nu}}{\partial x_\lambda}\frac{\partial\gamma_{\mu\nu}}{\partial x_\lambda}-\frac{1}{2}\frac{\partial\gamma}{\partial x_\lambda}\frac{\partial\gamma}{\partial x_\lambda}\right)-\frac{\kappa}{2}(\gamma_{\mu\nu}-\tfrac{1}{2}\delta_{\mu\nu}\gamma)T_{\mu\nu}, \quad \ldots\ldots(54)$$

which gives for the field equations

$$\Box^2\gamma_{\mu\nu}=\kappa T_{\mu\nu}, \qquad \Box^2\gamma=\kappa T_{\mu\mu}. \qquad \ldots\ldots(55)$$

In the presence of interaction, the supplementary conditions (34) and (35) have also to be modified. Following A, we may state the supplementary conditions in the Heisenberg representation as

$$\left[\frac{\partial\gamma_{\mu\nu}}{\partial x_\mu}\right]^+\Psi=0, \qquad [\gamma_{\mu\mu}-\gamma]^+\Psi=0, \qquad \ldots\ldots(56)$$

where $[\ ]^+$ denotes the positive frequency part. These conditions are, of course, identical with (34) and (35) in the absence of interaction. But the necessity of writing them in the form (56) arises from the fact that in the Heisenberg representation $\gamma_{\mu\nu}$ and γ cannot be split into the positive and the negative frequency parts in the presence of interaction. However, such a splitting is still possible for $\partial\gamma_{\mu\nu}/\partial x_\mu$ and $\gamma_{\mu\mu}-\gamma$. For, according to (55), $\partial\gamma_{\mu\nu}/\partial x_\mu$ and $\gamma_{\mu\mu}-\gamma$ still satisfy the wave equation for plane waves:

$$\Box^2\frac{\partial\gamma_{\mu\nu}}{\partial x_\mu}=0, \qquad \Box^2(\gamma_{\mu\mu}-\gamma)=0,$$

where we have taken into account the approximation used in §2.

When we pass over from the Heisenberg representation to the interaction representation, the required supplementary conditions may be obtained in the same way as in the case of the radiation field. Following the treatment given for the radiation field (Gupta 1951)*, we easily find in the interaction representation

$$\left.\begin{aligned}\left(\frac{\partial\gamma_{\mu\nu}^{(+)}(x)}{\partial x_\mu}+\kappa\int_{t'=t}D^{(+)}(x-x')T_{0\nu}(x')\,dv'\right)\Psi(t)=0,\\ (\gamma_{\mu\mu}^{(+)}-\gamma^{(+)})\Psi=0,\end{aligned}\right\} \qquad \ldots\ldots(57)$$

where $D^{(+)}(x-x')$ is the positive frequency part of $D(x-x')$. It should be observed that, due to the occurrence of the $T_{0\nu}$-term in (57), those gravitons which could not exist in a pure gravitational field can now appear in virtual states in the presence of interaction.

For practical purposes it is most convenient to use the invariant perturbation theory based on the interaction representation. For this we require, in addition to the commutation relations (23) and (24), the vacuum expectation values of the anticommutators. Using the vacuum conditions (40), we easily find, by following Schwinger (1949),

$$\left.\begin{aligned}\langle\{\gamma_{\mu\nu}(x),\,\gamma_{\lambda\varrho}(x')\}\rangle_0=(\delta_{\mu\lambda}\delta_{\nu\varrho}+\delta_{\mu\varrho}\delta_{\nu\lambda})D^{(1)}(x-x'),\\ \langle\{\gamma(x),\,\gamma(x')\}\rangle_0=-4D^{(1)}(x-x').\end{aligned}\right\} \qquad \ldots\ldots(58)$$

It should be noted that the use of an indefinite metric does not make any difference to the calculation of the vacuum expectation values, for the indefinite metric operator η, defined in A, is just equal to unity for the state of vacuum, which does not contain any gravitons.

§7. LORENTZ-INVARIANCE

In the present paper we have treated the components γ_{0i} of $\gamma_{\mu\nu}$ by means of an indefinite metric, while the other components have been treated in the usual way. Thus, though the expectation value of $\gamma_{\mu\nu}$ is always real, we have to regard $\gamma_{\mu\nu}$ as a complex tensor with γ_{0i} antiHermitian and the other components Hermitian. In this way the Lorentz-invariance of our treatment is not quite

* The letter, referred to above, contains an error. There the relation preceding eqn. (9) should read $[\delta D(x-x')/\delta t]_{t=t'}=-\delta(x_1-x_1')\delta(x_2-x_2')\delta(x_3-x_3')$.

obvious. However, the Lorentz-invariance of the present theory can be easily established by splitting up $\gamma_{\mu\nu}$ into the Hermitian and the antiHermitian components in a more general way, as we have done in A.

For this we take $\gamma_{\mu\nu}$ to be of the form

$$\begin{aligned}\gamma_{\mu\nu} = {} & N_\mu^{(1)}N_\nu^{(1)}\Lambda^{(11)} + N_\mu^{(1)}N_\nu^{(2)}\Lambda^{(12)} + N_\mu^{(1)}N_\nu^{(3)}\Lambda^{(13)} - N_\mu^{(1)}N_\nu^{(0)}\Lambda^{(10)} \\ & + N_\mu^{(2)}N_\nu^{(1)}\Lambda^{(21)} + N_\mu^{(2)}N_\nu^{(2)}\Lambda^{(22)} + N_\mu^{(2)}N_\nu^{(3)}\Lambda^{(23)} - N_\mu^{(2)}N_\nu^{(0)}\Lambda^{(20)} \\ & + N_\mu^{(3)}N_\nu^{(1)}\Lambda^{(31)} + N_\mu^{(3)}N_\nu^{(2)}\Lambda^{(32)} + N_\mu^{(3)}N_\nu^{(3)}\Lambda^{(33)} - N_\mu^{(3)}N_\nu^{(0)}\Lambda^{(30)} \\ & - N_\mu^{(0)}N_\nu^{(1)}\Lambda^{(01)} - N_\mu^{(0)}N_\nu^{(2)}\Lambda^{(02)} - N_\mu^{(0)}N_\nu^{(3)}\Lambda^{(03)} + N_\mu^{(0)}N_\nu^{(0)}\Lambda^{(00)}, \qquad \ldots\ldots(59)\end{aligned}$$

where, as in A, $N_\mu^{(1)}$, $N_\mu^{(2)}$, $N_\mu^{(3)}$ and $N_\mu^{(0)}$ are a set of orthogonal unit four-vectors, $N_\mu^{(1)}$, $N_\mu^{(2)}$, $N_\mu^{(3)}$ being space-like, and $N_\mu^{(0)}$ time-like. Further, $\Lambda^{(11)}$, $\Lambda^{(12)}$, ... are scalars, of which $\Lambda^{(10)}$, $\Lambda^{(20)}$, $\Lambda^{(30)}$, $\Lambda^{(01)}$, $\Lambda^{(02)}$ and $\Lambda^{(03)}$ are antiHermitian, while the rest are Hermitian. Thus, according to (59), we have split $\gamma_{\mu\nu}$ into sixteen components in a formally Lorentz-invariant way. We can now follow the entire treatment of the present paper with two differences: Firstly, instead of $\gamma_{\mu\nu}$, we have to expand the Λ's into Fourier expansions of the form (25). Secondly, instead of taking the x_3 axis along $\mathbf{k}$, we have to choose, as in A, $N_\mu^{(1)}$, $N_\mu^{(2)}$, $N_\mu^{(3)}$ in such a way that

$$k_\mu N_\mu^{(1)} = k_\mu N_\mu^{(2)} = 0, \qquad k_\mu N_\mu^{(3)} = -k_\mu N_\mu^{(0)}. \qquad \ldots\ldots(60)$$

The treatment for γ, of course, remains unchanged, because γ is a scalar independent of $\gamma_{\mu\nu}$. In this way the vacuum conditions (40) and all the other results remain unchanged.

Since (59) is a tensor equation, all our results will now be formally Lorentz-invariant. Still, in order to establish the relativistic invariance of our treatment one further point remains to be clarified. According to (59), if we choose a frame of reference in which $N_\mu^{(0)} = (0, 0, 0, i)$, i.e. the time-axis coincides with $N_\mu^{(0)}$, the components γ_{0i} of $\gamma_{\mu\nu}$ will be antiHermitian while the other components will be Hermitian. Since this property of $\gamma_{\mu\nu}$ is not preserved in all frames of reference, our treatment has singled out those frames of reference in which the time-axis coincides with $N_\mu^{(0)}$. Thus, in the present theory $N_\mu^{(0)}$ appears as a preferred direction. However, this does not matter, for $N_\mu^{(0)}$ can be chosen in an arbitrary way, and the results of physical interest are independent of its direction. In fact, after the vacuum conditions (40) have been established, $N_\mu^{(0)}$ never occurs explicitly in the interaction representation.

REFERENCES

EINSTEIN, A., 1918, *Berliner Berichte*, p. 154.

GUPTA, S. N., 1950, *Proc. Phys. Soc.* A, **63**, 681; 1951, *Ibid.*, **64**, 850.

ROSENFELD, L., 1930, *Z. Phys.*, **65**, 589.

SCHWINGER, J., 1948, *Phys. Rev.*, **74**, 1439; 1949, *Ibid.*, **75**, 651.

WENTZEL, G., 1949, *Quantum Theory of Fields* (New York : Interscience), p. 217.

The Equations of Motion and Coordinate Condition in General Relativity

By J. H. HAYWOOD
The University, Manchester

Communicated by L. Rosenfeld; *MS. received* 17*th September* 1951

ABSTRACT. A new coordinate condition has been considered and the equations of motion of two bodies in their weak and quasistatic gravitational field have been derived to the second approximation. A number of additional second order terms appear in the new equations which, however, have no influence on either the secular motion of the centre of mass or the rotation of periastron of the two-body system.

§ 1.

In recent years two independent methods have been developed for the derivation of the equations of motion of bodies in weak and quasistatic gravitational fields from the field equations of general relativity. The method of Einstein and his co-workers (1938, 1940, 1949) considers the bodies to be spherically symmetric singularities, and derives their equations of motion from the field equations of empty space surrounding the singularities. Fock (1939) and Papapetrou (1951a) employ the field equations inside the bodies as well as in empty space; their method can, in principle, be applied also to bodies without spherical symmetry.

An essential step in both methods is the use of four first order differential equations which are subsequently referred to as the coordinate condition. The coordinate condition used by Einstein and co-workers is

$$\eta^{\alpha\beta}(h_{\mu\alpha}-\tfrac{1}{2}\eta_{\mu\alpha}\eta^{\varrho\sigma}h_{\varrho\sigma})_{,\beta}=0, \qquad \ldots\ldots(1.1)$$

where, as usual, $h_{\mu\nu}=g_{\mu\nu}-\eta_{\mu\nu}$ and an index after a comma denotes ordinary differentiation. Fock and Papapetrou use the coordinate condition

$$\mathfrak{g}^{\mu\nu}{}_{,\nu}=0. \qquad \ldots\ldots(1.2)$$

Both coordinate conditions are identical to the first approximation, i.e. when retaining terms up to the order $1/\mathbf{c}^2$ only; however, they differ in the higher approximations, i.e. when terms of the order $1/\mathbf{c}^4$, $1/\mathbf{c}^6$ etc. are retained.

The question arises whether the choice of the coordinate condition will influence the form of the equations of motion. Einstein and Infeld (1949) have proved that if the coordinate condition (1.1) is changed arbitrarily, but in the second approximation only (i.e. being kept unchanged in the first approximation), then the equations of motion up to the second approximation will remain unchanged. This result explains why the methods of Einstein and Fock lead to the same equations of motion, though the conditions (1.1) and (1.2) coincide in the first approximation only.

A systematic discussion of the role of the coordinate condition has been given by Papapetrou (1951b). He finds that in the first approximation the equations

of motion do not depend on the coordinate condition, the assumption of a weak and quasistatic field leading necessarily to the Newtonian equations of motion. To any higher approximation the equations of motion will depend on the coordinate condition, though for the equations of motion up to the nth approximation only the form of the coordinate condition up to the $(n-1)$th approximation will be of importance.

In the present paper a new coordinate condition, which differs from (1.1) and (1.2) already in the first approximation, will be considered and the corresponding change of the equations of motion to the second approximation will be calculated explicitly. The new coordinate condition is $g^{\mu\nu}{}_{,\nu}=0$, or to the first approximation

$$\eta^{\alpha\beta}h_{\mu\alpha,\beta}=0. \qquad \ldots\ldots(1.3)$$

The equations of motion will, then, acquire a number of additional second order terms. These terms will be calculated by means of an appropriate transformation of coordinates.

§ 2.

We denote by an asterisk a system of coordinates in which the coordinate condition (1.1) holds. This is the system employed by Einstein, Infeld and Hoffman (1938) in which the equations of motion of two bodies up to the second approximation have been calculated. With a slight change of notation we write

$$\left.\begin{aligned} h^*_{00} &= \underset{2}{h^*_{00}}+\underset{4}{h^*_{00}}+\ldots. \\ h^*_{0n} &= \underset{1}{h^*_{0n}}+\underset{3}{h^*_{0n}}+\ldots. \\ h^*_{mn} &= \underset{2}{h^*_{mn}}+\underset{4}{h^*_{mn}}+\ldots. \end{aligned}\right\} \qquad \ldots\ldots(2.1)$$

the subscripts under the terms on the right-hand side indicating the order of magnitude of each term.†

We now consider a transformation of the form

$$x^{*\mu}=x^\mu+\sum_{r=1}^{\infty}\underset{r}{a^\mu}, \qquad \ldots\ldots(2.2)$$

which differs from the identical transformation $x^{*\mu}=x^\mu$ by terms of at least the first order. It will be shown in § 3 that, if we retain the basic assumption of the field being weak and quasistatic, a transformation of the type (2.2) will be sufficient for fulfilling, in the frame x^μ, the new coordinate condition (1.3). Moreover, we may retain Einstein's demand that quantities with an odd (or even) number of indices 0 be developed in an odd (or even) power series. Thus our transformation will be of the form

$$\left.\begin{aligned} x^{*0} &= x^0+\underset{1}{a^0}+\underset{3}{a^0}+\ldots., \\ x^{*s} &= x^s+\underset{2}{a^s}+\underset{4}{a^s}+\ldots. \end{aligned}\right\} \qquad \ldots\ldots(2.3)$$

It is seen immediately that in order to get the equations of motion in the frame x^μ, to the second approximation, it will be necessary to calculate the quantities $\underset{1}{a^0}$ and $\underset{2}{a^s}$ only. This calculation will be given in § 3. We simplify

† As usual, Latin indices take the values 1, 2, 3 only, while Greek indices take the values 1, 2, 3 and 0.

the present calculations by anticipating a result of §3, namely that $\overset{1}{m}{}^0 = 0$. Thus if we put $x^0 = t$,

$$t^* = t. \qquad \ldots\ldots (2.3\,a)$$

According to Einstein, Infeld and Hoffman (1938) the equations of motion of a body of gravitational mass $\overset{1}{m}$ and space coordinates η^{*s} in the presence of a second body of mass $\overset{2}{m}$ and coordinates ζ^{*s} are

$$\frac{d^2\eta^{*n}}{dt^{*2}} - \overset{2}{m}\frac{\partial}{\partial\eta^{*n}}\left(\frac{1}{r^*}\right) = \overset{2}{m}\left\{\left[\frac{d\eta^{*s}}{dt^*}\frac{d\eta^{*s}}{dt^*} + \frac{3}{2}\frac{d\zeta^{*s}}{dt^*}\frac{d\zeta^{*s}}{dt^*} - 4\frac{d\eta^{*s}}{dt^*}\frac{d\zeta^{*s}}{dt^*} - 4\frac{\overset{2}{m}}{r^*} - 5\frac{\overset{1}{m}}{r^*}\right]\right.$$
$$\times\frac{\partial}{\partial\eta^{*n}}\left(\frac{1}{r^*}\right) + \left[4\frac{d\eta^{*s}}{dt^*}\left(\frac{d\zeta^{*n}}{dt^*} - \frac{d\eta^{*n}}{dt^*}\right) + 3\frac{d\eta^{*n}}{dt^*}\frac{d\zeta^{*s}}{dt^*} - 4\frac{d\zeta^{*n}}{dt^*}\frac{d\zeta^{*s}}{dt^*}\right]$$
$$\times\frac{\partial}{\partial\eta^{*s}}\left(\frac{1}{r^*}\right) + \left.\frac{1}{2}\frac{\partial^3 r^*}{\partial\eta^{*n}\partial\eta^{*s}\partial\eta^{*r}}\frac{d\zeta^{*s}}{dt^*}\frac{d\zeta^{*r}}{dt^*}\right\}, \qquad \ldots\ldots (2.4)$$

where
$$(r^*)^2 = (\eta^{*s} - \zeta^{*s})(\eta^{*s} - \zeta^{*s}).$$

The equations of motion of the second body are obtained by replacing $\overset{1}{m}$, $\overset{2}{m}$, η^{*s} and ζ^{*s} by $\overset{2}{m}$, $\overset{1}{m}$, ζ^{*s} and η^{*s} respectively.

The equations of motion in the frame x^μ will be obtained by introducing (2.3) into (2.4). We notice that the left-hand side of (2.4) is of the order $1/c^2$ since t^* actually stands for ct^* and $\overset{1}{m}$, $\overset{2}{m}$ are the masses multiplied by G/c^2), while the right-hand side is of the order $1/c^4$. Since eqn. (2.4) is correct only up to terms of the order $1/c^4$ we see that the transformation (2.3) will change the left-hand side only. Let us write

$$\left.\begin{aligned}\delta\eta^s &= \eta^{*s} - \eta^s = \text{value of } \overset{2}{a}{}^s \text{ for } x^s = \eta^s,\\ \delta\zeta^s &= \zeta^{*s} - \zeta^s = \text{value of } \overset{2}{a}{}^s \text{ for } x^s = \zeta^s,\end{aligned}\right\} \qquad \ldots\ldots (2.5)$$

and
$$r^2 = (\eta^s - \zeta^s)(\eta^s - \zeta^s). \qquad \ldots\ldots (2.6)$$

An elementary calculation gives

$$\frac{d^2\eta^{*n}}{dt^{*2}} = \frac{d^2\eta^n}{dt^2} + \frac{d^2}{dt^2}(\delta\eta^n),$$

$$\frac{\partial}{\partial\eta^{*n}}\left(\frac{1}{r^*}\right) = \frac{\partial}{\partial\eta^n}\left(\frac{1}{r}\right) + \frac{\partial^2}{\partial\eta^n\partial\eta^s}\left(\frac{1}{r}\right)(\delta\eta^s - \delta\zeta^s) - \frac{\partial}{\partial\eta^s}\left(\frac{1}{r}\right)\frac{\partial}{\partial\eta^n}(\delta\zeta^s).$$

Hence in the frame x^μ we shall have in the left-hand side of the equations of motion the additional terms

$$\frac{d^2}{dt^2}(\delta\eta^n) - \overset{2}{m}\frac{\partial^2}{\partial\eta^n\partial\eta^s}\left(\frac{1}{r}\right)(\delta\eta^s - \delta\zeta^s) + \overset{2}{m}\frac{\partial}{\partial\eta^s}\left(\frac{1}{r}\right)\frac{\partial}{\partial\eta^n}(\delta\zeta^s). \qquad \ldots\ldots (2.7)$$

We notice that there has been no necessity for assuming any change of the masses $\overset{1}{m}$ and $\overset{2}{m}$ in the transformation from $x^{*\mu}$ to x^μ. This is why we did not put asterisks on $\overset{1}{m}$ and $\overset{2}{m}$ in eqn. (2.4).†

† The more general assumption would be that in the transformation from $x^{*\mu}$ to x^μ described by (2.3) we should have $m^* = m + \delta m$ where δm is small of the first order. Hence a term $\delta\overset{2}{m}(\partial/\partial\eta^n)(1/r)$ would appear on the right-hand side of the final equations of motion (3.14). Such a term might have some physical meaning only if it would be possible to determine the quantity m by some independent method. Actually the mass of a star is determined by observations of the motion of other bodies in its gravitational field, and is by definition the coefficient of the term $(\partial/\partial\eta^n)(1/r)$ in the equations of motion. Thus the splitting of this coefficient into $m + \delta m$ will remain arbitrary and, therefore, physically meaningless.

§ 3.

The functions $\overset{1}{a}{}^0$ and $\overset{2}{a}{}^s$ will be determined from the demand that in the frame x^μ the new coordinate condition (1.3) be fulfilled. Using the transformation formula connecting $g_{\mu\nu}$ with $g^*_{\mu\nu}$ we find,

$$\left.\begin{aligned} \overset{2}{h}{}_{00} &= \overset{2}{h}{}^*_{00} + 2\overset{1}{a}{}^0{}_{,0} \\ \overset{1}{h}{}_{0n} &= \overset{1}{h}{}^*_{0n} + \overset{1}{a}{}^0{}_{,n} \\ \overset{2}{h}{}_{mn} &= \overset{2}{h}{}^*_{mn} - \overset{2}{a}{}^m{}_{,n} - \overset{2}{a}{}^n{}_{,m} + \overset{1}{a}{}^0{}_{,n}\overset{1}{a}{}^0{}_{,m} + \overset{1}{a}{}^0{}_{,m}\overset{1}{h}{}^*_{0n} + \overset{1}{a}{}^0{}_{,n}\overset{1}{h}{}^*_{0m}. \end{aligned}\right\} \quad \ldots\ldots(3.1)$$

The values of the quantities $h^*_{\mu\nu}$ are previously known to be (Einstein, Infeld and Hoffman 1938),

$$\overset{2}{h}{}^*_{00} = -2\frac{\overset{1}{m}}{\overset{1}{r^*}} - 2\frac{\overset{2}{m}}{\overset{2}{r^*}}, \quad \overset{1}{h}{}^*_{0n} = 0, \quad \overset{2}{h}{}^*_{mn} = \delta_{mn}\overset{2}{h}{}^*_{00}, \qquad \ldots\ldots(3.2)$$

where $(\overset{1}{r^*})^2 = (x^{*s} - \eta^{*s})(x^{*s} - \eta^{*s})$, $(\overset{2}{r^*})^2 = (x^{*s} - \zeta^{*s})(x^{*s} - \zeta^{*s})$. $\ldots\ldots(3.3)$

The coordinate condition (1.3), up to terms of the order $1/c^2$, is

$$\overset{1}{h}{}_{0s,s} = 0, \qquad \overset{1}{h}{}_{n0,0} - \overset{2}{h}{}_{ns,s} = 0. \qquad \ldots\ldots(3.4)$$

Introducing (3.1) and (3.2) into (3.4) we find that $\overset{1}{a}{}^0$ and $\overset{2}{a}{}^s$ must satisfy the differential equations

$$\overset{1}{a}{}^0{}_{,ss} = 0, \qquad \overset{2}{a}{}^n{}_{,ss} + \overset{2}{a}{}^s{}_{,sn} + \overset{1}{a}{}^0{}_{,0n} - (\overset{1}{a}{}^0{}_{,n}\overset{1}{a}{}^0{}_{,s})_{,s} = \overset{2}{h}{}^*_{00,n}. \qquad \ldots\ldots(3.5)$$

The coordinate condition is valid throughout space, i.e. inside as well as outside the material bodies. Therefore it follows from the first of eqns. (3.5) that $\overset{1}{a}{}^0 = 0$. The second of eqns. (3.5) then becomes

$$\overset{2}{a}{}^n{}_{,ss} + \overset{2}{a}{}^s{}_{,sn} = \overset{2}{h}{}^*_{00,n}. \qquad \ldots\ldots(3.6)$$

If eqn. (3.6) is differentiated with respect to x^n, we find $2\overset{2}{a}{}^n{}_{,nss} = \overset{2}{h}{}^*_{00,nn}$. Since this equation is valid throughout space, it follows $\overset{2}{a}{}^s{}_{,s} = \frac{1}{2}\overset{2}{h}{}^*_{00}$. Equation (3.6) then reduces to

$$\overset{2}{a}{}^n{}_{,ss} = \tfrac{1}{2}\overset{2}{h}{}^*_{00,n}. \qquad \ldots\ldots(3.7)$$

The solution of this equation can be written in the form

$$\overset{2}{a}{}^n = \frac{\partial \omega}{\partial x^n}, \qquad \ldots\ldots(3.8)$$

where the function ω satisfies the equation

$$\omega_{,ss} = \tfrac{1}{2}\overset{2}{h}{}^*_{00}. \qquad \ldots\ldots(3.9)$$

To solve this equation we must first of all express $\overset{2}{h}{}^*_{00}$ in terms of the coordinates x^μ. Remembering (2.3) we see that this is done by simply neglecting the asterisks on the right-hand side of the first equation in (3.2) and in eqns. (3.3). Now $\overset{2}{h}{}^*_{00}$ is the sum of two terms and (3.9) is a linear equation. Therefore, ω will also be the sum of two terms, one for each of the two bodies.

Let us, then, first discuss eqn. (3.9) for one body only. In order to determine ω we shall have to consider the values of $\overset{2}{h}{}^*_{00}$ throughout space (i.e. outside as well as inside the body). Temporarily, we denote by r the distance from the centre

of the body and by $\rho(r)$ the mass density at the distance r. From the equation $\Delta \overset{*}{h}_{00} = 8\pi\rho$, we find the general formula

$$\overset{*}{h}_{00} = -\frac{8\pi}{r}\int_0^r \rho r^2\,dr - 8\pi\int_r^\infty \rho r\,dr. \qquad \ldots\ldots(3.10)$$

Since $\overset{*}{h}_{00}$ is a function of r only, the same will be true also for ω. Remembering that

$$\omega_{,\,ss} \equiv \Delta\omega = \frac{d^2\omega}{dr^2} + \frac{2}{r}\frac{d\omega}{dr},$$

we find from (3.9) and (3.10)

$$\frac{d^2\omega}{dr^2} + \frac{2}{r}\frac{d\omega}{dr} = -\frac{8\pi}{r}\int_0^r \rho r^2\,dr - 8\pi\int_r^\infty \rho r\,dr.$$

It will be sufficient to integrate this equation once only since

$$\frac{\partial\omega}{\partial x^n} = \frac{d\omega}{dr}\frac{x^n}{r};$$

i.e. for the calculation of $\overset{2}{a}{}^n$ only the quantities $d\omega/dr$ are needed.

The constant of integration will be determined by the demand that $d\omega/dr$ be finite throughout space, since otherwise the transformation (2.3) would have no meaning. We find,

$$\frac{d\omega}{dr} = -2\pi\int_0^r \rho r^2\,dr + \frac{2\pi}{3r^3}\int_0^r \rho r^4\,dr - \frac{4\pi r}{3}\int_r^\infty \rho r\,dr. \qquad \ldots\ldots(3.11)$$

It follows from this formula firstly that

$$d\omega/dr = 0, \quad \text{for} \quad r = 0. \qquad \ldots\ldots(3.12)$$

Outside the body the last term of (3.11) vanishes. For $r \gg R$, R denoting the radius of the body, the second term on the right-hand side of (3.11) becomes negligible compared with the first. Therefore, remembering that $4\pi\int_0^R \rho r^2\,dr = m$,

$$d\omega/dr = -\tfrac{1}{2}m \quad \text{for} \quad r \gg R. \qquad \ldots\ldots(3.13)$$

The total ω will now be $\omega = \overset{1}{\omega} + \overset{2}{\omega}$, $\overset{1}{\omega}$ being a function of $\overset{1}{r}$ and $\overset{2}{\omega}$ a function of $\overset{2}{r}$. Remembering (3.8) and taking into account (3.12) and (3.13) we find for the quantities $\delta\eta^s$ and $\delta\zeta^s$ defined by (2.5) the values $\delta\eta^s = -\tfrac{1}{2}\overset{2}{m}(\eta^s - \zeta^s)/r$, $\delta\zeta^s = \tfrac{1}{2}\overset{1}{m}(\eta^s - \zeta^s)/r$ where r now has the value defined by (2.6).

From these expressions we calculate the additional terms (2.7) which appear on the left-hand side of the equations of motion. In calculating these terms we substitute the Newtonian approximation for $d^2\eta^n/dt^2$ and $d^2\zeta^n/dt^2$, i.e.

$$\frac{d^2\eta^n}{dt^2} = \overset{2}{m}\frac{\partial}{\partial\eta^n}\left(\frac{1}{r}\right), \quad \frac{d^2\zeta^n}{dt^2} = \overset{1}{m}\frac{\partial}{\partial\zeta^n}\left(\frac{1}{r}\right) = -\overset{1}{m}\frac{\partial}{\partial\eta^n}\left(\frac{1}{r}\right).$$

Taking into account the relations

$$\frac{\partial}{\partial\eta^s}\left(\frac{1}{r}\right)\frac{\partial^2 r}{\partial\eta^s\partial\eta^n} = 0, \quad \frac{\partial^2}{\partial\eta^n\partial\eta^s}\left(\frac{1}{r}\right)\frac{\partial r}{\partial\eta^s} = -\frac{2}{r}\frac{\partial}{\partial\eta^n}\left(\frac{1}{r}\right),$$

we find that the additional terms (2.7) have the value

$$\frac{\overset{2}{m}(\overset{1}{m}+\overset{2}{m})}{r}\frac{\partial}{\partial\eta^n}\left(\frac{1}{r}\right) + \frac{\overset{2}{m}}{2}\frac{\partial^2 r}{\partial\eta^n\partial\eta^r\partial\eta^s}\left(\frac{d\eta^s}{dt} - \frac{d\zeta^s}{dt}\right)\left(\frac{d\eta^r}{dt} - \frac{d\zeta^r}{dt}\right).$$

The final equations of motion in a coordinate system which satisfies the coordinate condition (1.3) are therefore

$$\frac{d^2\eta^n}{dt^2} - \frac{2}{m}\frac{\partial}{\partial\eta^n}\left(\frac{1}{r}\right) = \frac{2}{m}\left\{\left[\frac{d\eta^s}{dt}\frac{d\eta^s}{dt} + \frac{3}{2}\frac{d\zeta^s}{dt}\frac{d\zeta^s}{dt} - 4\frac{d\eta^s}{dt}\frac{d\zeta^s}{dt} - 3\frac{\overset{2}{m}}{r} - 4\frac{\overset{1}{m}}{r}\right]\frac{\partial}{\partial\eta^n}\left(\frac{1}{r}\right)\right.$$
$$+\left[4\frac{d\eta^s}{dt}\left(\frac{d\zeta^n}{dt} - \frac{d\eta^n}{dt}\right) + 3\frac{d\eta^n}{dt}\frac{d\zeta^s}{dt} - 4\frac{d\zeta^n}{dt}\frac{d\zeta^s}{dt}\right]\frac{\partial}{\partial\eta^s}\left(\frac{1}{r}\right)$$
$$\left.+\frac{\partial^2 r}{\partial\eta^n\partial\eta^s\partial\eta^r}\left(\frac{d\zeta^s}{dt}\frac{d\zeta^r}{dt} + \frac{1}{2}\frac{d\eta^s}{dt}\frac{d\eta^r}{dt} - \frac{d\zeta^s}{dt}\frac{d\eta^r}{dt}\right)\right\}, \quad \ldots\ldots(3.14)$$

§ 4.

Robertson (1938) has integrated the equations of motion (2.4). Robertson's method may be repeated for the eqns. (3.14). The result of this calculation, which need not be described here in any detail, is that the additional terms in the new equations of motion do not influence the two quantities which Robertson discusses, i.e. the secular motion of the centre of gravity and the periastron advance of a double star system. If one assumes that these quantities are the only observables of the motion, then our result would mean that the coordinate condition (1.3) is fully equivalent, from the physical point of view, to (1.1) or (1.2). Such a statement, however, is not plausible at all since one would expect that an observer, on one of the two stars, for example, might be able to observe many more details of the motion; if this is so, then—according to the point of view expressed by Papapetrou (1951 b)—the conditions (1.1) and (1.3) need not be equivalent.

ACKNOWLEDGMENT

The author wishes to thank Dr. A. Papapetrou for valuable advice and stimulating discussions.

REFERENCES

EINSTEIN, A., and INFELD, L., 1940, *Ann. Math.*, **41**, 455; 1949, *Canad. J. Math.*, **1**, 209.
EINSTEIN, A., INFELD, L., and HOFFMAN, B., 1938, *Ann. Math.*, **39**, 65.
FOCK, V. A., 1939, *J. Phys., U.S.S.R.*, **1**, 81.
PAPAPETROU, A., 1951 a, *Proc. Phys. Soc.* A, **64**, 57; 1951 b, *Ibid.*, **64**, 302.
ROBERTSON, H., 1938, *Ann. Math.*, **39**, 101.

On Polarized Particle Beams

BY R. H. DALITZ
Department of Mathematical Physics, University of Birmingham

Communicated by R. E. Peierls; MS. received 28th November 1951

ABSTRACT. A partially polarized beam of particles is represented by a statistical operator in spin space. For nucleon–nucleon scattering a theorem stated by Wolfenstein in 1949 connecting the two simplest experiments involving polarized nucleons is shown to depend on the invariance of the interaction potential under time-reflection.

NUCLEON–NUCLEON scattering experiments which study the scattering of polarized beams and the polarization of scattered nucleons are logically the next step in the unravelling of the nucleon–nucleon scattering matrix. Such experiments have been proposed by Wolfenstein

(1949 b) and by Lepore (1950), who have evaluated the polarization produced in a single scattering, and the azimuthal asymmetry in scattering of a polarized beam, for some tensor–force interactions. Here it is our purpose to discuss the concept of polarization of a beam and to study the structure of the nucleon–nucleon scattering matrix.

Since a wave function ψ will always describe a particle completely polarized in some direction, a partially polarized beam cannot be a pure state, but is in fact a statistical mixture of pure states. Such a mixture may be specified by giving the set $\{\psi^\alpha\}$ of normalized states occurring, together with the relative frequency $P(\alpha)$ with which each ψ^α is represented in the beam. If a basic set of states $\{\psi_i\}$ is chosen, so that we may write $\psi^\alpha=\Sigma_i C_i^\alpha \psi_i$, the expectation value of an observable O in the beam is

$$\begin{aligned}\bar{O}&=\Sigma_\alpha P(\alpha)(\psi^{\alpha\dagger}, O\psi^\alpha)=\Sigma_{ij\alpha}P(\alpha)C_i^{\alpha *}C_j^\alpha O_{ij}\\&=\Sigma_{ij}U_{ji}O_{ij}=\text{Trace }(UO),\end{aligned}\qquad\ldots\ldots(1)$$

where U is the matrix (U_{ji}) where $U_{ji}=\Sigma_\alpha P(\alpha)C_j^\alpha C_i^{\alpha *}$. From the properties of the probability $P(\alpha)$, $U_{ii}=\text{Trace }(U)=1$. This statistical matrix U now contains all information concerning the beam necessary for prediction of the results of experiments with the beam. Except for the case of a completely polarized beam (which is a pure state), many different probability distributions $P(\alpha)$ and sets of states $\{\psi^\alpha\}$ will lead to the same matrix U.

For example, a linear beam of spin $\frac{1}{2}$ particles may be represented by a statistical operator U in spin space. Such a 2×2 matrix may always be written in the form $A+\mathbf{B}.\boldsymbol{\sigma}$. Since the normalization condition implies $A=\frac{1}{2}$, it is convenient to write $U=\frac{1}{2}(1+\mathbf{p}.\boldsymbol{\sigma})$. The pseudo-vector $\mathbf{p}$ thus specifies completely the polarization nature of the beam and may be referred to as the polarization of the beam. At once $\mathbf{p}=\text{Trace }(\boldsymbol{\sigma}U)$.

For spin greater than $\frac{1}{2}$, U will be more complicated, e.g. for deuterons $U=\{1+p_iS_i+T_{ij}(S_iS_j+S_jS_i)\}/3$, S_i being the spin operator for total spin 1, so that the specification of the state of the beam requires both the pseudo-vector p_i and the symmetric traceless tensor T_{ij}. In particular, for such a beam it is possible that $p_i=0$, yet $T_{ij}\neq 0$, so that the ordering in spin-space is generally more complicated than a simple polarization. These considerations may clearly be generalized to any total spin, and it is noteworthy that the analysis is at once applicable also to relativistic particles, for example electrons.

In spin space the scattering of a particle may be described by an operator $\mathscr{S}(\boldsymbol{\sigma}, \mathbf{k}_i, \mathbf{k}_f)$, which transforms the initial to the final spin state, $\mathbf{k}_i$, $\mathbf{k}_f$ being unit vectors in the initial and final directions. The outgoing beam $\mathbf{k}_f$ will be represented now by the statistical matrix

$$U'=(\mathscr{S}U\mathscr{S}^\dagger)/\text{Trace }(\mathscr{S}U\mathscr{S}^\dagger),\qquad\ldots\ldots(2)$$

so that, for example, the polarization after the collision will be

$$\mathbf{p}'=\text{Trace }(\boldsymbol{\sigma}U')=\text{Trace }(\boldsymbol{\sigma}\mathscr{S}U\mathscr{S}^\dagger)/\text{Trace }(\mathscr{S}U\mathscr{S}^\dagger).\qquad\ldots\ldots(3)$$

On the other hand, the differential cross section for the collision is

$$d\sigma/d\Omega=\text{Trace }(\mathscr{S}U\mathscr{S}^\dagger)=\tfrac{1}{2}\{\text{Trace }(\mathscr{S}\mathscr{S}^\dagger)+\mathbf{p}.\text{Trace }(\mathscr{S}\boldsymbol{\sigma}\mathscr{S}^\dagger)\}.\qquad\ldots\ldots(4)$$

It is of interest to compare these considerations with earlier work on the scattering of polarized thermal neutrons by unpolarized nuclei (e.g. Borowitz and Hamermesh 1948) or by ferromagnets (e.g. Halpern and Johnston 1939).

In the former case the scattering operator is $\mathscr{S}=a+b\boldsymbol{\sigma}.\mathbf{I}$, $\mathbf{I}$ being the nucleon spin operator. By evaluation of (3) for unpolarized nuclei it is easily shown that the direction of the neutron polarization is unchanged by the collision, though the magnitude of the polarization is always reduced. A choice of basic spin states directed along this constant direction leads to the representation usual in this study, i.e. by a polarization factor $(P_+-P_-)/(P_++P_-)$, P_+, P_- being the probabilities of the two spin orientations. A similar representation has been used in the study of scattering by a ferromagnet, in which case the justification lies in the precession of the spin about the internal magnetic field by a random amount between collisions, as noted by Halpern and Johnston (1939).

The elastic collision of two nucleons is of special interest. The operator describing the scattering from relative momentum direction $\mathbf{k}_i$ to direction $\mathbf{k}_f$ may be written $\mathscr{S}(\boldsymbol{\sigma}_1, \boldsymbol{\sigma}_2; \mathbf{k}_i, \mathbf{k}_f)$. Since the Hamiltonian will be invariant for rotations and reflections of the coordinate system, the most general form† possible for $\mathscr{S}$ is

$$\mathscr{S}=A+B\boldsymbol{\sigma}_1.\mathbf{k}_i\times\mathbf{k}_f+C\boldsymbol{\sigma}_2.\mathbf{k}_i\times\mathbf{k}_f+D\boldsymbol{\sigma}_1.\mathbf{k}_i\boldsymbol{\sigma}_2.\mathbf{k}_i+E\boldsymbol{\sigma}_1.\mathbf{k}_f\boldsymbol{\sigma}_2.\mathbf{k}_f$$
$$+F\boldsymbol{\sigma}_1.\mathbf{k}_i\boldsymbol{\sigma}_2.\mathbf{k}_f+G\boldsymbol{\sigma}_1.\mathbf{k}_f\boldsymbol{\sigma}_2.\mathbf{k}_i+H\boldsymbol{\sigma}_1.\mathbf{k}_i\times\mathbf{k}_f\boldsymbol{\sigma}_2.\mathbf{k}_i\times\mathbf{k}_f+J\boldsymbol{\sigma}_1.\boldsymbol{\sigma}_2, \quad \ldots\ldots(5)$$

where A, B, C, D, E, F, G, H, J are functions of $\mathbf{k}_i.\mathbf{k}_f=\cos\theta$.

It is natural to suppose that the Hamiltonian is invariant also for reversal of the time axis, which implies further restriction on the structure of $\mathscr{S}$. Under time reflection, $\mathscr{S}$ behaves as follows:

$$t\rightarrow t'=-t:\ \mathscr{S}(\boldsymbol{\sigma}_1,\boldsymbol{\sigma}_2;\mathbf{k}_i,\mathbf{k}_f)\rightarrow\mathscr{S}'=\mathscr{S}(-\boldsymbol{\sigma}_1,-\boldsymbol{\sigma}_2;-\mathbf{k}_i,-\mathbf{k}_f). \quad \ldots\ldots(6)$$

However, the time-reversed scattering process is the scattering of an incident wave of direction $-\mathbf{k}_f$ to final direction $-\mathbf{k}_i$, so that

$$\mathscr{S}(-\boldsymbol{\sigma}_1,-\boldsymbol{\sigma}_2;-\mathbf{k}_i,-\mathbf{k}_f)=\mathscr{S}(\boldsymbol{\sigma}_1,\boldsymbol{\sigma}_2;-\mathbf{k}_f,-\mathbf{k}_i). \quad \ldots\ldots(7)$$

This equation implies that $D=E$, $F=G$ in the form (5), so that

$$\mathscr{S}=\{A+U(\boldsymbol{\sigma}_1+\boldsymbol{\sigma}_2).\mathbf{k}_i\times\mathbf{k}_f+V(\boldsymbol{\sigma}_1-\boldsymbol{\sigma}_2).\mathbf{k}_i\times\mathbf{k}_f+D(\boldsymbol{\sigma}_1.\mathbf{k}_i\boldsymbol{\sigma}_2.\mathbf{k}_i+\boldsymbol{\sigma}_1.\mathbf{k}_f\boldsymbol{\sigma}_2.\mathbf{k}_f)$$
$$+F(\boldsymbol{\sigma}_1.\mathbf{k}_i\boldsymbol{\sigma}_2.\mathbf{k}_f+\boldsymbol{\sigma}_1.\mathbf{k}_f\boldsymbol{\sigma}_2.\mathbf{k}_i)+J\boldsymbol{\sigma}_1.\boldsymbol{\sigma}_2\}, \quad \ldots\ldots(8)$$

where $U=(B+C)/2$, $V=(B-C)/2$.

It has been stated, but not proved, by Wolfenstein (1949 a, b) that the polarization produced by scattering of an unpolarized nucleon is equal to the proportional value of the term not azimuthally symmetric in the differential cross section for scattering of a completely polarized beam by unpolarized target nucleons. This important connection between the two simplest polarization experiments is, from (3) and (4), equivalent to the statement that Trace $(\boldsymbol{\sigma}_1\mathscr{S}\mathscr{S}^\dagger)=$ Trace $(\mathscr{S}\boldsymbol{\sigma}_1\mathscr{S}^\dagger)$. By direct calculation, using (8), each of these quantities is

$$\text{Trace}\,(\mathscr{S}\boldsymbol{\sigma}_1\mathscr{S}^\dagger)=\text{Trace}\,(\boldsymbol{\sigma}_1\mathscr{S}\mathscr{S}^\dagger)=\mathbf{k}_i\times\mathbf{k}_f\,8\mathscr{R}\{A^*(U+V)+J^*(U-V)\}. \quad \ldots(9)$$

It is significant to note, however, that this relation is not valid for the more general scattering operator (5). This connection between the simplest polarization experiments holds in virtue of the invariance of the interaction

† *Note added in proof.* In later equations H has been taken zero since the term proportional to H is linearly related to the terms D, E, J. This has been pointed out to me by Drs. Ashkin and Wolfenstein.

potential under time-reversal. For collisions of identical particles, $\mathscr{S}$ must be symmetrical for the interchange (1, 2), which requires at once that $B=C$, $D=E$, $F=G$ in (5), whence $V=0$ in (8) and (9).

The complete elucidation of the scattering operator (8) requires the study of more complicated collisions, for instance of polarized nucleons with polarized target, somewhat beyond available techniques at present. Bhatia (1950) has, for some simple cases, studied theoretically the change in polarization of a fast nucleon in a collision with unpolarized nucleons, an experiment which provides the additional information given by Trace $(\boldsymbol{\sigma}_{14}\mathscr{S}\boldsymbol{\sigma}_{13}\mathscr{S}^{\dagger})$.

The only term of (8) which couples singlet and triplet states is that proportional to V. In the collision of unpolarized nucleons, because of this term the polarization produced in the recoil nucleons is not equal to the polarization produced in the deflected nucleons, since Trace $(\boldsymbol{\sigma}_2\mathscr{S}\mathscr{S}^{\dagger})$ – Trace $(\boldsymbol{\sigma}_1\mathscr{S}\mathscr{S}^{\dagger})$ is not zero but is proportional to V. However, for the nucleon potentials currently proposed, $\mathscr{S}$ is symmetrical for the interchange (1, 2), whence the two polarizations are predicted to be equal. An experimental test of this consequence would be of considerable interest.

REFERENCES

BHATIA, A. B., 1950, *Proc. Phys. Soc.* A, **63**, 502.
BOROWITZ, S., and HAMERMESH, M., 1948, *Phys. Rev.*, **74**, 1285.
HALPERN, O., and JOHNSTON, M. H., 1939, *Phys. Rev.*, **55**, 898.
LEPORE, J. V., 1950, *Phys. Rev.*, **79**, 137.
WOLFENSTEIN, L., 1949 a, *Phys. Rev.*, **75**, 1664 ; 1949 b, *Ibid.*, **76**, 541.

On the Polarizability of the Hydrogen Molecule

BY EIICHI ISHIGURO
Physics Department, Ochanomizu University, Tokyo, Japan

TADASHI ARAI
Chemistry Department, Kyoto University, Kyoto, Japan

MASATAKA MIZUSHIMA AND MASAO KOTANI
Physics Department, Tokyo University, Tokyo, Japan

Communicated by C. A. Coulson; MS. received 28th September 1951

ABSTRACT. The polarizability of the hydrogen molecule is calculated theoretically. The energy of the molecule, under an external electrostatic field, is calculated by the variation method, using 11+10 terms and 11+9 terms James–Coolidge type wave functions, for the polarizability parallel to and perpendicular to the molecular axis respectively. By expanding the energy in powers of the field strength, the polarizability is determined. By using a Morse function for the adiabatic potential of the molecule, the 0–0 and 0–1 matrix elements of the polarizability between vibrational states are calculated, with the result: $\alpha_{00}=7{\cdot}89$, $\gamma_{00}=2{\cdot}78$, $\alpha_{01}=1{\cdot}39$, $\gamma_{01}=0{\cdot}90$ for ordinary hydrogen H_2, and $\alpha_{00}=7{\cdot}75$, $\gamma_{00}=2{\cdot}68$, $\alpha_{01}=1{\cdot}13$, $\gamma_{01}=0{\cdot}71$ for heavy hydrogen D_2 (in units of 10^{-25} cm^3), where α is the mean polarizability and γ the anisotropy.

§ 1. INTRODUCTION

THE polarizability is one of the fundamental quantities characteristic of each molecule, and its value is often required when we want to study various phenomena concerning the molecule. Experimentally, the measurement of the dielectric constant and of the refractive index gives us fairly accurate values of the mean polarizability, at least in the vibrational ground state, but the anisotropy of the polarizability tensor is obtainable only with low accuracy. Especially in the case of non-polar molecules, we have no experimental means of determining the sign of the anisotropy. A purely theoretical calculation of the polarizability is, therefore, very desirable. In general this is also a difficult task, but in the case of the hydrogen molecule we can hope to obtain reliable results, since very accurate wave functions for the free hydrogen molecule, obtained by James and Coolidge, are fortunately available. The extension of their method to the case in which an applied electrostatic field is present enables us to find the polarizability. The results of our calculation along this line are reported in the present paper.

§ 2. DEFINITIONS. COMPARISON OF RESULTS HITHERTO OBTAINED

The polarizability of a molecule is a tensor, with three principal values α_{xx}, α_{yy} and α_{zz} in general. In the case of an axially symmetric molecule such as hydrogen, α_{xx} is equal to α_{yy} if we take the axis of the molecule as z axis, so that we have only to know two independent quantities α_{xx} and α_{zz}. We denote these quantities as $\alpha_\perp$ and $\alpha_\parallel$ respectively. It is convenient to introduce further α and γ by

$$\alpha = \tfrac{1}{3}(2\alpha_\perp + \alpha_\parallel), \quad \gamma = \alpha_\parallel - \alpha_\perp. \qquad \ldots\ldots(1)$$

α is called the mean polarizability and γ is the measure of the anisotropy.

Results of the quantum-mechanical calculation of the polarizability made hitherto by various authors are shown in table 1. Since all previous calculations were made using rather simple wave functions such as Heitler–London's, Wang's, Rosen's, and the m.o. of Coulson, the accuracy of those results might not be very high. Values obtained in this paper are also shown in this table.

Most of the authors calculated the polarizability for one or several fixed values of the internuclear distance R, but if we take the anharmonicity of vibration and the non-linearity of α in dependence on R into account, we find that the quantities which have direct relation to experiment are not the values of the polarizability or of its derivative at a fixed value of R, but the diagonal or non-diagonal matrix elements of the polarizability between vibrational states. $\alpha_{vv'}$ and $\gamma_{vv'}$ in the table are these matrix elements. It is to be noticed that there are fairly large differences between α_{00}, γ_{00} and $(\alpha)_{R_0}$, $(\gamma)_{R_0}$. For the sake of comparison we have given in table 1 also the values of α_{01} and γ_{01} multiplied by $2\pi(\nu M/h)^{1/2}$, which should be equal to $\partial\alpha/\partial R$, $\partial\gamma/\partial R$ if there were no anharmonicity and no non-linearity.

§ 3. GENERAL THEORY

The Hamiltonian of the hydrogen molecule in the presence of a uniform external electrostatic field $\mathbf{F}$ is given by

$$H = H^0 + H', \qquad H' = \frac{1}{F}\mathbf{F}.(\mathbf{r}_1 + \mathbf{r}_2), \qquad \ldots\ldots(2)$$

where H^0 is the Hamiltonian of the free hydrogen molecule and $\mathbf{r}_1$, $\mathbf{r}_2$ are the position vectors of the two electrons. In this paper atomic units are used throughout the calculation.

Table 1. Theoretical Values of the Polarizability of the Hydrogen Molecule

$\alpha_\perp$	$\alpha_\parallel$	α	γ	$\frac{\partial\alpha_\perp}{\partial R}$	$\frac{\partial\alpha_\parallel}{\partial R}$	$\frac{\partial\alpha}{\partial R}$	$\frac{\partial\gamma}{\partial R}$	References	
0·85	0·61	0·77	−0·24						
0·52	0·77	0·60	0·25						
0·74	0·75	0·74	0·01	0·95	1·10	1·00	0·15	(3 a)	
0·67	0·71	0·69	0·04	0·80	1·08	0·89	0·28	(3 b)	
0·73	0·75	0·73	0·02	0·98	1·02	0·99	0·04	(3 c)	
0·66	0·71	0·68	0·05	0·89	1·02	0·93	0·13	(3 d)	
0·59	0·72	0·63	0·13					(4)	
0·70	0·92	0·77	0·22					(5)	
0·66	0·68	0·67	0·02					(6 a)	
0·64	0·71	0·66	0·07					(6 b)	
0·62	0·71	0·65	0·09					(6 c)	
0·66	0·83	0·72	0·17	1·31	1·86	1·49	0·55	(7)	
0·659	0·906	0·741	0·247	1·132	1·969	1·411	0·838	(R=1·40)	Our values
$(\alpha_\perp)_{\infty}$	$(\alpha_\parallel)_{\infty}$	α_{∞}	γ_{∞}	$C(\alpha_\perp)_{01}$	$C(\alpha_\parallel)_{01}$	$C\alpha_{01}$	$C\gamma_{01}$		
0·697	0·975	0·789	0·278	1·253	2·285	1·596	1·033	for H_2	
0·686	0·954	0·775	0·268	1·218	2·190	1·542	0·971	for D_2	

$C=2\pi(\nu M/h)^{1/2}$, ν=frequency of vibration, M=mass of H or D.

(1) Mrowka (1932); H–L, perturbation. (2) Steensholt (1935); Wang, variation, one parameter. (3) Hirschfelder (1935); a Rosen, variation, two parameters, b Rosen, variation, one parameter, c Wang, variation, two parameters, d Wang, variation, one parameter. (4) Easthope (1936); H–L, perturbation. (5) Mulliken and Rieke (1941); H–L, perturbation. (6) Steensholt (1947); a m.o. of Coulson, variation, two parameters, b m.o. of Coulson, variation, three parameters, c m.o. of Coulson, variation, five parameters. (7) Bell and Long (1950); m.o., variation, one parameter. In this table, the unit of figures in the first four columns ($\alpha_\perp$, $\alpha_\parallel$, α and γ) is 10^{-24} cm^3, and that of figures in the last four columns ($\partial\alpha_\perp/\partial R$, $\partial\alpha_\parallel/\partial R$, $\partial\alpha/\partial R$ and $\partial\gamma/\partial R$) is 10^{-16} cm^2.

Now the electronic ground state of the free hydrogen molecule has the symmetry $^1\Sigma_g^+$, but when the electric field is applied the charge cloud is deformed, and the electronic eigen-function loses the character of Σ_g^+ more or less. If the field is not very strong, the wave function can be expressed as

$$\Psi=\Theta+\Phi, \qquad \ldots\ldots(3)$$

where Θ is of symmetry Σ_g^+, and Φ is of symmetry Σ_u^+ or Π_g according as the field is applied parallel or perpendicular to the molecular axis. Φ is at least of the first order in F. Normalization of (3) gives

$$\int\Theta^2\,d\tau+\int\Phi^2\,d\tau=1, \qquad \ldots\ldots(4)$$

since $\int\Theta\Phi\,d\tau=0$. If we calculate the average value of the total Hamiltonian with (3), we have

$$E=\int\Theta H^0\Theta\,d\tau+2F\int\Theta H'\Phi\,d\tau+\int\Phi H^0\Phi\,d\tau, \qquad \ldots\ldots(5)$$

dropping terms which vanish on account of symmetry. We try to minimize (5) under the auxiliary condition (4), and express the result in powers of F as follows:

$$E=E^0-\tfrac{1}{2}\alpha F^2+\ldots., \qquad \ldots\ldots(6)$$

from which we can find an approximate value of the polarizability α.

For this purpose we express Θ and Φ as linear combinations of functions of the respective symmetry:

$$\Theta = \sum_i c_i \theta_i, \qquad \Phi = \sum_k b_k \phi_k. \qquad \ldots\ldots(7)$$

The equations (4), (5) are written as

$$\sum_{i,j} c_i c_j S_{ij} + \sum_{k,h} b_k b_h T_{kh} = 1. \qquad \ldots\ldots(8)$$

$$E = \sum_{i,j} c_i c_j H^0_{ij} + 2F \sum_{i,k} c_i b_k H'_{ik} + \sum_{k,h} b_k b_h H^0_{kh}, \qquad \ldots\ldots(9)$$

where $S_{ij} = \int \theta_i \theta_j \, d\tau$, $T_{kh} = \int \phi_k \phi_h \, d\tau$. Differentiating (9) with respect to c_i and b_k, with the use of the well-known method of Langrangian multipliers, we get

$$\sum_j (H^0_{ij} - E S_{ij}) c_j + F \sum_k H'_{ik} b_k = 0, \qquad \ldots\ldots(10)$$

$$\sum_h (H^0_{kh} - E T_{kh}) b_h + F \sum_i H'_{ik} c_i = 0. \qquad \ldots\ldots(11)$$

In the limit of the vanishing field $F \to 0$, (10) gives

$$\sum (H^0_{ij} - E^{(0)} S_{ij}) c_j^{(0)} = 0. \qquad \ldots\ldots(12)$$

This is nothing but the variational treatment of the free hydrogen molecule, which has been solved by James and Coolidge if we identify θ_i as their functions. Now, in order to find E to the second order in F, we have to find b_k only to the first order in F, so that we can put $b_k = b_k^{(1)} F$. This gives a system of simultaneous inhomogeneous equations for $b_k^{(1)}$:

$$\sum_h (H^0_{kh} - E^{(0)} T_{kh}) b_h^{(1)} = - \sum_i H'_{ik} c_i^{(0)}, \qquad \ldots\ldots(13)$$

and the familiar formalism of the perturbation theory gives

$$E = E^{(0)} + F^2 \sum_{i,k} c_i^{(0)} H'_{ik} b_k^{(1)}. \qquad \ldots\ldots(14)$$

By comparing this with (6), we finally obtain the following formula for the polarizability

$$\alpha = - 2 \sum_i \sum_k c_i^{(0)} H'_{ik} b_k^{(1)}. \qquad \ldots\ldots(15)$$

The corresponding wave function is given by

$$\Psi = \sum_i c_i^{(0)} \theta_i + F \sum b_k^{(1)} \phi_k. \qquad \ldots\ldots(16)$$

§ 4. METHOD OF CALCULATION AND THE NUMERICAL RESULTS

As Θ we have adopted the eleven terms wave function of James and Coolidge (1933), that is, we have expressed Θ as a linear combination of $\theta[00000]$, $\theta[00020]$, $\theta[00110]$, $\theta[10000]$, $\theta[00001]$, $\theta[10200]$, $\theta[10020]$, $\theta[10110]$, $\theta[20000]$, $\theta[00111]$, $\theta[00002]$, where

$$\theta[M,N,J,K,P] = \frac{1}{2\pi} \{\xi_1^M \xi_2^N \eta_1^J \eta_2^K \rho^P + \xi_1^N \xi_2^M \eta_1^K \eta_2^J \rho^P\} \exp\{-c(\xi_1 + \xi_2)\}, \qquad \ldots\ldots(17)$$

ξ, η being elliptic coordinates of the electrons and ρ the inter-electronic distance divided by the internuclear distance R; c is fixed to be 0·75 throughout our calculation. The $c_i^{(0)}$ for this value of c are given in the paper by James and

Coolidge, for R (atomic units) = 1·2, 1·3, 1·4 and 1·5, and $E^{(0)}$ have also been obtained by them (private communication) as in table 2.

For the expansion of Φ we have used similar functions chosen as follows. In the case of $\alpha_{\parallel}$, $\phi[0010]$, $\phi[1010]$, $\phi[0110]$, $\phi[1110]$, $\phi[2010]$, $\phi[0021]$, $\phi[0030]$, $\phi[2001]$, $\phi[1012]$, $\phi[0112]$ have been adopted, where each set of integers has the same meaning as $MNJK$ of $\theta[MNJKP]$ (in all of our additional terms the quantity corresponding to P is taken to be zero, to avoid too involved calculation, so that they do not depend on ρ). In the case of $\alpha_{\perp}$,

$$\phi[m,n,j,k]=\frac{1}{2\pi}[\xi_1{}^m\xi_2{}^n\eta_1{}^j\eta_2{}^k\{(\xi_1{}^2-1)(1-\eta_1{}^2)\}^{1/2}\cos\phi_1 + \xi_1{}^n\xi_2{}^m\eta_1{}^k\eta_2{}^j\{(\xi_2{}^2-1)(1-\eta_2{}^2)\}^{1/2}\cos\phi_2]\exp\{-c(\xi_1+\xi_2)\}, \quad \ldots\ldots(18)$$

where ϕ_1 and ϕ_2 are the azimuthal angles of the two electrons. Here we adopted $\phi[0000]$, $\phi[1000]$, $\phi[0100]$, $\phi[0020]$, $\phi[0002]$, $\phi[0011]$, $\phi[1020]$, $\phi[1002]$, $\phi[2000]$.

The details of the numerical calculation are shown in Appendix 1.

The results of the calculation are shown in table 3. In this table the results are also shown for those cases in which only three, five and seven additional terms are adopted, in order to see the convergency of our calculation. These terms have been taken in the order written above, except in the 7 terms case for $\alpha_{\parallel}$.

Table 2

R (A.U.)	1·2	1·3	1·4	1·5
$E^{(0)}$ (A.U.)	−2·3260	−2·3414	−2·3460	−2·3422

Table 3 (*a*). $\alpha_{\parallel}$ (A.U.)

R (A.U.)	1·2	1·3	1·4	1·5
Three terms	4·329	4·900	5·487	6·110
Five terms	4·800	5·342	5·952	6·630
Seven terms*	4·860	5·420	6·051	6·753
Ten terms	4·876	5·451	6·107	6·862

* Out of ten terms $\phi[0030]$, $\phi[0021]$ and $\phi[2001]$ are omitted.

Table 3 (*b*). $\alpha_{\perp}$ (A.U.)

R (A.U.)	1·2	1·3	1·4	1·5
Three terms	3·596	3·881	4·209	4·584
Five terms	3·688	4·003	4·364	4·778
Seven terms	3·738	4·066	4·442	4·872
Nine terms	3·750	4·067	4·443	4·874

If we express our results in the form

$$\alpha=a+b(R-R_e)+c(R-R_e)^2+d(R-R_e)^3, \qquad R_e=1{\cdot}4, \quad \ldots\ldots(19)$$

we obtain a, b, c and d as in table 4. a and b are $(\alpha)_{R_e}$ and $(\partial\alpha/\partial R)_{R_e}$ respectively, and have been given in table 1, for the sake of comparison with results obtained by other authors.

Table 4

		a	b	c	d
$\alpha_{\parallel}$	(A.U.)	6·1144	7·0338	4·948	2·98
	(c.g.s.)	$0{\cdot}90593\times10^{-24}$	$1{\cdot}9695\times10^{-16}$	$2{\cdot}619\times10^{-8}$	2·98
$\alpha_{\perp}$	(A.U.)	4·44678	4·0424	2·803	−0·31
	(c.g.s.)	$0{\cdot}65885\times10^{-24}$	$1{\cdot}1319\times10^{-16}$	$1{\cdot}483\times10^{-8}$	−0·31

The adiabatic potential of the hydrogen molecule can be fairly well expressed by a Morse function, at least in the neighbourhood of $R=R_e$. According to Hirschfelder (1950), the numerical constants have been determined as follows:

$$U=109{\cdot}46(-2e^{-x}+e^{-2x})\ \text{kcal/mol}, \qquad \ldots\ldots(20)$$

$x=1{\cdot}0298(R/a_0-1{\cdot}401)$, $a_0=0{\cdot}529151\times10^{-8}$ cm. The vibrational wave functions ψ_v for this potential can be obtained analytically (v is the vibrational quantum number). They are slightly different for H_2, HD and D_2 due to the difference of their reduced masses. After a short calculation, we can also show that

$$D^p_{vv'}=\int_{-\infty}^{+\infty}\psi_v(R-R_e)^p\psi_{v'}\,dR, \qquad \ldots\ldots(21)$$

can be expressed as in Appendix 2. The numerical values of these integrals for the three types of hydrogen molecule are shown in table 5, and using these results and formula (19), the matrix elements of the polarizability are obtained as given in table 6.

Table 5. $D^p_{vv'}$ (A.U.)

	H_2	HD	D_2
D^0_{00}	1	1	1
D^1_{00}	0·0427 87	0·0369 57	0·0300 81
D^2_{00}	0·0301 72	0·0257 69	0·0206 94
D^3_{00}	0·0045 43	0·0033 69	0·0022 16
D^0_{01}	0	0	0
D^1_{01}	0·16703	0·15517	0·13991
D^2_{01}	0·02419	0·01937	0·01418
D^3_{01}	0·01727	0·01347	0·00956

Table 6. Matrix Elements of the Polarizability

	H_2	HD	D_2
$(\alpha_{\parallel})_{00}$	6·5782 (0·9746)	6·5119 (0·9651)	6·4350 (0·9537)
$(\alpha_{\perp})_{00}$	4·7029 (0·6968)	4·6674 (0·6917)	4·6257 (0·6856)
α_{00}	5·3280 (0·7894)	5·2822 (0·7829)	5·2288 (0·7749)
γ_{00}	1·8753 (0·2778)	1·8445 (0·2734)	1·8093 (0·2682)
$(\alpha_{\parallel})_{01}$	1·3461 (0·1994)	1·2275 (0·1819)	1·0828 (0·1605)
$(\alpha_{\perp})_{01}$	0·7377 (0·1093)	0·6774 (0·1004)	0·6024 (0·0893)
α_{01}	0·9405 (0·1393)	0·8608 (0·1276)	0·7625 (0·1130)
γ_{01}	0·6084 (0·0901)	0·5501 (0·0815)	0·4804 (0·0712)
$\epsilon-1$	0·0002666	0·0002643	0·0002616
ρ_n (Ray.)	0·0162	0·0160	0·0157
ρ_n (Raman)	0·052	0·0512	0·0500

In this table, the values of the polarizability in atomic units are given first, and their values in units of 10^{-24} cm^3 are given in brackets.

We see in table 3 that the calculated values of the polarizability increase with the number of added terms in the wave function. This is quite natural since we have made use of the variational method, and the energy is expressed as (14) in which $E^{(0)}$ is constant throughout our calculation. If the James–Coolidge value of $E^{(0)}$ is close enough to the actual value, which seems to be true, our theoretical values of the polarizability are a little lower than the true ones. There may be some additional errors in calculating the matrix elements of the polarizability, since we have approximated to the adiabatic potential by a Morse

function, and neglected terms higher than $(R-R_e)^4$ in the expansion (19), but our estimation of errors from various sources shows that the final errors in $(\alpha_0)_{00}$ and $(\alpha_1)_{00}$ do not amount to more than a few per cent. The percentages of the possible errors in the values of γ and $\alpha_H-\alpha_D$ may be somewhat higher.

§ 5. COMPARISON WITH EXPERIMENT

The dielectric constant ϵ and the refractivity n (extrapolated to zero frequency) of gases are given by the formula

$$\epsilon-1=n^2-1=4\pi N\alpha_{00}, \qquad \ldots\ldots(22)$$

where N is the number of molecules in a unit volume. Our theoretical value of ϵ or n^2 for the ordinary hydrogen H_2 at s.t.p. is 1·0002666, while the experimental values are 1·000273 (Tangl 1908), 1·000263 (Fritts 1924), 1·000259 (Braunmühl 1927), 1·000265 (Zahn 1924) for ϵ, and 1·000273 (Van Vleck 1932) for n^2.

Bell (1942) has analysed the values of the refractive index of D_2 measured by Larsén (1936), and has obtained the result: $(\alpha_{H_2}-\alpha_{D_2})/\alpha_{H_2}=13\%$, for which our theoretical value is 18·6%.

The depolarization factor in Rayleigh scattering of natural light is expressed as

$$\rho_n=6\gamma_{00}^2/(45\alpha_{00}^2+7\gamma_{00}^2). \qquad \ldots\ldots(23)$$

Our theoretical value for this quantity, for H_2, is 0·0162, while the experimental values are 0·022 (Cabannes and Granier 1928), 0·0274 (Rao 1927), 0·0257 (Partharasathy 1932) and 0·009 (Volkman 1935).

The same quantity for the vibrational Raman line can be expressed by the same formula if we put α_{01} and γ_{01} instead of α_{00} and γ_{00} respectively. The theoretical value is 0·052, while the experimental one is 0·13 (Bhagavantam 1932).

The ratio of the intensity of the vibrational Raman line to that of the Rayleigh line is

$$\frac{\nu_R^4}{\nu_0^4}\frac{\alpha_{01}^2+13\gamma_{01}^2/45}{\alpha_{00}^2+13\gamma_{00}^2/45}, \qquad \ldots\ldots(24)$$

where ν_R and ν_0 are the frequencies of Raman and Rayleigh lines respectively. In the case of the Stokes line due to 4046 Å of Hg, the theoretical value is 0·0154, while the experimental one is 0·0042 (Bhagavantam 1932), which is rather difficult to measure accurately.

One of the authors (Mizushima 1950) has estimated α_{01} to be about $0{\cdot}18\times10^{-24}\,\mathrm{cm}^3$ from the intensity of pressure absorption, which agrees with our result.

ACKNOWLEDGMENTS

We wish to express our sincere thanks to the members of the Kotani Laboratory of Tokyo University for their discussions and financial aid, to Professor James for his kindness in sending his unpublished data, and to Professor Coulson for his kindness in communicating our paper to the Physical Society. We are also much indebted to Misses S. Nakadate, H. Nishikubo, M. Iwano, K. Nagai, A. Uno, N. Fujita and T. Koide for the numerical calculations.

APPENDIX 1

Most of the integrals can be expressed in terms of the James–Coolidge $X(m,n,j,k;p)$, but H'_{ik} and T_{kh} can be written also with the use of another set of auxiliary functions. For example H'_{ik} can be reduced as follows:

(i) *Electric field parallel to the molecular axis*

$$\phi[m\,n\,j\,k](z_1+z_2)\theta[M\,N\,J\,K\,P]$$

$$=8(R/2)^7\{U(m+M+1,n+N,j+J+1,k+K;P)$$
$$+U(m+M,n+N+1,j+J,k+K+1;P)$$
$$+U(m+N+1,n+M,J+K+1,k+J;P)$$
$$+U(m+N,n+M+1,j+K,k+J+1;P)\} \qquad \ldots\ldots(A)$$

$$=2(R/2)^7\{X(m+M+1,n+N+2,j+J+1,k+K;P)$$
$$-X(m+M+1,n+N,j+J+1,k+K+2;P)$$
$$+X(m+M,n+N+3,j+J,k+K+1;P)$$
$$-X(m+M,n+N+1,j+J,k+K+3;P)$$
$$+X(m+N+1,n+M+2,j+K+1,k+J;P)$$
$$-X(m+N+1,n+M,j+K+1,k+J+2;P)$$
$$+X(m+N,n+M+3,j+K,k+J+1;P)$$
$$-X(m+N,n+M+1,j+K,k+J+3;P)\}. \qquad \ldots\ldots(B)$$

(ii) *Electric field perpendicular to the molecular axis*

$$\phi[m\,n\,j\,k](x_1+x_2)\theta[M\,N\,J\,K\,P]$$

$$=4(R/2)^7\{\overline{U}(m+M,n+N,j+J,k+K;P)+\overline{U}(m+N,n+M,j+K,k+J;P)\}$$
$$+2(R/2)^7\{V(m+M,n+N,j+J,k+K;P)$$
$$+V(m+N,n+M,j+K,k+J;P)\} \qquad \ldots\ldots(A)$$

$$=2(R/2)^7\{\overline{X}(m+M,n+N+2,j+J,k+K;P)$$
$$-\overline{X}(m+M,n+N,j+J,k+K+2;P)+\overline{X}(m+N,n+M+2,j+K,k+J;P)$$
$$-\overline{X}(m+N,n+M,j+K,k+J+2;P)+X(m+M,n+N+2,j+J,k+K;P)$$
$$-X(m+M,n+N,j+J,k+K+2;P)+X(m+N,n+M+2,j+K,k+J;P)$$
$$-X(m+N,n+M+2,j+K,k+J+2;P)\}, \qquad \ldots\ldots(B)$$

where
$$U(m,n,j,k;P)=\frac{1}{4}\frac{1}{(2\pi)^5}\int\int\int\int\int\int \exp\{-2c(\xi_1+\xi_2)\}\xi_1^{\,m}\xi_2^{\,n}\eta_1^{\,j}\eta_2^{\,k}$$
$$\times(\xi_1^{\,2}-\eta_1^{\,2})(\xi_2^{\,2}-\eta_2^{\,2})\rho^P\,d\xi_1\,d\xi_2\,d\eta_1\,d\eta_2\,d\phi_1\,d\phi_2,$$

$$\overline{U}(m,n,j,k;P)=U(m+2,n,j,k;P)+U(m,n,j+2,k;P)$$
$$-U(m+2,n,j+2,k;P)-U(m,n,j,k;P),$$

$$V(m,n,j,k;P)=\frac{1}{2}\frac{1}{(2\pi)^5}\int\int\int\int\int\int \exp\{-2c(\xi_1+\xi_2)\}\xi_1^{\,m}\xi_2^{\,n}\eta_1^{\,j}\eta_2^{\,k}$$
$$\times(\xi_1^{\,2}-1)(1-\eta_1^{\,2})\cos 2\phi_1(\xi_1^{\,2}-\eta_1^{\,2})(\xi_2^{\,2}-\eta_2^{\,2})\rho^P\,d\xi_1\,d\xi_2\,d\eta_1\,d\eta_2\,d\phi_1\,d\phi_2.$$

U, $\overline{U}$ and V can be integrated elementarily in those cases when $P=0$ or 2. In the case when $P=1$, the Neumann expansion of $1/\rho$ can be used, and, for example, $U(m,n,j,k;1)$ is expressed as follows:

$$\begin{aligned}U(m,n,j,k;1)=&\sum_{\tau=0}^{\infty} D_\tau^0[W_\tau(m+4,n+2)C_\tau(j)C_\tau(k)+W_\tau(m+2,n+4)C_\tau(j)C_\tau(k)\\&-W_\tau(m+4,n)C_\tau(j)C_\tau(k+2)-2W_\tau(m+2,n+2)C_\tau(j)C_\tau(k)\\&-W_\tau(m,n+4)C_\tau(j+2)C_\tau(k)+W_\tau(m+2,n)C_\tau(j)\{2C_\tau(k+2)-C_\tau(k+4)\}\\&+W_\tau(m,n+2)\{2C_\tau(j+2)-C_\tau(j+4)\}C_\tau(k)\\&-W_\tau(m,n)\{2C_\tau(j+2)C_\tau(k+2)-C_\tau(j+4)C_\tau(k+2)-C_\tau(j+2)C_\tau(k+4)\}\\&-2W_\tau(m+3,n+3)C_\tau(j+1)C_\tau(k+1)+2W_\tau(m+3,n+1)C_\tau(j+1)C_\tau(k+3)\\&+2W_\tau(m+1,n+3)C_\tau(j+3)C_\tau(k+1)-2W_\tau(m+1,n+1)C_\tau(j+3)C_\tau(k+3)]\\&-\sum_{\tau=1}^{\infty} D_\tau^1\{W_\tau^1(m+2,n+2)C_\tau^1(j)C_\tau^1(k)-W_\tau^1(m+2,n)C_\tau^1(j)C_\tau^1(k+2)\\&-W_\tau^1(m,n+2)C_\tau^1(j+2)C_\tau^1(k)+W_\tau^1(m,n)C_\tau^1(j+1)C_\tau^1(k+2),\end{aligned}$$

in which $D_\tau^0=2\tau+1$, $D_\tau^1=-2(2\tau+1)/\tau^2(\tau+1)^2$, and

$$C_\tau^\nu(k)=\tfrac{1}{2}\int_{-1}^{+1} P_\tau^\nu(\eta)(1-\eta^2)^{\nu/2}\eta^k\,d\eta,$$

$$W_\tau^\nu(m,n)=\iint \exp\{-2c(\xi_1+\xi_2)\}Q_\tau^\nu(\xi_+)P_\tau^\nu(\xi_-)(\xi_1^2-1)^{\nu/2}(\xi_2^2-1)^{\nu/2}\xi_1^m\xi_2^n\,d\xi_1\,d\xi_2,$$

$\xi_+(\xi_-)$ being the larger (smaller) one of ξ_1 and ξ_2. Superscript ν is omitted if it is zero.

We carried out the calculation of H'_{ik} and $T_{k\lambda}$ by both methods mentioned above, and, by comparing the two results, we could avoid numerical errors.

The numerical values of the integrals required in our calculation have been partly published by Kotani, Amemiya and Simose (1938) and Kotani and Amemiya (1940), and the remaining part may be published elsewhere.

APPENDIX 2

The vibrational wave function corresponding to the Morse function

$$U=D(-2\,e^{-x}+e^{-2x}),\qquad x=a(R-R_e)$$

is given by

$$\psi_v=A_v a^{1/2}\,e^{-z/2}z^{(k-1)/2}\sum_{s=0}^{v}\frac{(-1)^s z^{-s}}{s!(v-s)!\;\Gamma(k-v-s)},$$

where $z=k\exp\{-a(R-R_e)\}$, $k=4\pi(2\mu D)^{1/2}/ah$. With this wave function we can show that

$$D_{vv'}^p=\int_{-\infty}^{+\infty}\psi_v(R-R_e)^p\psi_{v'}\,dR.$$

This can be reduced to the following formulae:

$$D_{vv}^0=1,\qquad D_{vv'}^0=0\quad(v\neq v')$$

$$D_{00}^1=\frac{1}{a}\left\{\log k-\psi(k)+\frac{1}{k-1}\right\},\qquad D_{01}^1=\frac{(k-3)^{1/2}}{a}\,\frac{1}{k-2},$$

$$D_{00}^2=\frac{1}{a^2}\left\{\left(\log k-\psi(k)+\frac{1}{k-1}\right)^2+\frac{1}{(k-1)^2}+\psi^{(1)}(k)\right\},$$

$$D^2_{01} = \frac{(k-3)^{1/2}}{a^2}\,\frac{2}{k-2}\left\{\log k - \psi(k) + \frac{1}{k-1} + \frac{1}{k-2}\right\},$$

$$D^3_{00} = \frac{1}{a^3}\left\{\left(\log k - \psi(k) + \frac{1}{k-1}\right)^3 + \frac{3}{(k-1)^2}\left(\log k - \psi(k) + \frac{1}{k-1}\right) + \frac{2}{(k-1)^3} + 3\left(\log k - \psi(k) + \frac{1}{k-1}\right)\psi^{(1)}(k) - \psi^{(2)}(k)\right\},$$

$$D^3_{01} = \frac{(k-3)^{1/2}}{a^3}\,\frac{3}{k-2}\left\{\left(\log k - \psi(k) + \frac{1}{k-1} + \frac{1}{k-2}\right)^2 + \frac{1}{(k-1)^2} + \frac{1}{(k-2)^2} + \psi^{(1)}(k)\right\},$$

where

$$\log k - \psi(k) = \frac{1}{2k} + \frac{1}{12k^2} - \frac{1}{120k^4} + \frac{1}{252k^6} - \ldots\ldots,$$

$$\psi^{(1)}(k) = \frac{1}{k} + \frac{1}{2k^2} + \frac{1}{6k^3} - \frac{1}{30k^5} + \frac{1}{42k^7} - \ldots\ldots,$$

$$\psi^{(2)}(k) = -\frac{1}{k^2} - \frac{1}{k^3} - \frac{1}{2k^4} + \frac{1}{6k^6} - \frac{1}{6k^8} + \ldots\ldots$$

REFERENCES

Bell, R. P., 1942, *Trans. Faraday Soc.*, **38**, 422.

Bell, R. P., and Long, D. A., 1950, *Proc. Roy. Soc.* A, **203**, 364.

Bhagavantam, S., 1932, *Indian J. Phys.*, **7**, 549.

v. Braunmühl, H., 1927, *Phys. Z.*, **28**, 141.

Cabannes, J., and Granier, J., 1923, *J. Phys. Radium*, **4**, 429.

Easthope, C. E., 1936, *Proc. Camb. Phil. Soc.*, **32**, 260.

Fritts, E. C., 1924, *Phys. Rev.*, **23**, 345.

Hirschfelder, J. O., 1935, *J. Chem. Phys.*, **3**, 620; 1950, *Ibid.*, **18**, 130.

James, H. M., and Coolidge, A. S., 1933, *J. Chem. Phys.*, **1**, 825.

Kotani, M., Amemiya, A., and Simose, T., 1938, *Proc. Phys.-Math. Soc. Japan*, **20**, extra number.

Kotani, M., and Amemiya, A., 1940, *Proc. Phys.-Math. Soc. Japan*, **22**, extra number.

Larsén, T., 1936, *Z. Phys.*, **100**, 543.

Mizushima, M., 1950, *Phys. Rev.*, **77**, 150.

Mrowka, B., 1932, *Z. Phys.*, **76**, 300.

Mulliken, R. S., and Rieke, C., 1941, *Rep. Prog. Phys.*, **8**, 231 (London : Physical Society).

Partharasathy, S., 1932, *Indian J. Phys.*, **7**, 139.

Rao, R., 1927, *Indian J. Phys.*, **2**, 61.

Steensholt, G., 1935, *Z. Phys.*, **93**, 620; 1947, *Phil. Mag.*, **38**, 748.

Tangl, K., 1908, *Ann. Phys., Lpz.*, **26**, 59.

Van Vleck, J. H., 1932, *The Theory of Electric and Magnetic Susceptibilities* (Oxford : Clarendon Press), p. 67.

Volkman, H., 1935, *Ann. Phys., Lpz.*, **24**, 457.

Zahn, C. T., 1924, *Phys. Rev.*, **24**, 400.

On the Theory of Electrical Conductivities of Monovalent Metals

By A. B. BHATIA*
Physical Research Laboratory, Ahmedabad, India

Communicated by H. Fröhlich; MS. received 9th November 1951

ABSTRACT. It is shown that on the basis of the Bloch–Peierls–Bardeen theory of conductivity, the use of $\theta_R \simeq \theta_D$ in the Bloch–Grüneisen formula is a reasonable approximation in the temperature range $T \gtrsim \theta_D$. At very low temperatures $T \ll \theta_D$, however, $\theta_R = \theta_L$. This, it is shown, disagrees with experimental data much more than the *ad hoc* use of $\theta_R \simeq \theta_D$ in the Bloch–Grüneisen formula.

§1. INTRODUCTION

As far as we know, in all theoretical and experimental considerations on the electrical conductivities of metals, it is *tacitly* assumed that θ (in future denoted by θ_R) is equal to θ_D, the Debye characteristic temperature. Although this assumption has received remarkable experimental support—at least in the temperature range $T \sim \theta_D$—mainly from the work of Grüneisen (1933), so far its justification on theoretical grounds has not been attempted. Indeed, according to Bloch's (1928) treatment, where only the longitudinal elastic waves contribute to electrical resistance, one would expect $\theta_R = \theta$ corresponding to longitudinal elastic waves (which we shall denote by θ_L).† However, Blackman (1951) has shown that values for θ_L for most metals are appreciably larger than those for θ_R or θ_D.

It is the purpose of this paper to show that the conclusion $\theta_R = \theta_L$ is considerably modified when one also takes into account the so-called *Umklapprozesse*, which Bloch's treatment neglects. In fact, we shall see that the use of $\theta_R \simeq \theta_D$ in the Bloch–Grüneisen formula is a fair enough approximation for $T \gtrsim \theta_D$. For low temperatures ($T \ll \theta_D$), however, one should put $\theta_R = \theta_L$. As we shall see in §3, the use of $\theta_R = \theta_L$ in the Bloch–Grüneisen formula gives much more violent disagreement with the experimental data than the *ad hoc* use of $\theta_R \simeq \theta_D$. It is, therefore, felt that the assumptions of the theory for low temperatures need re-examination.

It may be mentioned here that, since any exact treatment of these topics is forbiddingly difficult—mainly because of the intractability of Bloch's integral equation under general conditions—our considerations are essentially of a semi-quantitative nature. Moreover, this discussion will be confined to monovalent metals only.

* Now at the Department of Mathematical Physics, University of Edinburgh.

† We wish to mention here that Dr. Blackman's (1951) emphasis on this point is, to a large extent, responsible for the present paper.

§ 2. THE CASE $T \gtrsim \theta_D$

In this section we consider the case $T \gtrsim \theta_D$. However, before proceeding further, we mention that the expression for the electrical resistance σ is derived in three steps, (*a*) the calculation of the probability $P(\mathbf{k}\mathbf{k}')\,dS(\mathbf{k}')$ per unit time for an electron in state $\mathbf{k}$ to jump into state $\mathbf{k}'$ in an area $dS(\mathbf{k}')$ of the Fermi surface, (*b*) to solve Bloch's integral equation for the mean free path l, and (*c*) to obtain σ, which is simple once l is known.

First we consider explicitly the case $T \gg \theta_D$. Then $P(\mathbf{k}\mathbf{k}')$ is given (cf. Bardeen 1937, Krishnan and Bhatia 1948) by

$$P(\mathbf{k}\mathbf{k}') = F(|\mathbf{k}-\mathbf{k}'|)\sum_m \sum_{j=1}^{3} \frac{(\mathbf{n}_{qj}\cdot\overline{\mathbf{q}+\mathbf{B}_m})^2}{\nu_{qj}^2} \equiv F(\phi)S, \text{ say,} \quad \ldots\ldots(1)$$

in which $F(|\mathbf{k}-\mathbf{k}'|)$ is a function of k (the electron wave number at the Fermi surface) and the angle of scattering ϕ only in the combination $k\sin\frac{1}{2}\phi$, the precise functional dependence of F on $k\sin\frac{1}{2}\phi$ being determined by the perturbing potential, $\mathbf{q}$ is the wave vector of the elastic wave, $\mathbf{n}_{qj}$ is the unit displacement vector of that wave of which the frequency is ν_{qj}, and $\mathbf{B}_m$ is a vector in the reciprocal lattice, corresponding to some lattice spacing of the crystal; $\mathbf{k}$ is related to $\mathbf{k}'$ by

$$\mathbf{k}-\mathbf{k}' = \mathbf{B}_m + \mathbf{q} \qquad \text{and} \qquad |\mathbf{k}'| \simeq |\mathbf{k}|. \qquad \ldots\ldots(2)$$

First consider $\mathbf{B}_m = (0,0,0)$. If we assume the velocities V_j of the elastic waves to be independent of q, then (1) reduces to

$$P(\mathbf{k}\mathbf{k}') = F(\phi)\sum_{j=1}^{3} \frac{\cos^2\gamma_j}{V_j^2} \equiv F(\phi)S_1, \text{ say,} \quad \ldots\ldots(3)$$

in which $\cos\gamma_j = (\mathbf{n}_{qj}\cdot\mathbf{q}_j/q_j)$. Here then only the longitudinal component of the elastic waves contributes to $P(\mathbf{k}\mathbf{k}')$. In an elastically anisotropic crystal $\epsilon = c_{11}-c_{12}-2c_{44} \neq 0$, the factor S_1 in (3) depends on the direction of $\mathbf{q}$ in a complicated manner (see for example Krishnan and Bhatia 1948). Now, in order that the step (*b*) above could be taken, one assumes $\epsilon = 0$, when

$$S_1 = 1/V_L^2 \simeq (hq_m/\kappa\theta_L)^2, \qquad \ldots\ldots(4)$$

in which q_m is the maximum possible value of q. However, in all usual treatments S_1 in (3) is replaced by

$$[\tfrac{1}{3}(1/V_L^3 + 2/V_T^3)]^{2/3} \simeq (hq_m/\kappa\theta_D)^2 \qquad \ldots\ldots(5)$$

instead of by (4); this procedure, in view of the above, is not justified. It may be mentioned that when $\epsilon \neq 0$ one might replace S_1 (as an approximation) by its average over all directions of $\mathbf{q}$ but *not* by the average of the left-hand side of (5) as is usually done.

Consider next terms for which $\mathbf{B}_m \neq 0$ of (1) (*Umklapprozesse*). These terms contribute to $P(\mathbf{k}\mathbf{k}')$ when ϕ is greater than about 80°. Now here, even under the assumption of elastic isotropy, $\epsilon = 0$, the sum $S - S_1$ would not be a function of ϕ alone. Hence any exact treatment is difficult. However, a qualitative estimate of the contribution from these terms to (1) can be easily obtained.

First we note that these terms for which $\mathbf{B}_m \neq 0$ depend upon the component of the displacement vector along $\mathbf{q}+\mathbf{B}_m$ and not along $\mathbf{q}$, as is the case for $\mathbf{B}_m = 0$. Now it is easy to see that the angles between the vectors $\mathbf{q}$ and $\mathbf{q}+\mathbf{B}_m$ cover a wide range, as the directions of incidence and scattering are varied. It is,

therefore, reasonable to conclude that the contributions to $S-S_1$ averaged over all directions of incidence and of scattering ($\phi \geqslant 80°$) from longitudinal and transverse waves are of comparable magnitude. Hence, if the *Umklapprozesse* alone were responsible for the electrical resistance of a metal, one would expect θ_R to be very close to θ_D.

Next we give some estimates for the relative contributions to the electrical resistance of sodium metal at room temperature ($T > \theta_L$ or θ_D) from the $\mathbf{B}_m = 0$ term and the *Umklapprozesse*. For a given direction of incident electrons in the crystal, let $R(l_1)$, $[R(x) = 1/x]$, and $R(l_2)$ denote the contributions to $R(l)$ from these two terms respectively.‡ Then the contributions σ_1 and σ_2 to σ are given by

$$\sigma = \sigma_1 + \sigma_2 = \text{constant} \times [\overline{R(l_1)} + \overline{R(l_2)}], \qquad \ldots\ldots(6)$$

in which $\overline{R(l)}$ denotes a suitable average of $R(l)$ over all directions of incident electrons in the crystal. Krishnan and Bhatia (1948) estimated the value of $\overline{R(l_2)}/\overline{R(l_1)} = \sigma_2/\sigma_1 = \nu$, say, by suitably integrating $P(\mathbf{k}\mathbf{k}')$ for a few directions of incident electrons. They obtain $\nu \simeq 3$. However, they have overestimated the value of ν since they took $F(\phi)$ to be nearly isotropic. Using the same method, but taking for $F(\phi)$ the function given by Bardeen (1937), one obtains $\nu \simeq 2$. We have also calculated ν making Bardeen's assumptions, which make $P(\mathbf{k}\mathbf{k}')$ a function of ϕ alone, and have obtained $\nu = 1{\cdot}2$. His assumptions, however, are of such a nature as to lead to an underestimate of ν (see Bardeen 1937, p. 695). Although these calculations are by no means exact, they demonstrate conclusively that at room temperatures *Umklapprozesse* contribute most to the electrical resistance of sodium. However, since about one-third of the total resistance comes from the term for which $\mathbf{B}_m = 0$, to which only longitudinal waves contribute, if one were to use a single value of θ_R, it should lie intermediate between θ_L and θ_D but closer to θ_D than to θ_L.

For noble metals, which are face-centred cubic and for which the ratio of the smallest $|\mathbf{B}_m|$ to the diameter of the Fermi sphere ($|\mathbf{B}_{111}|/2k = 1{\cdot}1$) is smaller than the corresponding ratio for the alkali metals ($|\mathbf{B}_{110}|/2k = 1{\cdot}14$), obviously the relative contribution from the *Umklapprozesse* would be still larger than that for alkali metals. Hence for noble metals the *effective* θ_R values would be much closer to θ_D than for alkali metals. This is demonstrated in the table.

	Metal	Li	Na	K	Cu	Ag	Au
*	θ_L	540	282	—	540	—	—
	θ_D	328	150	100	315	215	170
†	θ_R	363	202	163	333	223	175

* From Blackman (1951).
† As determined from resistivities in the temperature range $T \sim \theta_D$ (Grüneisen 1933).

The above arguments, qualitatively and to a large extent quantitatively, still remain valid at temperatures $T \sim \theta_D$, since these temperatures are large enough to excite appreciably all $\mathbf{q}$-quanta. Thus we see that, at least for $T \gtrsim \theta_D$, $\theta_R \sim \theta_D$ is a fair enough approximation. One may, therefore, take empirically the expression for σ to be given by the Bloch–Grüneisen formula:

$$\sigma/\sigma(T_0) = ATG(\theta_R/T) \quad \text{for} \quad T \gtrsim \theta_D, \qquad \ldots\ldots(7)$$

where $\theta_D \leqslant \theta_R < \theta_L$, $AT_0 \simeq 1$, $\sigma(T_0)$ is the specific resistance at temperature $T_0 \gg \theta_L$ or θ_D and $G(y)$ is the Grüneisen function of the variable y. As mentioned before,

‡ Although the separation of two contributions to $R(l)$ may not be possible under general conditions, we assume for convenience that this separation is possible.

(7) is in very good agreement with experimental data. An *empirical* formula for σ more appropriate than (7) would be ($T \gtrsim \theta_D$)

$$\sigma/\sigma(T_0) = AT[xG(\theta_L/T) + (1-x)G(\theta_D/T)], \qquad \ldots\ldots(8)$$

where $x = 0{\cdot}3$ to $0{\cdot}4$ for alkali metals and less than this for noble metals.

One should remember here, however, that the Bloch–Grüneisen formula is obtained under very restrictive assumptions which are not justified when one takes *Umklapprozesse* into account and (7) and (8) are more or less only *empirical* formulae. A detailed investigation regarding this point is now being carried out.

§ 3. THE CASE $T \ll \theta_D$

In the temperature range $T \sim \theta_D$, (since $\theta_D < \theta_L$) the second term in (8) decreases less rapidly with decrease of temperature than the first term. However, at still lower temperatures, the contribution to σ from *Umklapprozesse* will not be proportional to the Grüneisen function $G(\theta_D/T)$ for the following reason. As is obvious from (2), the smallest elastic wave number q_c which can give rise to *Umklapprozesse* is given by $q_c = (|\mathbf{B}| - 2k)$, where $\mathbf{B}$ is the smallest of the vectors $\mathbf{B}_m$ of the reciprocal lattice. Hence, the temperature θ_c below which the *Umklapprozesse* become *almost* completely ineffective may be taken as $\theta_c \simeq (q_c/q_m)\theta_D$. (For sodium and lithium, to take two examples, $\theta_c \sim 30°$ K and $70°$ K respectively.) Therefore, at temperatures below θ_c, the first term of (8) alone will contribute to σ. In this range of temperatures, obviously, this term would give both a very much sharper decrease of σ with decreasing T and a smaller absolute value of σ than (7). Recently MacDonald and Mendelssohn (1950) have made a detailed comparison of the observed resistivities of the alkali metals at low temperatures with the Bloch–Grüneisen formula (7). They find that, although in the temperature range $T \sim \theta_D$ the agreement with (7) is good when θ_R is chosen in accordance with the table, at very low temperatures ($T \lesssim \theta_c$) formula (7) gives for all the alkali metals (except for sodium where the discrepancy is small) a much sharper decrease of σ with T than is actually observed. For example, for K the value of θ_R needed in (7) for agreement at these temperatures is about $70°$ K which is even smaller than θ_D. In view of the above discussion, this discrepancy between calculated and experimental results is very much accentuated when one uses for σ, as one should at these low temperatures, the first term of (8) alone instead of (7).

Thus we see that, although the Bloch–Bardeen theory is satisfactory in the temperature range $T \gtrsim \theta_D$, it is in serious disagreement with experiments at very low temperatures. It may be mentioned that at these low temperatures the observed specific heats show a similar deviation from the Debye formula. Whether the discrepancy in the Bloch–Bardeen theory is due to its use of Debye vibrational spectrum or due to some other cause remains to be seen.

REFERENCES

BARDEEN, J., 1937, *Phys. Rev.*, **52**, 688.

BHATIA, A. B., and KRISHNAN, K. S., 1948, *Proc. Roy. Soc.* A, **194**, 185.

BLACKMAN, M., 1951, *Proc. Phys. Soc.* A, **64**, 681.

BLOCH, F., 1928, *Z. Phys.*, **52**, 555; 1929, *Ibid.*, **59**, 208.

GRÜNEISEN, E., 1933, *Ann. Phys., Lpz.*, **16**, 530.

MACDONALD, D. K. C., and MENDELSSOHN, K., 1950, *Proc. Roy. Soc.* A, **202**, 103.

Density of States Curve for the 3d Electrons in Nickel

By G. C. FLETCHER
Department of Mathematics, University College of the South-West, Exeter

Communicated by H. Jones ; MS. received 17th October 1951

ABSTRACT. A calculation is made of the energy density of electronic states for the 3d electrons in metallic nickel, using the approximation of tight binding. The early stages of the calculations and preliminary results have been previously summarized by Fletcher and Wohlfarth in 1951. The theoretical basis of the approximation is outlined and the validity of the underlying assumptions examined. The required overlap integrals are evaluated and the secular equation for the energy as a function of wave vector is solved exactly over the energy range of interest for nickel. The density of states curve is computed graphically. Among results of physical interest obtained are : bandwidth $2{\cdot}7_0$ ev, degeneracy temperature $1{\cdot}4_3\times10^3$ deg K, low temperature electronic heat coefficient $\gamma\ 1{\cdot}6_9\times10^{-3}$ cal. mol^{-1} deg^{-2} (compared with the experimental value of $1{\cdot}74\times10^{-3}$). The results are compared with those obtained by the cellular method of approximation used by Krutter in 1935, and Slater in 1936.

§1. INTRODUCTION

The transition metals are of particular interest in the theory of metals, since they display anomalous electronic properties, which are only explicable on the assumption that the energy density of electronic states $N(E)$ for certain critical values of energy E is much larger than for other metals (Mott 1936a, b). Results deduced from the only previous calculation of $N(E)$ for the 3d electrons in nickel (Krutter 1935, Slater 1936) do not agree very well with experiment and in the present work a re-calculation has been made using the approximation of tight binding (T.B.) (Bloch 1928 and others). The early stages of the calculations and preliminary results have previously been summarized (Fletcher and Wohlfarth 1951, to be referred to as I), and the purpose of the present paper is to give details of the complete work, together with a critical examination of the underlying assumptions and a discussion of the results obtained. Approximate wave functions for an electron in the metal were formed from the five atomic 3d functions and the resulting fifth-order secular equation has been solved exactly, whereas previously it has been the practice to make certain arbitrary approximations for the sake of simplicity (e.g. I, and Jones and Mott 1937). These approximations are shown to be invalid. In proceeding with the solution of this equation, numerical calculations have been made for the first time of the overlap integrals occurring in the matrix elements of energy. A feature of the calculation is the occurrence of the correct energy degeneracies as predicted by group theory. Certain results of physical interest are discussed in §4.

§2. THEORY OF THE APPROXIMATION

The complete theory of the T.B. approximation has been given by a number of authors (e.g. Mott and Jones 1936) and will not be repeated here. Bloch wave functions are built up from suitable atomic functions; those used here correspond to the five-fold degenerate 3d level of the isolated atom, i.e.

$$\left.\begin{aligned}\phi_1&=(15/4\pi)^{1/2}xyf(r)/r^2, \quad \phi_2=(15/4\pi)^{1/2}yzf(r)/r^2\\ \phi_3&=(15/4\pi)^{1/2}zxf(r)/r^2, \quad \phi_4=(15/16\pi)^{1/2}(x^2-y^2)f(r)/r^2\\ \phi_5&=(5/16\pi)^{1/2}(3z^2-r^2)f(r)/r^2\end{aligned}\right\} \quad \ldots\ldots(1)$$

where $f(r)$ is the normalized radial function of the isolated atom and the numerical factors are normalizing constants for the angular functions. From (1) the functions

$$\psi_{nk}=\sum_{\mathbf{l}}\exp(i\mathbf{a}\mathbf{l}\,.\,\mathbf{k})\phi_n(\mathbf{r}-\mathbf{a}\mathbf{l}),\ n=1\ldots.5 \qquad \ldots\ldots(2)$$

(where $\mathbf{k}$ is the wave-vector and $\mathbf{a}\mathbf{l}$ the position of any atom in the crystal lattice, summation being over all atoms) are constructed and may be shown to be of the correct Bloch form $\exp(i\mathbf{k}\,.\,\mathbf{r})u_k(\mathbf{r})$, where $u_k(\mathbf{r})$ has the periodicity of the lattice. For a cubic lattice a is simply the lattice constant and l_x, l_y, l_z may be integral or half-integral. Finally, the zero-order wave function for an electron in the crystal is assumed to be a linear combination of the functions (2)

$$\Psi_n(\mathbf{k}\,;\mathbf{r})=\sum_{m}a_{nm}(\mathbf{k})\psi_{mk}(\mathbf{r}). \qquad \ldots\ldots(3)$$

If $H=-(\hbar^2/2m)\nabla^2+V(\mathbf{r})$ denotes the Hamiltonian and E the energy for the electron in the crystal, then Ψ_n must satisfy

$$(H-E)\Psi_n=0. \qquad \ldots\ldots(4)$$

If the non-orthogonality of the ψ_{nk} with respect to n is neglected, an approximation to be discussed later, it is easily shown that E must satisfy the secular determinantal equation

$$|H_{nm}-E\delta_{nm}|=0,\ m=1\ldots.5\,;\ n=1\ldots.5, \qquad \ldots\ldots(5)$$

where $H_{nm}=[\int\psi_{nk}^{*}H\psi_{mk}\,d\tau]/\alpha_n\alpha_m$ and $\alpha_n^2=\int\psi_{nk}^{*}\psi_{nk}\,d\tau$. It can readily be shown that

$$\alpha_n^2=N\sum_{\mathbf{l}}\exp(-i\mathbf{a}\mathbf{l}\,.\,\mathbf{k})\int\phi_n^{*}(\mathbf{r}-\mathbf{a}\mathbf{l})\phi_n(\mathbf{r})\,d\tau\simeq N, \qquad \ldots\ldots(6)$$

where N is the total number of atoms in the crystal, on the assumption that the contributions to (6) from all other atoms ($\mathbf{l}\neq0$) is negligible compared with that from the central atom ($\mathbf{l}=0$). Finally, H_{nm} can be expressed in the form

$$H_{nm}=(\mathscr{E}_0+C)\delta_{nm}+\sum_{\mathbf{l}\neq0}\exp(-i\mathbf{a}\mathbf{l}\,.\,\mathbf{k})\int\phi_n^{*}(\mathbf{r}-\mathbf{a}\mathbf{l})(V-U)\phi_m(\mathbf{r})\,d\tau, \qquad \ldots\ldots(7)$$

where U is the potential due to an isolated atom at $\mathbf{l}=0$ and $\mathscr{E}_0$ is the energy of a 3d electron in the field of such an atom. The constant C, termed the self-energy of the central atom, will be defined below. For convenience, energies may be measured above and below the constant value $\mathscr{E}_0+C$. With the assumptions to be discussed below, the matrix elements H_{nm} are then found to have the following explicit values

$$\left.\begin{aligned}
&H_{11}=-4A_1\cos\xi\cos\eta+4A_2(\cos\eta\cos\zeta+\cos\zeta\cos\xi)\\
&H_{22}=-4A_1\cos\eta\cos\zeta+4A_2(\cos\zeta\cos\xi+\cos\xi\cos\eta)\\
&H_{33}=-4A_1\cos\zeta\cos\xi+4A_2(\cos\xi\cos\eta+\cos\eta\cos\zeta)\\
&H_{44}=4A_4\cos\xi\cos\eta-4A_5(\cos\eta\cos\zeta+\cos\zeta\cos\xi)\\
&H_{55}=-(4/3)(A_4+4A_5)\cos\xi\cos\eta+(4/3)(2A_4-A_5)(\cos\eta\cos\zeta+\cos\zeta\cos\xi)\\
&H_{12}=H_{21}=-4A_3\sin\zeta\sin\xi\,;\ H_{23}=H_{32}=-4A_3\sin\xi\sin\eta\\
&H_{31}=H_{13}=-4A_3\sin\eta\sin\zeta\,;\ H_{14}=H_{41}=0\\
&H_{24}=H_{42}=-4A_6\sin\eta\sin\zeta\,;\ H_{34}=H_{43}=4A_6\sin\zeta\sin\xi\\
&H_{15}=H_{51}=-(8/3^{1/2})A_6\sin\xi\sin\eta\,;\ H_{25}=H_{52}=(4/3^{1/2})A_6\sin\eta\sin\zeta\\
&H_{35}=H_{53}=(4/3^{1/2})A_6\sin\zeta\sin\xi\\
&H_{45}=H_{54}=(4/3^{1/2})(A_4+A_5)(\cos\eta\cos\zeta-\cos\zeta\cos\xi)
\end{aligned}\right\} \qquad \ldots\ldots(8)$$

where $\xi = \frac{1}{2}ak_x$; $\eta = \frac{1}{2}ak_y$; $\zeta = \frac{1}{2}ak_z$ and

$$\left.\begin{aligned}
A_1 &= -\int \phi_1^*(x-\tfrac{1}{2}a, y-\tfrac{1}{2}a, z)(V-U)\phi_1(x,y,z)\,d\tau \\
A_2 &= \int \phi_1^*(x, y-\tfrac{1}{2}a, z-\tfrac{1}{2}a)(V-U)\phi_1(x,y,z)\,d\tau \\
A_3 &= \int \phi_1^*(x-\tfrac{1}{2}a, y, z-\tfrac{1}{2}a)(V-U)\phi_2(x,y,z)\,d\tau \\
A_4 &= \int \phi_4^*(x-\tfrac{1}{2}a, y-\tfrac{1}{2}a, z)(V-U)\phi_4(x,y,z)d\tau \\
A_5 &= -\int \phi_4^*(x, y-\tfrac{1}{2}a, z-\tfrac{1}{2}a)(V-U)\phi_4(x,y,z)\,d\tau \\
A_6 &= \int \phi_2^*(x, y-\tfrac{1}{2}a, z-\tfrac{1}{2}a)(V-U)\phi_4(x,y,z)\,d\tau.
\end{aligned}\right\} \quad \ldots\ldots(9)$$

The assumptions inherent in the above treatment will now be briefly considered.

(i) The fundamental assumption of 'tight binding' is that the atoms in the crystal are far enough apart for interaction between them to be small. It is this interaction that causes the discrete energy levels of the isolated atom to broaden into bands of allowed energy for the crystal, and the assumption can only be justified on the grounds of consistency if the widths obtained for these bands are comparatively small. The value of $2{\cdot}7_0$ ev obtained for the bandwidth in the present calculation satisfies this criterion on comparison with bandwidths obtained for electrons farther from the atomic nucleus and therefore affected to a greater extent by neighbouring atoms in the crystal.

(ii) The non-orthogonality of the ψ_{nk} with respect to n is neglected, that is, the approximation is made that

$$\sum_{\mathbf{l}\neq\mathbf{l}'}\sum \exp\{ia(\mathbf{l}-\mathbf{l}').\mathbf{k}\}\int \phi_n^*(\mathbf{r}-a\mathbf{l}')\phi_m(\mathbf{r}-a\mathbf{l})\,d\tau = 0\,(n\neq m). \quad \ldots(10)$$

This approximation is linked up with another mentioned above, viz. that $\alpha_n^2 \simeq N$ and it is convenient to consider them together. As far as the derivation of eqns. (5) and (7) is concerned the neglect of non-orthogonality may be expressed in the alternative form

$$\int \psi_{nk}^*\psi_{mk}\,d\tau \ll \int \psi_{nk}^*\psi_{nk}\,d\tau \quad (n\neq m) \qquad \ldots\ldots(11)$$

$$\text{or} \sum_{\mathbf{l}}\sum_{\mathbf{l}'} \exp\{ia(\mathbf{l}-\mathbf{l}').\mathbf{k}\}\int \phi_n^*(\mathbf{r}-a\mathbf{l}')\phi_m(\mathbf{r}-a\mathbf{l})\,d\tau$$

$$\ll \sum_{\mathbf{l}}\sum_{\mathbf{l}'} \exp\{ia(\mathbf{l}-\mathbf{l}').\mathbf{k}\}\int \phi_n^*(\mathbf{r}-a\mathbf{l}')\phi_n(\mathbf{r}-a\mathbf{l})\,d\tau$$

$$\text{or} \sum_{\mathbf{l}\neq\mathbf{l}'}\sum \exp\{ia(\mathbf{l}-\mathbf{l}').\mathbf{k}\}\int \phi_n^*(\mathbf{r}-a\mathbf{l}')\phi_m(\mathbf{r}-a\mathbf{l})\,d\tau$$

$$\ll N + \sum_{\mathbf{l}\neq\mathbf{l}'}\sum \exp\{ia(\mathbf{l}-\mathbf{l}').\mathbf{k}\}\int \phi_n^*(\mathbf{r}-a\mathbf{l}')\phi_n(\mathbf{r}-a\mathbf{l})\,d\tau. \quad \ldots\ldots(12)$$

The integrals involved will obviously be much greater for nearest neighbours than for other pairs of atoms; considering nearest neighbours only for $n=1$, $m=2$, for example, a calculation gave for the left- and right-hand sides of (12) respectively the values

$$-0{\cdot}028N\sin\zeta\sin\xi \text{ and } N[1+0{\cdot}08\cos\xi\cos\eta - 0{\cdot}02(\cos\eta\cos\zeta+\cos\zeta\cos\xi)]$$

so that both approximations appear to be reasonable. It is stressed that, at least in the present problem, the actual orthogonality of the ψ_{nk} is immaterial, provided the inequality (12) is obeyed.

(iii) It is assumed in deriving (7) that

$$\int \phi_n^*(\mathbf{r})(V-U)\phi_m(\mathbf{r})\,d\tau = C\delta_{nm}. \qquad \ldots\ldots(13)$$

Now $V-U$ is an even function of x, y, z, $x-y$ or $x+y$ because of the symmetry of the lattice and hence, from considerations of the parity of $\phi_n^*\phi_m$ with respect to one or other of these variables, it is easily shown that $\int \phi_n^*(\mathbf{r})(V-U)\phi_m(\mathbf{r})\,d\tau = 0\ (n \neq m)$. Also $V-U$ must be symmetrical in x, y and z so that $\int \phi_n^*(\mathbf{r})(V-U)\phi_n(\mathbf{r})\,d\tau$ will have the same value for $n=1$, 2 and 3. An approximate calculation shows that the absolute values of this integral for $n=4$ and 5 are slightly less than that for $n=1$, 2 and 3 as would be expected since ϕ_1, ϕ_2 and ϕ_3 have antinodes in the directions of nearest neighbours while ϕ_4, ϕ_5 have antinodes in the directions of next nearest neighbours. Owing to the assumption (see §3) that $V=U$ for $r<a/2^{3/2}$, however, the differences are very small and the assumption expressed in (13) is unlikely to introduce any serious error.

(iv) The usual assumption was made that the major contribution to the H_{nm} arises from nearest neighbouring atoms and only these were considered. Any given atom in the face-centred cubic lattice has twelve nearest neighbours given by $\mathbf{l}=(\pm\frac{1}{2}, \pm\frac{1}{2}, 0)$, $(\pm\frac{1}{2}, 0, \pm\frac{1}{2})$, $(0, \pm\frac{1}{2}, \pm\frac{1}{2})$ and six next nearest given by $\mathbf{l}=(\pm 1, 0, 0)$, $(0, \pm 1, 0)$, $(0, 0, \pm 1)$. It seems probable, therefore, that the latter will also make a fairly large contribution, since they are only $\sqrt{2}$ times as far away as the nearest neighbours. This approximation seems the most likely to introduce serious error but is unavoidable without seriously increasing the complexity of the expressions for the H_{nm} and hence of the calculation.

§3. DETAILS OF COMPUTATION

In order to calculate the numerical values of the coefficients A_i some assumption must be made regarding the radial wave function $f(r)$ and the potential $V-U$. For the latter it was assumed that (i) $V=U$ within a sphere about the central atom of radius A equal to half the distance between nearest neighbours ($A=a/2^{3/2}$) (Mott and Jones 1936, p. 67), and (ii) $U=0$ elsewhere. For V outside this sphere an atomic potential centred on the nearest neighbour was used, which should be a good approximation in the regions where the product of the two wave functions is large. Since the atomic wave functions and potential have not been calculated for Ni, Hartree and Hartree's figures for Cu^+ with exchange (1936) were used, as this ion contains the same number of electrons as the Ni atom. For ease of computation as close a fit as possible was made to these values by explicit algebraic expressions. With primed symbols referring to the nearest neighbour, the range $r'<2A/5$ was found to be relatively unimportant and the expressions

$$f(r') = 85{\cdot}88r'^2 \exp(-5r') + 1{\cdot}979r'^2 \exp(-2r') \qquad \ldots\ldots(14)$$

$$V(r') = -\{1+28\exp(-3r')\}/r' \qquad \ldots\ldots(15)$$

were obtained (V is in atomic units). Integration was carried out over all space T less the atomic sphere τ of the central atom. Within this range

$$f(r) = 1{\cdot}979r^2 \exp(-2r) \qquad \ldots\ldots(16)$$

is a sufficiently good approximation, while for integration over τ it was also assumed that $f(r')=1{\cdot}979r'^2\exp(-2r')$ and $V(r')=-1/r'$. Although the $r^2\exp(-5r)$ term would not be small in integrating over τ, it must be omitted as it has been neglected in integrating over T. Thus for instance

$$A_1 \propto \int [1{\cdot}979\exp(-2r)\{1+28\exp(-3r')\} \times\{85{\cdot}88\exp(-5r')+1{\cdot}979\exp(-2r')\}xyx'y'/r']\,dT - \int [1{\cdot}979\exp(-2r)\times 1{\cdot}979\exp(-2r')xyx'y'/r']\,d\tau. \quad \ldots\ldots(17)$$

In carrying out the integrations, prolate spheroidal coordinates with the central atom and nearest neighbour as foci were used. The values obtained for the A_i may then be put in the convenient form

$$A_1=0{\cdot}1928E_0,\ A_2=0{\cdot}0572E_0,\ A_3=0{\cdot}0776E_0,\ A_4=0{\cdot}1348E_0,$$
$$A_5=0{\cdot}0247E_0,\ A_6=0{\cdot}0862E_0, \quad \ldots\ldots(18)$$

where
$$E_0=4(A_1+A_2)=1{\cdot}349\,\text{ev}. \quad \ldots\ldots(19)$$

A qualitative consideration of the various approximations indicated above shows that their effects on the A_i are all likely to be small, some being additive and some subtractive. Their total effect appears negligible compared with that arising from neglect of next-nearest neighbours.

Owing to the difficulty in solving a fifth order equation with coefficients as complex as (5), it was decided as a first approximation to neglect arbitrarily H_{nm} for $n=1, 2, 3$; $m=4, 5$, as has been done by previous workers (e.g. Jones and Mott 1937), and solve the resulting cubic and quadratic equations. Details of this work have already been given in I. Apart from giving correctly the total width of the band ($2{\cdot}7_0$ ev) which is unaffected by the neglected terms, this preliminary calculation served to reduce greatly the work involved in solving the complete quintic equation and also demonstrated the effect of neglecting the above terms (see §4).

From a study of the $N(E)$ curve obtained in I it was decided to calculate the more exact curve over the range of energy values $0{\cdot}5<E/E_0<0{\cdot}771$ ($2{\cdot}35<E<2{\cdot}70$ ev for diagram in I), a complete calculation being excessively laborious and unnecessary for most purposes. In effect only those solutions of (5) were found, which fell within this range; further reference to the previous calculation indicated in what regions of the Brillouin zone such solutions were likely to be found.

Along certain directions in **k**-space it is found that the secular eqn. (5) can be solved exactly as follows. Solutions marked * are identical with those obtained in I.

(100) *direction*. $E_{1,2}=4A_2+4(A_2-A_1)\cos\xi$ *

$E_3=-4A_1+8A_2\cos\xi$ *

$E_4=4A_4-8A_5\cos\xi$ *

$E_5=(4/3)[-A_4-4A_5+(4A_4-2A_5)\cos\xi]$ *

(110) *direction*. $E_1=4A_4\cos^2\xi-8A_5\cos\xi$ *

$E_{2,3}=4A_3\cos^2\xi+4(A_2-A_1)\cos\xi\pm 4A_3\sin^2\xi$ *

E_4 and E_5 given by

$$E^2+[(4A_1+16A_5/3+4A_4/3)q^2+(8A_5/3-16A_4/3-8A_2)q]E$$
$$+(16q^2/3)[(4A_1A_5+A_1A_4)q^2-(8A_2A_5+2A_2A_4+4A_1A_4-2A_1A_5)q$$
$$+(8A_2A_4-4A_2A_5)]-64A_6^2p^4/3=0$$

where $p=\sin\xi$; $q=\cos\xi$.

(111) *direction.* $E_1=4[(2A_3+2A_2-A_1)\cos^2\xi-2A_3]$. *

The other four roots occur in two doubly-degenerate pairs given by

$$E^2-4[(2A_2-A_1+A_4-2A_5-A_3)\cos^2\xi+A_3]E$$
$$+16\{[(A_4-2A_5)(2A_2-A_1-A_3)-2A_6^2]\cos^4\xi$$
$$+[A_3(A_4-2A_5)+4A_6^2]\cos^2\xi-2A_6^2\}=0.$$

$\xi=\pi$; $\zeta=0$ *direction.* $E_{1,2}=\pm4(A_1+A_2)\cos\eta-4A_2$ *

$E_3=4A_1$ *

$E_{4,5}=(4/3)[2A_5-A_4\pm2(A_4+A_5)(1+3\cos^2\eta)^{1/2}]$. *

The general effect of solving the quintic equation exactly, that is the effect of including the elements H_{nm} neglected in I, is to separate the solutions from each other and to remove some of the points of degeneracy which occurred in I and which were accidents of that approximation.

Returning to a consideration of eqn. (5) for a general vector **k**, various methods have been devised for solving such an equation, either in its determinantal or expanded form. Investigation of these methods showed, however, that none was suitable in the present case owing to the complexity of the H_{nm} and the fact that the roots of (5) are not, in general, well separated. An estimate of the required solution for a given vector **k** was therefore made from the approximate solutions already obtained in I. This was substituted in the determinant, which was evaluated, a correction was applied to the solution and the process repeated until a solution correct to three decimal places was obtained. The symmetry of eqn. (5) reduced considerably the region of the Brillouin zone to be investigated, and in all some 270 roots were obtained by the above method and checked at symmetrically equivalent points.

For each wave vector **k**, eqn. (5) has five roots, and a major problem is that of collecting these roots into five sets, each set belonging to one Brillouin zone and having an associated energy band. As a first step the energy degeneracies arising from symmetry considerations, reality of the Hamiltonian and accidental degeneracy may be investigated as indicated by Bouckaert, Smoluchowski and Wigner (1936) and by Herring (1937).

Following the arguments of the above papers the following deductions regarding degeneracy can be made for the present case.

(*a*) Due to symmetry there should be one triply degenerate level and one doubly degenerate level at $\mathbf{k}=0$. A double degeneracy, arising from the former, should occur along the (100) direction and two along the (111) direction. There is no other symmetry degeneracy apart from a double degeneracy at the point $\mathbf{k}=(2\pi/a, \pi/a, 0)$.

(*b*) If the Hamiltonian of a problem is real, it is possible for degeneracy, additional to that due to symmetry, to occur between a wave function and its complex conjugate. For a face-centred cubic crystal it is easily shown that no degeneracy of this type can occur.

(*c*) In addition to the above, various points of accidental degeneracy must occur in the present case. Their prediction, however, depends on a knowledge of the relative energies of the five wave functions Ψ_n (which will, in general, have different symmetry properties) for certain special wave vectors, e.g. $\mathbf{k}=(0, 0, 0)$, $(2\pi/a\ 0, 0)$, etc., so that most of these degeneracies are probably a result of the approximations of the calculation. They are indicated in fig. 1.

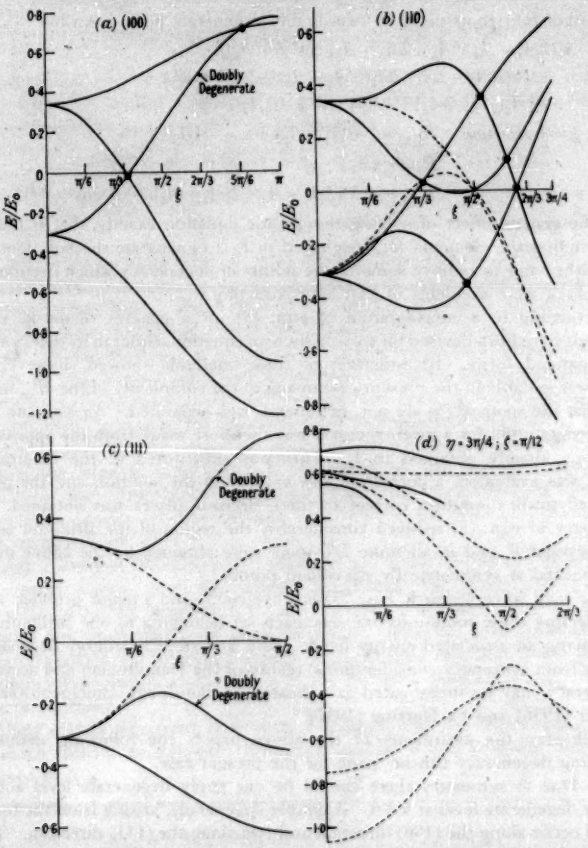

Fig. 1. Variation of energy with wave vector along certain directions in **k**-space. Broken curves indicate approximate solutions obtained in *I*. ○ Predicted points of accidental degeneracy.

(*d*) The normal derivative of E vanishes over the square faces of the Brillouin zone and along every line joining two opposite corners of a hexagonal face. E must have six-fold rotational symmetry over each hexagonal face.

From the solutions of eqn. (5), curves showing the variation of E with $\mathbf{k}$ were drawn for each value of k_y, and each value of k_z from 0 to $2\pi/a$ at intervals of $\pi/6a$. Only one other point of accidental degeneracy (see fig. 1(*b*)) was discovered, apart from those predicted. Attempts to collect the energy values into sets, as mentioned above, indicated quite conclusively that there is only one possible way of doing this. Solutions must be interchanged at all points

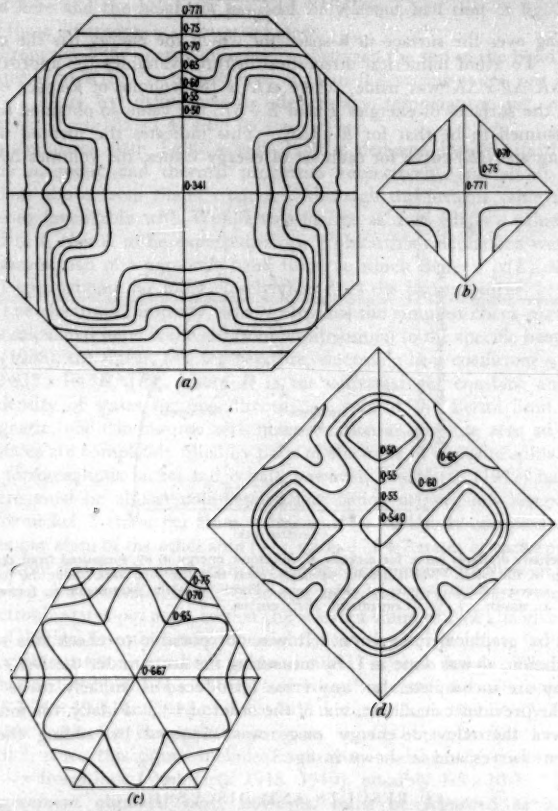

Fig. 2. Contours of constant energy for certain planes of the Brillouin zone for the high energy set of solutions of (5) drawn at energy intervals of 0·05 E_0. (*a*) $\zeta=0$ plane. (*b*) Square face ($\zeta=\pi$). (*c*) Hexagonal face. (*d*) $\zeta=\pi/2$ plane.

of accidental degeneracy in such a way that for every value of $\mathbf{k}$ the highest energy value belongs to Brillouin zone I, the next highest to Brillouin zone II, and so on. This is a perfectly valid procedure (Bouckaert, Smoluchowski and Wigner 1936), and the resulting discontinuities in grad E do not affect $N(E)$ since on any given surface of constant energy of $\mathbf{k}$-space such discontinuities occur only at isolated points and not over an area.

As in the previous calculation in I constant energy contours were drawn in the planes $k_z = \nu\pi/6a$ ($\nu = 0 \ldots . 12$) at intervals of $0{\cdot}025\,E_0$ for each of the three sets of energy values involved in the energy range considered. Examples of the (E, $\mathbf{k}$) curves and the constant energy contours are shown in figs. 1 and 2.

It follows directly from the definition of $N(E)$ that

$$N(E) \propto \iint \frac{dS}{|\text{grad } E|},$$

integrating over the surface in $\mathbf{k}$-space for which the energy has the constant value E. To avoid numerical integration in three variables the approximation $N(E) \propto \Delta K/\Delta E \propto \Delta K$ was made, where ΔK is the volume of $\mathbf{k}$-space enclosed between the surfaces of energies E and $E+\Delta E$, the value so obtained for $N(E)$ being assumed to be that for $E+\frac{1}{2}\Delta E$. This indicates the method used for calculating an $N(E)$ curve for each set of energy values, the volumes ΔK being

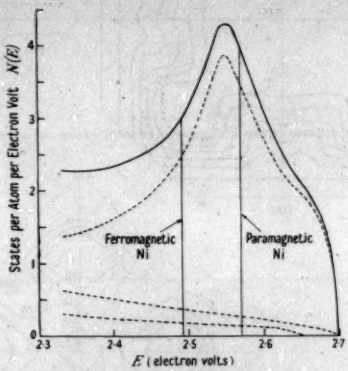

Fig. 3. Density of states curve for nickel. E, electronic energy in ev, measured from zero at the bottom of the band. $N(E)$, density of states, such that the total area under the (complete) curve corresponds to 5 states of either spin. Fermi limit for paramagnetic, ferromagnetic nickel as shown. - - - - - Constituent $N(E)$ curves.

obtained by graphical integration. It was not possible to check this stage of the calculation, as was done in I, by measuring the areas under the $N(E)$ curves, since they are incomplete, but any error introduced is unlikely to be greater than in the previous calculation, viz. of the order of 1%. Finally, the total $N(E)$ curve over the relevant energy range was obtained by adding the three constituent curves and is shown in fig. 3.

§ 4. RESULTS AND DISCUSSION

(*a*) The total width of the 3d band is 2·70 ev, as obtained already in I, since the highest and lowest energy values occur when $\mathbf{k} = (2\pi/a, 0, 0)$ for which $H_{nn} = 0$ ($n = 1, 2, 3$; $m = 4, 5$). On comparison of fig. 3 with the curve obtained in I it is seen that the right-hand peak has moved to a higher energy value nearly at the top of the band. This is readily understood on reference to fig. 1. Consider the (111) direction in particular, since here the effect of the previously neglected elements H_{nm} is greatest. Fig. 1 (*c*) then shows clearly that the result of including these elements is to force the higher solutions of eqn. (5) to still

higher energy values and the lower ones to lower values, i.e. to increase the number of states near the limits of the band and decrease the number near the middle. This suggests also, therefore, that the left-hand peak of the $N(E)$ curve would occur nearer the bottom of the band than in I. The $N(E)$ curve would then resemble that given by Slater (1936), but there are important differences between the two curves. The width of Slater's curve is twice that obtained here and the height of his peak only about half that of fig. 3. The effect of these differences is illustrated below.

(*b*) From fig. 3 the energy difference ϵ_0 between the top of the band and the right-hand vertical line, which corresponds to 0·3 vacant states per atom, is 0·125 ev. Then by definition the degeneracy temperature for nickel is $T=(\boldsymbol{e}/\boldsymbol{kc})\times 10^8\times 0{\cdot}125=1{\cdot}4_5\times 10^3\,°\text{K}$.

This compares with 1600° K and 2400° K deduced by Wohlfarth (1949) from the magnetic and thermal properties respectively, and about 2000° K deduced as above from Slater's curve. Although the present value does not compare so favourably with Wohlfarth's figures as does Slater's value or that deduced in I, this is to be expected, since Wohlfarth's calculations were based on the assumption of a parabolic band form, to which Slater's $N(E)$ curve and that in I approximate far more closely than does the present curve.

(*c*) The electronic property, which provides the simplest check on an $N(E)$ curve as calculated here, is the electronic contribution to the specific heat. From Stoner (1936), the linear, low temperature, electronic heat coefficient γ is given by $\gamma=2{\cdot}835\times 10^{-4}\boldsymbol{R}N(E)_0$, where $\boldsymbol{R}$ is the universal gas constant and $N(E)_0$ is the density of states for one direction of spin at the Fermi limit. For a paramagnetic, one can assume zero magnetization at absolute zero so that the lowest states are completely filled by pairs of electrons of opposite spins. In the case of ferromagnetic nickel and cobalt, however, Wohlfarth (1949) has shown that there must be almost complete magnetization at very low temperatures. Thus, for nickel, 5 states per atom of one spin (+) are fully occupied and only 4·4 states per atom of the other spin (−), instead of 4·7 states of each spin. The only electrons which can take part in the specific heat process are those of (−) spin near the top of this unfilled band. The area under the curve of fig. 3 corresponds to 5 electronic states per atom so that the relevant value of $N(E)_0$ is given by the left-hand vertical line, the area to the right of which corresponds to 0·6 state per atom, i.e. this is the Fermi limit in the unfilled (−) spin band. The resulting value obtained for γ is $1{\cdot}6_9\times 10^{-3}$ cal mol^{-1} deg^{-2} as compared with an observed value of $1{\cdot}74\times 10^{-3}$, and one of $1{\cdot}1\times 10^{-3}$ deduced from Slater's $N(E)$ curve. A suitable value for comparison purposes would be somewhat lower than $1{\cdot}74\times 10^{-3}$, since this figure includes contributions from the s electrons and from d→s transitions (Wohlfarth 1948, 1949), possibly $1{\cdot}5\times 10^{-3}$. The very close agreement obtained here, however, must be regarded as somewhat fortuitous, owing to the approximations made and the fact that the Fermi limit occurs at a steeply sloping part of the $N(E)$ curve so that any error in its position would introduce a comparatively large error in γ.

It may also be noted, by comparison with I, that consideration of the previously neglected elements H_{nn} has brought the theoretical value of γ into closer agreement with experiment; these elements have been neglected in previous calculations of a similar nature to the present one (Jones and Mott 1937). A more interesting point, however, is that the 'ferromagnetic Fermi limit' now falls to

the left of the band peak. If this does in fact occur, then a number of theoretical calculations of other electronic properties, based on a parabolic variation of $N(E)$ with E at the Fermi limit, would appear to be in need of revision.

(*d*) As mentioned in §3 (*a*) a triple and a double degeneracy should occur between the wave functions at $\mathbf{k}=0$. This is confirmed in the present calculation with an energy separation between the two degenerate levels of 0·88 ev. In all applications of the cellular method, however, five-fold degeneracy is obtained at the centre of the Brillouin zone, a result due to the method of approximation.

(*e*) Returning to a general consideration of the $N(E)$ curve, Wohlfarth (1951) points out that the collective electron treatment of ferromagnetism was originally developed by Stoner (1938, 1939, 1948, 1951) for a 'parabolic' energy band, for which $N(E) \propto (E_M - E)^{1/2}$, where E_M is the upper energy limit of the band. Wohlfarth carries out similar calculations for a 'rectangular' energy band, for which $N(E)$ is constant, and shows that the observed values of several electronic properties of nickel lie between the values calculated for parabolic and rectangular bands. Use of a band form intermediate between these two might therefore be expected to yield results in good agreement with experiment. The present curve may therefore be of use as a basis for a new calculation of suitable electronic properties for nickel.

Another problem, to which the present work is related, is that of ferromagnetic anisotropy. The view has been put forward that this is due to spin–orbit coupling and Brooks (1940) has treated the problem theoretically on these lines, using 'tight-binding' wave functions and obtaining qualitative agreement with experiment for iron and nickel. In his treatment, however, the matrix elements H_{nm} ($n=1, 2, 3$; $m=4, 5$) are neglected (as in I), whereas it has been shown here that this approximation is not a valid one. It is possible, therefore, that the results obtained by Brooks would be considerably modified if these elements were taken into consideration.

ACKNOWLEDGMENTS

The author is indebted to Professor H. Jones and Dr. E. P. Wohlfarth for much helpful advice and assistance in this work, and also to London University for a postgraduate studentship.

REFERENCES

Bloch, F., 1928, *Z. Phys.*, **52**, 555.
Bouckaert, L. P., Smoluchowski, R., and Wigner, E. P., 1936, *Phys. Rev.*, **50**, 58.
Brooks, H., 1940, *Phys. Rev.*, **58**, 909.
Fletcher, G. C., and Wohlfarth, E. P., 1951, *Phil. Mag.*, **42**, 106.
Hartree, D. R., and Hartree, W., 1936, *Proc. Roy. Soc.* A, **157**, 490.
Herring, C., 1937, *Phys. Rev.*, **52**, 361.
Jones, H., and Mott, N. F., 1937, *Proc. Roy. Soc.* A, **162**, 49.
Krutter, H. M., 1935, *Phys. Rev.*, **48**, 664.
Mott, N. F., 1936 a, *Proc. Roy. Soc.* A, **153**, 699 ; 1936 b, *Proc. Roy. Soc.* A, **156**, 368.
Mott, N. F., and Jones, H., 1936, *Properties of Metals and Alloys* (Oxford : Clarendon Press).
Slater, J. C., 1936, *Phys. Rev.*, **49**, 537 and 931 ;
Stoner, E. C., 1936, *Phil. Mag.*, **21**, 145 ; 1938, *Proc. Roy. Soc.* A, **165**, 372 ; 1939, *Ibid.*, **169**, 339 ; 1948, *Rep. Prog. Phys.*, **11**, 43 (London : Physical Society) ; 1951, *J. Phys. Radium*, **12**, 372.
Wohlfarth, E. P., 1948, *Proc. Leeds Phil. Lit. Soc.*, **5**, 89 ; 1949, *Proc. Roy. Soc.* A, **195**, 434 ; 1951, *Phil. Mag.*, **52**, 374.

A Determination of the Rate of Emission of Spontaneous Fission Neutrons by Natural Uranium

By D. J. LITTLER

Atomic Energy Research Establishment Harwell, Didcot, Berks.

MS. received 4th October 1951

ABSTRACT. By comparison with a calibrated neutron source, the total rate of emission of primary neutrons in the Graphite Low Energy Experimental Pile has been found. The rate of emission of spontaneous fission neutrons from natural uranium is computed to be $59{\cdot}5 \pm 3{\cdot}3$ neutrons/g/hr of uranium.

§1. INTRODUCTION

In the experiment described here, a calibrated Ra–Be neutron source was used to determine the total rate of emission of primary neutrons in the Graphite Low Energy Experimental Pile at Harwell (the G.L.E.E.P.). From a knowledge of the total amount of uranium in the G.L.E.E.P. the rate of emission of spontaneous fission neutrons from natural uranium was computed.

The G.L.E.E.P. was made sub-critical by about 0·1% (reproduction constant 0·999) by inserting the control rods into the pile beyond the balance position. The neutron counting rate recorded by a boron trifluoride proportional counter, which was located near the boundary of the pile, was observed as a function of the position of a calibrated Ra–Be neutron source along the pile axis.

It may be shown, see Appendix, that if C_1 is the counting rate recorded by the counter with the source in the pile and C_0 is the counting rate recorded with the source out of the pile

$$\frac{C_1}{C_0} = \frac{1+(S/\Sigma)(\rho_s/\bar{\rho})}{1+\alpha\rho_s^2/p\Sigma\bar{\rho}}, \qquad \ldots\ldots(1)$$

where S is the neutron strength of the Ra–Be source, Σ is the total rate of emission of primary neutrons by the pile, p is the probability that a fast neutron will escape resonance capture in the pile, α is a constant proportional to the thermal neutron absorption cross section of the neutron source, $\bar{\rho}$ is the average neutron density in the pile before the source is introduced, and ρ_s is the neutron density at the source position before the source is introduced.

If an absorber which has the same effective thermal neutron absorption cross section as the Ra–Be source be introduced, the observed counting rate will be C_2, where

$$\frac{C_2}{C_0} = \frac{1}{1+\alpha\rho_s^2/p\Sigma\bar{\rho}}. \qquad \ldots\ldots(2)$$

Thus from (1) and (2)

$$\frac{C_1-C_2}{C_2} = \frac{S}{\Sigma}\frac{\rho_s}{\bar{\rho}}. \qquad \ldots\ldots(3)$$

The experiment consisted in observing C_1 and C_2 for various values of $\rho_s/\bar{\rho}$. $(C_1-C_2)/C_2$ was then plotted as a function of $\rho_s/\bar{\rho}$, and the slope of the line obtained gave S/Σ. Since S was known absolutely, the absolute value of Σ could be obtained.

It should be noted that in the derivation of the foregoing formulae (see Appendix) it is assumed that the neutron density distribution is the same with the Ra–Be source present as with it absent. This assumption is true provided that the pile is close to criticality.

On the other hand, the closer the pile is brought to criticality, the larger becomes the value of $\alpha\rho_s^2/p\Sigma\bar{\rho}$ in the denominator of eqn. (1). This means that, with the pile very close to criticality, the effect of absorption of neutrons by the source tends to become of more importance than the emission of neutrons by it.

A compromise between these two conflicting requirements had to be made. An analysis more detailed than that given in the Appendix was made, and showed that, provided the reproduction constant of the pile were closer to unity than 0·1%, the neutron density distribution in the pile would be the same as for a critical pile, both with the source present and with it absent.

The pile was therefore made sub-critical by 0·1% for the experiment. The experimental results obtained showed that, with this setting, the effect of absorption by the source was small compared with the effect of emission by the source. That is, the variations in C_2 due to changing the absorber position were very much less than the variations in C_1 due to changing the source position.

§ 2. EXPERIMENTAL PROCEDURE AND RESULTS

The boron trifluoride counter used was 3 in. in diameter and 12 in. long, and contained BF_3 gas at a pressure of 6 cm Hg and argon at a pressure of 6 cm Hg. It was located near the boundary of the pile core and reflector in order to obtain a suitable counting rate. The electronic equipment used with the counter was of a standard pattern and consisted of a linear amplifier, a discriminator and two scalers in cascade. With the discriminator setting used, no counts were obtained when the high tension supply was disconnected from the counter. There was a small dead time (16 μsec) in the electronic equipment, and all counting results were corrected for this.

The Ra–Be source used was the one described by Littler (1951); it had a neutron strength of $9{\cdot}7\times10^6(\pm4\frac{1}{2}\%)$ n/sec. The effective thermal neutron absorption cross section of this source was also known from the source calibration experiment (this was obtained by running the G.L.E.E.P. at high power and then modulating the power by oscillating the source through the pile).

The absorber used was a brass cylinder. This had been shown by modulation experiments to have the same effective thermal neutron absorption cross section as the Ra–Be source.

The G.L.E.E.P. was shut down for several hours before the experiment was started. This ensured that there would be no contribution to the primary sources in the pile from delayed neutron emitters, as a result of previous high power running.

The neutron density distribution in the G.L.E.E.P. had been previously measured by the use of indium foils (Colmer and Littler 1951). From these measurements the values of $\rho_s/\bar{\rho}$ for each source position used were computed. The source was placed at standard positions along the axis of the pile, these positions being at intervals of two pile pitches (one pitch is $7\frac{1}{4}$ in.). Source positions near the core-reflector boundary were not used, since the theory of the method assumes a bare pile, and the results would be erroneous if the source

were nearer to the boundary than two migration lengths (~ 50 cm). After changing the source position (or the position of the brass absorber) no counting was done for fifteen minutes. This allowed the neutron density to reach a new steady state for each measurement.

The results obtained are shown in the figure. The statistical accuracy of the counting rate ratios is within the order of 1%, and the accuracy of the values of $\rho_s/\bar{\rho}$ is within the order of 3%.

The slope of the straight line in the figure was determined by the method of least squares and was found to be 16·9. Since $S = 9{\cdot}7 \times 10^6$ n/sec, we may deduce the value of Σ, the total primary neutron strength of the pile: $\Sigma = 5{\cdot}73 \times 10^5$ n/sec ($\pm 5\frac{1}{2}$%).

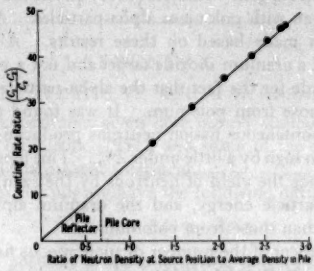
Counting Rate Ratio $\frac{(S+S_0)}{S_0}$
Pile Reflector
Pile Core
Ratio of Neutron Density at Source Position to Average Density in Pile

The G.L.E.E.P. became divergent in August 1947, and it then contained 12 tons of uranium metal and 21 tons of uranium dioxide (Colmer and Littler 1951). Since that time it has had more uranium added to it, to give it an excess reproduction constant of 0·2%, and it now contains $3{\cdot}462 \times 10^4$ kg of uranium element.

Thus, assuming that all the primary neutrons in the pile are produced by the spontaneous fission of uranium, the spontaneous fission neutron strength is $16{\cdot}5 \pm 0{\cdot}9$ n/kg/sec, or $59{\cdot}5 \pm 3{\cdot}3$ n/g/hr.

§3. DISCUSSION OF RESULTS

The figure quoted in the previous section for the number of spontaneous fission neutrons emitted per hour per gramme of uranium will be in error if there are other sources of primary neutrons in the G.L.E.E.P. Two other possible sources of primary neutrons are those produced by cosmic rays and those produced by (α, n) reactions.

The rate of production of neutrons in the atmosphere by cosmic rays is too small to have any effect on the figure quoted in the last section. (Apart from the low rate of production of neutrons, only a small fraction of those produced can enter the pile because it is surrounded by a thick concrete shield.) An order of magnitude calculation on the production of neutrons from uranium by the capture of negative μ-mesons has been made. It was assumed that the stopping power of uranium for μ-mesons is the same as that of lead, and for the latter the value quoted by Koenig (1946) was used, that at sea level the flux of μ-mesons is one per cm^2 per minute (Rossi 1948), and that two neutrons are

produced per μ-meson stopped. It was found that the neutron production from uranium by the capture of μ-mesons was much less than 0·1% of the production from spontaneous fission.

It has been assumed that there is only a very small production of neutrons by the stopping of μ-mesons in graphite. This assumption is based on the experiments of Conversi, Pancini and Piccioni (1947), who showed that nearly all μ-mesons stopped in graphite undergo decay and do not interact with the carbon nucleus.

The rate of production of neutrons by (α, n) reactions in the uranium metal in the G.L.E.E.P. should be very small as the metal is of high purity. In the uranium dioxide core of the pile there may be a contribution to the primary rate by (α, n) reactions with oxygen. Roberts (1947) quotes the neutron yield obtained by bombarding oxygen with polonium alpha-particles. An order of magnitude calculation has been made based on these results. Allowance was made for the fact that we have a uranium dioxide target and not a pure oxygen target, but no allowance was made for the fact that the alpha-particles from uranium are of lower energy than those from polonium. It was found that the figure quoted for the number of spontaneous fission neutrons produced per hour per gramme of uranium may be too high by a little under 2%. This figure represents an upper limit to the error, since the yield of neutrons by the (α, n) reaction may change rapidly with alpha-particle energy, and the uranium alpha-particles are about 1 MeV less energetic than those from polonium.

An early measurement of the number of spontaneous fission neutrons emitted by uranium was made by Rotblat (1941). He obtained a value of 53 ± 10 n/g/hr, which is in agreement with the value quoted in this paper. Other measurements of the number of spontaneous fission neutrons produced per hour per gramme of uranium have been made by Scharff-Goldhaber and Klaiber (1946) and Pose (1943). Scharff-Goldhaber and Klaiber quote a partial decay constant for uranium of 7×10^{-24} sec^{-1} on the assumption that only one neutron is emitted per spontaneous fission. This figure leads to a value of 64 n/g/hr emitted from uranium. Pose quotes a partial half-life for the decay of uranium by spontaneous fission, from which a value of 65 n/g/hr emitted from uranium may be deduced. These authors do not quote the accuracy of their determinations, but there must be some uncertainty in Pose's value, since he assumes a figure for the calibration of a neutron source.

Whitehouse and Galbraith (1950) quote a value for the spontaneous fission rate in natural uranium of $24{\cdot}2 \pm 1{\cdot}5$ fissions/g/hr. If we combine their value with the value quoted in this paper for the rate of production of neutrons from spontaneous fission we have, for the number of neutrons per fission, $\nu = 59{\cdot}5/24{\cdot}2 = 2{\cdot}5 \pm 0{\cdot}2$ n/fission.

It is of interest to note that this value for the number of neutrons per spontaneous fission in natural uranium is the same as the value for the number of neutrons per thermal neutron induced fission in natural uranium, namely $2{\cdot}5 \pm 0{\cdot}1$ n/fission (Atomics 1951).

ACKNOWLEDGMENTS

This work is published by permission of the Director of the Atomic Energy Research Establishment. The author wishes to express his thanks to Mr. E. E. Lockett, who measured the neutron density distributions in the G.L.E.E.P.

REFERENCES

ATOMICS, 1951, **2**, No. 1, 15.
COLMER, F. C. W., and LITTLER, D. J., 1951, *Nucleonics*, **8**, 3.
CONVERSI, M., PANCINI, E., and PICCIONI, O., 1947, *Phys. Rev.*, **71**, 209.
KOENIG, H. P., 1946, *Phys. Rev.*, **69**, 590.
LITTLER, D. J., 1951, *Proc. Phys. Soc.* A, **64**, 638.
POSE, H., 1943, *Z. Phys.*, **121**, 293.
ROBERTS, J. H., 1947, *Manhattan District Declassification Committee Report*, No. 731.
ROSSI, B., 1948, *Rev. Mod. Phys.*, **20**, 537.
ROTBLAT, J., 1941, *British Report* 241.
SCHARFF-GOLDHABER, G., and KLAIBER, G. S., 1946, *Phys. Rev.*, **70**, 229.
WALLACE, P. R., and LECAINE, J., 1946, *National Research Council of Canada Report*, No. M.T. 12.
WHITEHOUSE, W. J., and GALBRAITH, W., 1950, *Phil. Mag.*, **61**, 429.

APPENDIX

THEORY OF THE EXPERIMENT USING A ONE-GROUP MODEL

The theory of the experiment given here is very similar to the three-group diffusion theory given by Littler (1951), and some of the results of this latter analysis are assumed in the present treatment.

For a steady state in the pile we have the following diffusion equation:

$$D\nabla^2\rho-\rho/\tau+ps=-k\rho/\tau, \qquad \ldots\ldots(A\,1)$$

where ρ, a function of position in the pile, is the density of thermal neutrons, k is the reproduction constant for the pile, p is the probability that a fast neutron will escape resonance capture in ^{238}U, s is the rate of production of primary fast neutrons per unit volume, and D and τ are the diffusion coefficient and mean lifetime of the neutrons.

We assume that there is a small cavity in the pile, and that initially it is empty. Equation (A 1) then describes the state of affairs everywhere in the pile except in the cavity itself.

We now suppose that a neutron source is introduced into the cavity, and that the pile can again be in a steady state with ρ changed to ρ_1 and k changed to k_1. We have, therefore,

$$D\nabla^2\rho_1-\rho_1/\tau+ps=-k_1\rho_1/\tau. \qquad \ldots\ldots(A\,2)$$

If we now apply Green's theorem in the same way as in the three-group treatment, and assume that the pile is bare, so that ρ and ρ_1 will both be zero at the outer boundary of the pile, we have

$$\rho_c(T-pS)+ps\int(\rho_1-\rho)\,dV+\frac{k-k_1}{\tau}\int\rho\rho_1\,dV=0, \qquad \ldots\ldots(A\,3)$$

where ρ_c is the value of the neutron density at the cavity, T is the rate of absorption of thermal neutrons by the neutron source, S is the strength of the neutron source, and the volume integrals extend over the whole pile. If the reproduction constant is not changed, then $k=k_1$, and hence,

$$\rho_c(T-pS)+psV(\bar{\rho}_1-\bar{\rho})=0, \qquad \ldots\ldots(A\,4)$$

where $\bar{\rho}$ and $\bar{\rho}_1$ are the average neutron densities in the pile, and V is the volume of the pile.

If we write $T=\alpha\rho_{1c}$ (where α is a constant proportional to the absorption cross section of the neutron source) and $sV=\Sigma$, the total primary source strength in the pile, then we have

$$\rho_c(\alpha\rho_{1c}-pS)+p\Sigma(\bar{\rho}_1-\bar{\rho})=0. \qquad \ldots\ldots(A5)$$

If we suppose that the neutron density distribution in the pile is the same when the neutron source is present as when it is absent, we may write

$$\frac{\rho_{1c}}{\rho_c}=\frac{\bar{\rho}_1}{\bar{\rho}}=\frac{C_1}{C_0}, \qquad \ldots\ldots(A6)$$

where C_0 and C_1 are the counting rates obtained with a neutron counter in a given position in the pile, before and after introducing the neutron source.

The assumption that the neutron density distribution is not altered by inserting a neutron source into a sub-critical pile is only justified provided that the pile is very close to criticality (Wallace and LeCaine 1946). However, calculations of the change in the density distribution with the pile initially sub-critical by 0·1% showed that no serious error is incurred by making the assumption in this case. Furthermore, the calculations show that the density distribution with the pile sub-critical by 0·1% may be taken to be the same as with the pile critical, without introducing any serious error.

Using (A 5) and (A 6), we have, finally,

$$\frac{C_1}{C_0}=\frac{1+(S/\Sigma)(\rho_c/\bar{\rho})}{1+\alpha\rho_c^2/p\Sigma\bar{\rho}}. \qquad \ldots\ldots(A7)$$

In deriving this formula we have assumed that the G.L.E.E.P. has a uniform core. This is not so, since in the G.L.E.E.P. there are two regions, one containing uranium dioxide and one containing uranium metal. The problem should therefore have been solved as a two-core problem. A separate calculation has been carried out using a one-group two-core model. It was shown that, provided that ps is the same in the two cores, the result is identical with (A 7). However, s is not quite the same in the two cores since the amount of uranium element in a dioxide channel is not quite the same as the amount of uranium in a metal channel; also the values of the resonance escape probability differ by a few per cent in the two cores. Even in this case, however, the calculations showed that eqn. (A 7) is correct to well within 1%.

One other point is worthy of mention. If in eqn. (A 3) we take $\rho=\rho_1$ over the whole pile, we have, for the change in reproduction constant on inserting a neutron source into the pile,

$$k-k_1=\frac{\tau\rho_c(pS-T)}{\int\rho^2\,dV}.$$

This result is the one-group equivalent of that obtained by Littler (1951). It should be noted that it is independent of s, i.e. independent of the strength of primary sources in the pile.

Matrix Elements and Operator Equivalents Connected with the Magnetic Properties of Rare Earth Ions

By K. W. H. STEVENS
The Clarendon Laboratory, Oxford

Communicated by B. Bleaney ; MS. received 16th August 1951

ABSTRACT. An account is given of the methods used to determine the matrix elements of crystal field potentials with particular reference to rare earth ions. Emphasis is laid on the importance of Wigner coefficients in such problems and the idea of using equivalent angular momentum operators is developed. For convenience in applying the results tables of matrix elements are included.

§ 1. INTRODUCTION

In the course of some recent work on rare earth ions in crystals it has been necessary to evaluate the matrix elements of certain potential functions in representations in which the states are eigen states of the total angular momentum. Somewhat similar problems arise in connection with the magnetic properties of iron group ions in crystals, with the difference that the usual representations are then those in which the states are eigen states of the total orbital angular momentum and it is not necessary to include spin variables. In the case of rare earth ions the perturbations due to the crystal fields are usually small compared with the spin–orbit couplings, whereas in the iron group the inequality is reversed. This difference means that the evaluation of the relevant rare earth matrix elements is generally more complicated than is the case for iron group ions. It is the purpose of the paper to give an account of a method for obtaining their values in terms of one-electron radial integrals.

§ 2. PERTURBATIONS AND STATES

The potential functions which have been considered in detail are:

$$V_2^0 = \Sigma(3z^2 - r^2)$$
$$V_4^0 = \Sigma(35z^4 - 30r^2z^2 + 3r^4)$$
$$V_6^0 = \Sigma(231z^6 - 315r^2z^4 + 105r^4z^2 - 5r^6)$$
$$V_6^6 = \Sigma(x^6 - 15x^4y^2 + 15x^2y^4 - y^6)$$

where the summations are taken over the coordinates of all electrons. It will be noticed that each V can be written in the form $f(r)P_n^m(\theta, \phi)$ and thus transforms under rotation according to an irreducible representation of the rotation group. This property is extremely useful in determining matrix elements; as a first application it follows that the matrix elements of V_6^6 can be obtained from those of V_6^0 purely by symmetry arguments. Alternatively, once the matrix elements of V_2^0, V_4^0 and V_6^0 are known, the matrix elements of all even potentials up to the sixth degree can be found from symmetry. This will be discussed more fully later in the paper.

The states considered are formed by taking linear combinations of determinantal product states of 4f one-electron states. The rare earth ions show

Russell–Saunders coupling so the product states are first combined to form states for which **L** and **S** are constants and these are then combined to form states for which **J** is constant. The final states can be conveniently written as $|4f^n;\ \mathbf{LSJ}J_z\rangle$ where n denotes the number of electrons not in closed shells. The evaluation of the matrix elements of the potentials would be quite straightforward if the expressions of all states such as $|4f^n;\ \mathbf{LSJ}J_z\rangle$ in terms of basic products states were known. This, however, is not usually the case and rather than go through the tedious process of obtaining them it is more profitable to determine the matrix elements by methods which do not require this information.

§ 3. OPERATOR EQUIVALENTS

The methods used depend largely on the result that within a manifold of states for which **J** is constant there are simple relations between the matrix elements of potential operators and appropriate angular momentum operators. For example, inside **J** = constant,

$$\Sigma xy \equiv \alpha[J_xJ_y+J_yJ_x]$$

$$\Sigma(35z^4-30r^2z^2+3r^4) \equiv \beta[35J_z^4-30J(J+1)J_z^2+25J_z^2-6J(J+1)+3J^2(J+1)^2],$$

where α and β are numerical factors. That such operator equivalents hold can be verified by using the Wigner coefficients to give the values of the matrix elements of the potential functions. The Wigner coefficients are given (van der Waarden 1932) by:

$$c^J_{m,m'} = \Sigma_\nu \frac{(-1)^\nu[(j+m)!(j-m)!(j'+m')!(j'-m')!(J+M)!(J-M)!]^{1/2}}{(j-m-\nu)!(j+m-\lambda-\nu)!(j'+m'-\nu)!(j'-m'-\lambda+\nu)!\nu!(\lambda-\nu)!}$$

with $M=m+m'$ and $J=j+j'-\lambda$ ($\lambda=0,1,2,\ldots.$), using van der Waarden's notation. The element $\langle J,J_z|V_4^0|J,J_z\rangle$ is obtained, apart from the factor α from $c^J_{m,m'}$ with $j=J$, $m=J_z$, $j'=4$, $m'=0$ and $\lambda=4$, since V_4^0 can be regarded as a component of a vector in a D_4 space having $m'=0$. This method can be used to check the equivalents once they are obtained, but it does not provide a very good method for determining them. The Wigner coefficients will give the matrix elements, apart from the factor, but it is not always easy to pass from these to an angular momentum operator with the same elements. The following method is, however, available.

Each potential transforms under rotation according to an irreducible representation of the rotation group. For an operator equivalence to hold, the equivalent must transform in exactly the same way, and it is a matter of determining an angular momentum expression which has this property. There is no difficulty in doing this provided allowance is made for the non-commutation of J_x, J_y and J_z. For example, the two sets of functions x^2-y^2, $3z^2-r^2$, xy, yz, zx and $J_x^2-J_y^2$, $3J_z^2-J(J+1)$, $\frac{1}{2}(J_xJ_y+J_yJ_x)$, $\frac{1}{2}(J_yJ_z+J_zJ_y)$, $\frac{1}{2}(J_zJ_x+J_xJ_z)$ each transform according to D_2 and it is clear that they give the same transformation matrices. Thus $x^2-y^2 \equiv \alpha(J_x^2-J_y^2)$, $xy \equiv \frac{1}{2}\alpha(J_xJ_y+J_yJ_x)$ etc., within a manifold for which **J** is constant. This process is readily adapted to more complicated expressions. Suppose an operator equivalent to $x^4-6x^2y^2+y^4$ is required. This can be written as $\frac{1}{2}[(x+iy)^4+(x-iy)^4]$ and the equivalent operator is $\frac{1}{2}\alpha[(J_x+iJ_y)^4+(J_x-iJ_y)^4]$. On the other hand, the operator equivalent to $35z^4-30r^2z^2+3r^4$ is not $\alpha[35J_z^4-30J_z^2J(J+1)+3J^2(J+1)^2]$ since, for example, it is not correct to replace x^2z^2 (which occurs in r^2z^2) by $J_x^2J_z^2$. It should be

replaced by an expression consisting of all possible different combinations of J_x, J_y, J_z and J_z. Some equivalences are given in table 1.

Table 1

Operator Equivalents inside a Manifold for which **J** is Constant

$$\Sigma(3z^2-r^2) \equiv \alpha\overline{r^2}\,[3J_z^2-J(J+1)]$$

$$\Sigma(35z^4-30r^2z^2+3r^4) \equiv \beta\overline{r^4}[35J_z^4-30J(J+1)J_z^2+25J_z^2-6J(J+1)+3J^2(J+1)^2]$$

$$\Sigma(231z^6-315r^2z^4+105r^4z^2-5r^6) \equiv \gamma\overline{r^6}\left[\begin{array}{l} 231J_z^6-315J(J+1)J_z^4+735J_z^4+105J^2(J+1)^2J_z^2 \\ -525J(J+1)J_z^2+294J_z^2-5J^3(J+1)^3+40J^2(J+1)^2-60J(J+1)\end{array}\right]$$

Values of α, β and γ for Ground States of Rare Earth Ions

Ion	α	β	γ
$Ce^{+++}4f^1\ ^2F_{5/2}$	$-2/35$	$2/7.45$	0
$Pr^{+++}4f^2\ ^3H_4$	$-52/11.15^2$	$-4/55.33.3$	$17.16/7.11^2.13.5.3^4$
$Nd^{+++}4f^3\ ^4I_{9/2}$	$-7/33.33$	$-8.17/11.11.13.297$	$-17.19.5/13^2.11^2.3^2.7$
$Pm^{+++}4f^4\ ^5I_4$	$14/11.11.15$	$952/13.3^2.11^2.5$	$2584/11^2.13^2.3.63$
$Sm^{+++}4f^5\ ^6H_{5/2}$	$13/7.45$	$26/33.7.45$	0
$Eu^{+++}4f^6\ ^7F_0$	0	0	0
$Gd^{+++}4f^7\ ^8S$	0	0	0
$Tb^{+++}4f^8\ ^7F_6$	$-1/99$	$2/11.1485$	$-1/13.33.2079$
$Dy^{+++}4f^9\ ^6H_{15/2}$	$-2/9.35$	$-8/11.45.273$	$4/11^2.13^2.3^2.7$
$Ho^{+++}4f^{10}\ ^5I_8$	$-1/30.15$	$-1/11.2730$	$-5/13.33.9009$
$Er^{+++}4f^{11}\ ^4I_{15/2}$	$4/45.35$	$2/11.15.273$	$8/13^2.11^2.3^2.7$
$Tu^{+++}4f^{12}\ ^3H_6$	$1/99$	$8/3.11.1485$	$-5/13.33.2079$
$Yb^{+++}4f^{13}\ ^2F_{7/2}$	$2/63$	$-2/77.15$	$4/13.33.63$

For a single 4f electron, $\alpha=-2/45$, $\beta=2/45.11$, $\gamma=-4/9.13.33$.

§ 4. MULTIPLYING FACTORS

There then remains the problem of finding the multiplying factors. This is done by using the fact that the potential functions do not show any dependence on the spin, so that similar operator equivalents hold inside manifolds in which **L** is constant. A convenient state in **L**, **S**, **J**, J_z quantization is chosen and expressed in **L**, **S**, L_z, S_z quantization and an equation obtained by equating the two expectation values of the function. Another state in **L**, **S**, L_z, S_z quantization is then chosen and expressed in one electron product states and again expectation values are equated. In this way sufficient relations are obtained to determine the factors in terms of radial integrals over 4f wave functions. The technique for doing this is best demonstrated by means of an example.

The ground term of Sm^{+++} is $4f^5$; $^6H_{5/2}$ and the problem of finding the matrix elements of $V_4^0=\Sigma(35z^4-30r^2z^2+3r^4)$ inside the manifold of states spanning $\mathbf{J}=\frac{5}{2}$ is considered. From the operator equivalence it follows that the matrix elements of V_4^0 are equal to those of

$$\alpha[35J_z^4-30.\tfrac{5}{2}.\tfrac{7}{2}J_z^2+25J_z^2-6.\tfrac{5}{2}.\tfrac{7}{2}+3.(\tfrac{5}{2})^2.(\tfrac{7}{2})^2].$$

The most general expression for $|\mathbf{L}=5, \mathbf{S}=\frac{5}{2}, \mathbf{J}=\frac{5}{2}, J_z=\frac{5}{2}\rangle$ in **L**, **S**, L_z, S_z quantization is:

$$|\mathbf{J}=\tfrac{5}{2}, J_z=\tfrac{5}{2}\rangle \equiv a|L_z=5, S_z=-\tfrac{5}{2}\rangle+b|L_z=4, S_z=-\tfrac{3}{2}\rangle+c|3,-\tfrac{1}{2}\rangle$$
$$+d|2,\tfrac{1}{2}\rangle+e|1,\tfrac{3}{2}\rangle+f|0,\tfrac{5}{2}\rangle, \qquad \ldots\ldots(1)$$

where $a^2+b^2+c^2+d^2+e^2+f^2=1$ and all states have $\mathbf{L}=5$ and $\mathbf{S}=\frac{5}{2}$. Thus, using table 3, and noting that column F gives multiplying factors (see remark near end of paper)

$$\begin{aligned}60\alpha &= \langle \mathbf{J}=\tfrac{5}{2}, J_z=\tfrac{5}{2}|V_4^0|\mathbf{J}=\tfrac{5}{2}, J_z=\tfrac{5}{2}\rangle \\ &= a^2\langle L_z=5, S_z=-\tfrac{5}{2}|V_4^0|L_z=5, S_z=\tfrac{5}{2}\rangle + b^2\langle 4,-\tfrac{3}{2}|V_4^0|4,-\tfrac{3}{2}\rangle + \ldots. \\ &= a^2\langle 5|V_4^0|5\rangle + b^2\langle 4|V_4^0|4\rangle + \ldots. + f^2\langle 0|V_4^0|0\rangle,\end{aligned}$$

where, in the last line, the value of S_z has been omitted since V_4^0 does not contain spin variables. Inside a manifold for which $\mathbf{L}=5$

$$V_4^0 \equiv \beta[35L_z^4-30.5.6L_z^2+25L_z^2-6.5.6+3.(5)^2.(6)^2]$$

so that $60\alpha = 420\beta[6a^2-6b^2-6c^2-d^2+4e^2+6f^2]$ using values from table 3 appropriate to $\mathbf{L}=5$. The state $|L_z=5, S_z=\frac{5}{2}\rangle$ is equivalent to $\{\overset{+}{3}\overset{+}{2}\overset{+}{1}\overset{+}{0}\overset{+}{-1}\}$ using the usual notation for determinantal product states. Hence

$$\begin{aligned}\langle 5,\tfrac{5}{2}|V_4^0|5,\tfrac{5}{2}\rangle &= 2520\beta = \{\overset{+}{3}\overset{+}{2}\overset{+}{1}\overset{+}{0}\overset{+}{-1}\}V_4^0\{\overset{+}{3}\overset{+}{2}\overset{+}{1}\overset{+}{0}\overset{+}{-1}\} \\ &= \gamma[180-420+60+360+60] = 240\gamma\end{aligned}$$

since inside a manifold for which $\mathbf{l}=3$ (f-electrons)

$$35z^4-30r^2z^2+3r^4 = \gamma[35l_z^4-30.3.4.l_z^2+25l_z^2-6.3.4+3.(3)^2.(4)^2].$$

Also $\gamma.180 = \langle \mathbf{l}=3, l_z=3|35z^4-30r^2z^2+3r^4|\mathbf{l}=3, l_z=3\rangle = \frac{8}{11}\overline{r^4}$ where the wave function (not normalized) corresponding to $|\mathbf{l}=3, l_z=3\rangle$ is $f(r)P_3^3(\cos\theta)\exp 3i\phi$.

Thus $$\beta = \frac{240}{2520}\gamma = \frac{240.8}{2520.11.180}\overline{r^4} = \frac{4}{21.45.11}\overline{r^4}.$$

There remains the problem of determining the coefficients $a, b, c\ldots$ etc. in (1). A convenient way of doing this is to operate on both sides of (1) with $2\mathbf{L}.\mathbf{S}$. This operator has the property of commuting with $\mathbf{J}$ and inside a manifold in which $\mathbf{L}$, $\mathbf{S}$ and $\mathbf{J}$ are constant it is equivalent to $[J(J+1)-S(S+1)-L(L+1)]$. In the present case $2\mathbf{L}.\mathbf{S}=-30$. Then, for example,

$$\begin{aligned}-30a &= \langle L_z=5, S_z=-\tfrac{5}{2}|-30|\{a|5,-\tfrac{5}{2}\rangle + b|4,-\tfrac{3}{2}\rangle + \ldots\} \\ &= \langle L_z=5, S_z=-\tfrac{5}{2}|2\mathbf{L}.\mathbf{S}|\{a|5,-\tfrac{5}{2}\rangle + b|4,-\tfrac{3}{2}\rangle + \ldots\} \\ &= -25a+\sqrt{50}b.\end{aligned}$$

Enough equations can be obtained in this way to determine $a, b, c\ldots$ etc., the final values being

$$a=\left(\frac{6}{11}\right)^{1/2},\quad b=-\left(\frac{3}{11}\right)^{1/2},\quad c=\left(\frac{4}{33}\right)^{1/2},\quad d=-\left(\frac{1}{22}\right)^{1/2},\quad e=\left(\frac{1}{77}\right)^{1/2},\quad f=\left(\frac{1}{6.77}\right)^{1/2}.$$

These values give

$$60\alpha = \frac{4}{21.45.11}\overline{r^4}.420\left[6.\frac{6}{11}-6.\frac{3}{11}-6.\frac{4}{33}-\frac{1}{22}+4.\frac{1}{77}+6.\frac{1}{6.77}\right]$$

or $$\alpha = \frac{26}{45.33.7}\overline{r^4}.$$

In this way the matrix elements of V_4^0 inside $\mathbf{J}=\frac{5}{2}$ for Sm^{+++} can be obtained in terms of the average of r^4 over the radial part of the 4f wave function. A similar procedure is clearly available for V_2^0 and V_6^0.

At this point it is convenient to make several general remarks. In the example, the passage from L_z, S_z quantization to l_z, s_z quantization by

$$|L_z=5, S_z=\tfrac{5}{2}\rangle \equiv \{\overset{+}{3}\overset{+}{2}\overset{+}{1}\overset{+}{0}\overset{+}{-1}\},$$

is readily made because the determinantal state is the only state for which $L_z=5$, $S_z=\frac{5}{2}$. It is a property of the ground multiplets of all ions obeying Hund's

Table 2

Values of $3J_z^2-J(J+1)$

$J_z=$	J	F	$\pm 1/2$	$\pm 3/2$	$\pm 5/2$	$\pm 7/2$	$\pm 9/2$	$\pm 11/2$	$\pm 13/2$	$\pm 15/2$
1/2	0	0	0							
3/2	3	−1	1							
5/2	2	−4	−1	5						
7/2	3	−5	−3	1	7					
9/2	6	−4	−3	−1	2	6				
11/2	1	−35	−29	−17	1	25	45			
13/2	6	−8	−7	−5	−2	2	7	13		
15/2	3	−21	−19	−15	−9	−1	9	21	35	

$J_z=$	J	F	0	± 1	± 2	± 3	± 4	± 5	± 6	± 7	± 8
0	0	0	0								
1	1	−2	1								
2	3	−2	−1	2							
3	3	−4	−3	0	5						
4	1	−20	−17	−8	7	28					
5	3	−10	−9	−6	−1	6	15				
6	3	−14	−13	−10	−5	2	11	22			
7	1	−56	−53	−44	−29	−8	19	52	91		
8	3	−24	−23	−20	−15	−8	1	12	25	40	

Table 3

Values of $35J_z^4-30J(J+1)J_z^2+25J_z^2-6J(J+1)+3J^2(J+1)^2$

$J_z=$	J	F	$\pm 1/2$	$\pm 3/2$	$\pm 5/2$	$\pm 7/2$	$\pm 9/2$	$\pm 11/2$	$\pm 13/2$	$\pm 15/2$
1/2	0	0	0							
3/2	0	0	0	0						
5/2	60	2	−3	1						
7/2	60	9	−3	−13	7					
9/2	84	18	3	−17	−22	18				
11/2	120	28	12	−13	−33	−27	33			
13/2	60	108	63	−13	−92	−132	−77	143		
15/2	60	189	129	23	−101	−201	−221	−91	273	

$J_z=$	J	F	0	1	2	3	4	5	6	7	8
0	0	0	0								
1	0	0	0	0							
2	12	6	−4	1							
3	60	6	1	−7	3						
4	60	18	9	−11	−21	14					
5	420	6	4	−1	−6	−6	6				
6	60	84	64	11	−54	−96	−66	99			
7	12	756	621	251	−249	−704	−869	−429	1001		
8	420	36	31	17	−3	−24	−39	−39	−13	52	

rule that such a relation holds, for the rule states that the ground multiplets have maximum **S** and maximum **L**. The state with maximum S_z and L_z is then always particularly simple in l_z, s_z quantization. In the case where no such obvious relation exists, such as for excited states, the passage from L_z, S_z to l_z, s_z quantization is more difficult and is somewhat analogous to the passage from J_z to L_z, S_z already considered. It is suggested that the operator $\Sigma \mathbf{l}_i.\mathbf{l}_j$ could be used for this in a process similar to that in which **L**.**S** was used.

Table 4

Values of $231J_z^6-315J(J+1)J_z^4+735J_z^4+105J^2(J+1)^2J_z^2-525J(J+1)J_z^2+294J_z^2-5J^3(J+1)^3+40J^2(J+1)^2-60J(J+1)$

	J	F									
$J_z=$			$\pm 1/2$	$\pm 3/2$	$\pm 5/2$	$\pm 7/2$	$\pm 9/2$	$\pm 11/2$	$\pm 13/2$	$\pm 15/2$	
	1/2	0	0								
	3/2	0	0	0							
	5/2	0	0	0	0						
	7/2	1260	− 5	9	− 5	1					
	9/2	5040	− 8	6	10	− 11	3				
	11/2	7560	− 20	4	25	11	−31	11			
	13/2	2160	−200	−25	185	227	−11	−319	143		
	15/2	13860	− 75	−25	45	87	59	− 39	−117	65	

	J	F									
$J_z=$			0	1	2	3	4	5	6	7	8
	0	0	0								
	1	0	0	0							
	2	0	0	0	0						
	3	180	− 20	15	− 6	1					
	4	1260	− 20	1	22	− 17	4				
	5	2520	− 40	− 12	36	29	− 48	15			
	6	7560	− 40	− 20	22	43	8	−55	22		
	7	3780	−200	−125	50	197	176	−55	−286	143	
	8	13860	−120	− 85	2	93	128	65	− 78	−169	104

Having discussed the determination of matrix elements coupling states in the same **J** manifold the next step is to consider elements joining states in different **J** manifolds. It is not now possible to use operator equivalents and it is usually most convenient to use the Wigner coefficients directly. The variation of the elements with J_z is readily obtained and there remains again the problem of the multiplying constant.

Suppose for example that $\langle \mathbf{J}, J_z | V_6^0 | \mathbf{J}+2, J_z \rangle$ is required. Regarding V_6^0 as the component of a vector in a D_6 space with $m'=0$ the coefficient of $|\mathbf{J}, J_z\rangle$ in $V_6^0|\mathbf{J}+2, J_z\rangle$ is required. This is equal to a constant multiplying $c^{j'}_{j,0}$ with $j'=6$, $m'=0$, $j=J+2$, $m=J_z$ and $\lambda=8$. The value of the constant is obtained by evaluating the matrix element coupling a chosen pair of states in a manner analogous to that already described.

Thus the problem of reducing the matrix element of any potential function which transforms like the component of a vector with $m'=0$ in an irreducible representation space to a radial integration is, in principle, solved. It is often convenient to work with the components having $m'=0$, but the reasoning is easily extended to potentials other than these, since once the multiplying factor has been

found the variation with J_z is exactly that given by the corresponding Wigner coefficient. This dependence can be written as follows. Suppose V^0 and V^k are two components of a vector in a D_z space. Then

$$\langle \mathbf{J}, J_z | V^0 | \mathbf{J}', J_z \rangle = \alpha c^{J}_{m,m'} \quad \text{with} \quad j' = s, m' = 0, j = J', m = J_z, \lambda = s + J' - J,$$

and

$$\langle \mathbf{J}, J_z + k | V^k | \mathbf{J}', J_z \rangle = \alpha c^{J}_{m,m'} \quad \text{with} \quad j' = s, m' = k, j = J', m = J_z, \lambda = s + J' - J,$$

where the α's are the same and depend on $\mathbf{J}$ and $\mathbf{J}'$ but not on J_z. It will be noted that V^k only has matrix elements between states for which $\Delta J_z = k$. There is no difficulty in recognizing that a potential forms, say, the V^k component of a vector in D_z for, this being so, it must transform under rotation in the same way as $P_s^k(\theta, \phi)$, an associated Legendre function, which is such that a rotation through ψ about Oz multiplies it by $\exp(ik\psi)$.

In the accompanying tables are given the operator equivalents of certain functions together with the corresponding matrix elements. The elements for a given J value have common factors which are given in the columns under F. The actual elements are obtained by multiplying the elements in the table by the factors in the corresponding positions in column F. In table 1 are given the factors for V_2^0, V_4^0 and V_6^0 appropriate to the ground states of all the rare earth ions.

ACKNOWLEDGMENTS

I am much indebted to Mr. R. J. Elliott for his assistance in checking the numerical work and also for obtaining some of the values quoted in the tables. This work has been done during the tenure of a Research Fellowship founded by The Pressed Steel Company Ltd.

REFERENCE

VAN DER WAARDEN, B. L., 1932., *Die Gruppentheoretische Methode in der Quantenmechanik* (Berlin : Springer).

The Possible Effects of κ-Mesons in the Cosmic Radiation

BY S. HAYAKAWA*
Birkbeck College, University of London

Communicated by E. P. George; MS. received 6th November 1951

ABSTRACT. The decay and nuclear interaction schemes of κ-mesons are discussed. A tentative interpretation is made of some anomalous interactions of penetrating particles observed recently below ground. Further possible experiments testing the hypotheses made are suggested.

§1. INTRODUCTION

IT is generally accepted that the μ-mesons form the penetrating component of the cosmic radiation. They are thought to arise from the decay of π-mesons, the latter being produced in energetic collisions of the primary radiation with the nuclei of nitrogen and oxygen atoms in the atmosphere.

* On leave from Osaka City University, Japan.

There are, however, several properties of the cosmic radiation observed below ground that do not fit in well with this picture. Thus, there is the question of the variation with depth of the intensity of the penetrating component. This has been discussed by Hayakawa and Tomonaga (1949) on the basis of the above picture. These authors find it difficult to obtain a satisfactory agreement with observation at all depths. Also there is the existence of the pairs of penetrating particles discovered underground by Braddick and Hensby (1939). Observations by George and Trent (1949) and by Braddick, Nash and Wolfendale (1951) have shown that if these are produced by μ-mesons, then the cross section for their production is 5×10^{-29} cm^2 per nucleon, a figure which does not agree at all well with that found for the nuclear interaction of μ-mesons by George and Evans (1950), viz. 5×10^{-30} cm^2 per nucleon. Finally, several cloud chamber pictures have been obtained underground by George and Trent showing anomalous scatter of single penetrating particles on passing through lead plates in the chamber. Assuming the particles to be μ-mesons, the cross section for anomalous scatter is found to be of the order of 2×10^{-28} cm^2 per nucleon. Such a large cross section is difficult to understand in view of the known weak interaction of μ-mesons with nucleons, and in any case is about 100 times larger than the values found by Amaldi and Fidecaro (1950) at sea level.

An investigation has been made of the extent to which the above anomalies might be attributed to the effects of the κ-mesons recently discovered by O'Ceallaigh (1951). The results are briefly reported below.

§2. THE OBSERVED PROPERTIES OF κ-MESONS

According to O'Ceallaigh (1951) the following properties of κ-mesons have been found using nuclear emulsions: (i) the mass is approximately 1000 times that of the electron; (ii) the κ-meson decays at rest into a secondary charged particle of mass 200 to 300 times that of the electron; (iii) the momenta of the secondaries are not unique, various values up to 250 Mev/c having been observed; (iv) in one example, the secondary decay particle was brought to rest in the emulsion and decayed in turn into a relativistic tertiary particle; in this case the secondary particle may be identified as a μ-meson; (v) the lifetime is not established with certainty, but probably lies in the range 10^{-10} to 10^{-9} sec; (vi) the frequency of κ-mesons observed to come to rest in nuclear emulsions exposed under 30 cm Pb at the Jungfraujoch is approximately 10% of that of π–μ decay events.

§3. THE INTERACTION SCHEME OF κ-MESONS

In the light of the above properties, the following interaction scheme of the κ-meson is tentatively suggested.

3.1. μ-*Decay*

The μ-decay of κ-mesons appears to be similar to that of the β-decay of μ-mesons:

$$\kappa^{\pm} \rightarrow \kappa^0 + \mu^{\pm} + \mu^0 \qquad \ldots\ldots(1)$$

where both $(\kappa^{\pm}, \kappa^0)$ and $(\mu^{\pm}, \mu^0)$ behave according to pair-theory, whatever their values of spin. The mass of the κ^0–particle may eventually be determined from the properties (1) and (iii) in §2, though at present the results are not sufficiently accurate. The decay of the charged κ-mesons via a nucleon pair must be allowed as an alternative possibility, but it can be at least partially forbidden by selection

rules (cf. Fukuda and Hayakawa 1951). The coupling constant for the process (1) is of order of magnitude similar to that for the β-decay of nucleons or μ-mesons, a more precise determination being prevented by the uncertainties in (i), (iii) and (v) in § 2.

3.2. *Nuclear Coupling*

The interaction between κ-mesons and nucleons may be treated in a manner similar to that between leptons and nucleons except for a difference in coupling constant:

$$\mathrm{P(N)} \rightarrow \mathrm{N(P)} + \kappa^{+}(\kappa^{-}) + \kappa^{0} \qquad \ldots\ldots(2)$$

From (vi) § 2, it appears that the interaction is quite strong, and may thus be an important source of nuclear forces at short distances. At high energies, therefore, the κ-meson behaves in a manner similar to the π-meson: the cross section for their production in nucleon–nucleon collisions is large, and the probability of the production of secondary κ-mesons by collisions between incident κ-mesons and nucleons is considerable.

The strong interaction for the process (2) results in the production of many κ-mesons in the cosmic radiation in the upper atmosphere. The charged κ-mesons decay quickly into μ-mesons via process (1), and this process competes with the usually considered origin of the μ-mesons in the decay of π-mesons. From a study of the underground radiation, Bollinger (1951) has shown the latter source to be predominant up to energies of the order of 10^{12} ev. This suggests, therefore, that the production of κ-mesons in nucleon–nucleon collisions may be ten or more times less than that of π-mesons at high energies. Furthermore, the nuclear interaction of κ-mesons will be smaller than that of π–mesons by a similar factor. In what follows, an interaction length of a few tens of metres of water will be assumed for κ-mesons.

§ 4. POSSIBLE EFFECTS IN COSMIC RAYS

Whereas most of the charged κ-mesons produced in the atmosphere decay into μ-mesons on account of their short life, the neutral, κ^{0}-mesons produced either directly in nucleon–nucleon collisions or resulting from the decay of charged κ-mesons can survive down to ground level on account of their lack of ionization, their fairly long interaction length, and also presumably of their lack of decay. The frequency of κ^{0}-mesons at sea level is then estimated to be as large as that of $\mu^{\pm}$-mesons.

The κ^{0}-mesons which penetrate into the earth can produce charged κ-mesons through the process

$$\kappa^{0} + \mathrm{P(N)} \rightarrow \mathrm{N(P)} + \kappa^{+}(\kappa^{-}), \qquad \ldots\ldots(2')$$

if their energy is sufficiently high. The charged κ-mesons thus produced are lost mainly by decay and nuclear absorption, the ionization loss being negligible at the moderate depths and high energies in which we are interested. The author has solved the diffusion equations for the charged κ-mesons and their μ-meson decay products under simplified assumptions. As is usual in such problems, a critical energy is defined, determined by the lifetime and interaction length of the $\kappa^{\pm}$-mesons, which is found to be of order 10^{11} ev. Below the critical energy, decay is predominant, and the $\kappa^{\pm}$-mesons are in equilibrium with the parent κ^{0}-mesons, and their intensity is small. On the other hand they supply a large intensity of $\mu^{\pm}$-mesons which increases up to a certain depth and then reaches saturation. Above the critical energy, the intensity of $\kappa^{\pm}$-mesons follows a

characteristic transition curve, possessing a maximum at a depth equal to the absorption length. At the maximum, the intensity of $\kappa^{\pm}$-mesons is found to be as high as that of the $\mu^{\pm}$-mesons of the same energy. All effects resulting from the κ^0-mesons striking the ground are found to be negligible at depths greater than say 200 m water.

The above picture suggests that there may well be an additional source of penetrating particles at moderate depths below ground, consisting of the charged κ-mesons and their μ-meson decay products. If this is so, at intermediate depths the depth–intensity curve should lie above that calculated from the energy spectrum of the $\mu^{\pm}$-mesons at sea level, coinciding with it at depths greater than about 200 m of water. Indeed, the experimental curve shows a gradual change of slope (Rossi 1948) while the momentum spectrum of the $\mu^{\pm}$-mesons at sea level is well represented by a simple power law expression between 3×10^9 and 3×10^{10} ev/c. Although the measurements have not great accuracy, the difference between the two curves seems to be significant, and is very difficult to understand on the basis of our commonly accepted ideas.

The appreciable number of high-energy $\kappa^{\pm}$-mesons expected to exist should give rise to nuclear interactions underground. The first order process is similar to (2′) and would be observed as the annihilation of $\kappa^{\pm}$-mesons in flight. The second order process

$$\kappa^+(\kappa^-)+(\mathrm{NP})\rightarrow \mathrm{N(P)}+\kappa^0+\kappa^+(\kappa^-)+\kappa^0, \qquad \ldots\ldots(3)$$

would be observed as the nuclear scatter of a fast particle and the third order process

$$\kappa^+(\kappa^-)+\mathrm{N(P)}\rightarrow \mathrm{P(N)}+\kappa^0+\kappa^-(\kappa^+)+\kappa^0+\kappa^+(\kappa^-)+\kappa^0, \qquad \ldots\ldots(4)$$

would be observed as the production of an additional penetrating particle.* The cross sections for these processes become smaller by a factor of about ten at each step.

These nuclear interactions may be contrasted to the nuclear interactions of $\mu^{\pm}$-mesons, which latter are thought to be responsible for most of the nuclear disintegrations observed underground by George and Evans (1950) and Cocconi and Cocconi-Tongiorgi (1951). In the case of these μ-meson induced disintegrations, the mechanism appears to be first the production of a π-meson in an encounter between the incident μ-meson and a nuclear nucleon, followed by the re-absorption of the π-meson inside the same nucleus (Hayakawa 1951). In the case of the κ-meson interactions, the nuclear interactions of the secondary κ-mesons are not strong enough to produce further nuclear collisions in the nucleus in which they are produced. Furthermore, on account of this weak interaction, the nucleon recoil will not be large and the processes under consideration should occur mainly without associated nuclear disintegrations.

The processes (3) and (4) are suggested as a possible interpretation of the underground observations of scattering and penetrating pairs mentioned in the introduction. The cross sections resulting from a detailed calculation are consistent with those observed, as also are the fairly frequent cases of consecutive scattering in each of two lead plates, and the small angular divergence of the pairs. Without some such speculation these phenomena are very difficult to explain.

* I am indebted to Professor Rosenfeld for pointing out the possibility of the following alternative scheme for the production of a penetrating secondary particle :

$$\kappa^+(\kappa^-)+\mathrm{N(P)}\rightarrow \mathrm{P(N)}+\kappa^0+\kappa^-(\kappa^+)+\kappa^0+\pi^+(\pi^-).$$

The cross section for this process is found to be smaller than that of scheme (4).

The above picture is admittedly tentative, and only points favourable to the model have been discussed: it is quite easy to argue against it just as forcibly. The author's intention has been to stimulate further experiments which might confirm or disprove the speculation. The experiments are not difficult and some are repetitions of old ones in which greater accuracy and reliability is needed. Possible experiments are as follows:

(i) From reaction (2′), the frequent annihilation of charged particles in flight, and the frequent production of charged by neutral particles should be observed. This could be checked by a simple anticoincidence arrangement.

(ii) An accurate re-determination of the intensity–depth curve, preferably in water, in order to decide whether this curve shows significant departures from that inferred from the measured energy spectrum of penetrating particles at sea level would be useful.

(iii) According to processes (3) and (4), the particles involved in anomalous scatter and in penetrating pair production should all be heavy mesons, of mass of the order of $1000\,m_e$. Observations with a cloud chamber in a magnetic field might be useful in this respect.

ACKNOWLEDGMENTS

I would like to express my sincere thanks to Dr. E. P. George for his kind hospitality while I was at Birkbeck College. His stimulating discussions on the underground experiments carried out by him and his collaborators gave me the direct motive for this work.

REFERENCES

Amaldi, E., and Fidecaro, G., 1950, *Helv. phys. Acta*, **23**, 93.
Bollinger, L. M., 1951, Ph.D. Thesis, Cornell University.
Braddick, H. J. J., and Hensby, G., 1939, *Nature, Lond.*, **144**, 1012.
Braddick, H. J. J., Nash, W. F., and Wolfendale, A., 1951, *Phil. Mag.*, **42**, 1277.
Cocconi, G., and Cocconi-Tongiorgi, V., 1951, *Phys. Rev.*, **84**, 29.
Fukuda, H., and Hayakawa, S., 1951, *Prog. Theor. Phys.*, **5**, 993.
George, E. P., and Trent, P. T., 1949, *Nature, Lond.*, **164**, 838.
George, E. P. and Evans, J., 1950, *Proc. Phys. Soc.* A, **63**, 1248.
Hayakawa, S., 1951, *Phys. Rev.*, **84**, 37.
Hayakawa, S., and Tomonaga, S., 1949, *Prog. Theor. Phys.*, **4**, 287.
O'Ceallaigh, C., 1951, *Phil. Mag.*, **42**, 1032.
Rossi, B., 1948, *Rev. Mod. Phys.*, **20**, 537.

Experiments on Production of Auroral Radiation

By N. D. Sayers and K. G. Emeléus
Queen's University, Belfast

MS. received 22nd October 1951

ABSTRACT. Further experiments have been made on the production in the laboratory of the 'forbidden' red and green auroral lines, and the ultra-violet transauroral line of O I. The mean concentration of oxygen atoms in the 1^1S_0 and 5^5D states in the columns has been found from absolute intensity measurements. The decay of the green radiation produced by a Tesla discharge through a high-pressure source has been investigated with a photo-multiplier tube. It occurs at approximately the rate to be expected if the atoms in the ^1S state are undergoing spontaneous transitions to lower atomic levels, but complicating factors make it difficult to deduce transition probabilities from the experiment.

§1. INTRODUCTION

THE principal 'forbidden' lines resulting from transitions between low terms of OI, most of which appear in the spectrum of the night sky and aurora, have been repeatedly produced in the laboratory. Much still remains obscure, however, about the conditions under which they are excited. This paper contains an account of some quantitative experiments which have been done with discharge tubes containing gas at low pressure (§§ 2, 3) and atmospheric

Forbidden Transitions in OI

Transition	λ (Å)	A (sec^{-1})
$^3P_1-{}^1S_0$	2972·3	0·090
$^1D_2-{}^1S_0$	5577·3	2·20
$^3P_2-{}^1D_2$	6300·2	0·0078
$^3P_1-{}^1D_2$	6363·9	0·0026

pressure (§4) with the aim of determining the excitation conditions more precisely. The approximate wavelengths of the observed lines, and the transition probabilities (A) calculated from the electron configurations (Pasternack 1940), are shown in the table.

§2. DISCHARGE TUBES

The evidence on which design of low-pressure discharge tubes for production of the forbidden transitions can be based appears somewhat contradictory. Our earlier investigations (Emeléus, Sloane and Cathcart 1939) and those of Kvifte and Vegard (1947) showed that strong excitation was likely to occur in positive column tubes, if they were wide and the gas pressure relatively high, to hinder loss of metastable atoms by diffusion to the wall. Herman and Herman (1944) have, however, obtained both the green and red lines readily in tubes of only 1 cm radius passing feeble currents, whilst Hopfield (1931) has obtained them with narrow tubes passing heavy currents. Probe analyses which might account for these differences are lacking, and likely to be difficult to obtain because of the occurrence of irregular ionic oscillations (Sloane and Minnis 1937). The tubes made for the present investigation have been larger versions of the π-shaped tubes used previously (Emeléus, Sloane and Cathcart 1939), with large hollow iron electrodes in the side arms and horizontal sections up to 6 cm in diameter and 110 cm long. A graded quartz seal was recessed longitudinally into one end of the horizontal section for observation of the ultra-violet line. In our earlier investigations it was found that the green auroral line could only be obtained when the positive column had irregular moving striations. As there appeared, therefore, to be little advantage in use of d.c., we have used 50 c/s a.c. at between 1500 and 4000 v. Moving striations were present in each half cycle. Most experiments were done with the oxygen diluted with argon, and a few with oxygen and neon. The former gave the better source. The forbidden lines were not emitted from the negative glow and Faraday dark space.

The tubes behaved in most respects as had been anticipated and the green line was obtained consistently. Using argon, it was also found, in agreement with our earlier results, that it appeared almost in isolation at the periphery of the discharge and where the discharge diffused into the corner at the junction of the horizontal and vertical sections of the tubes. The dipole lines of OI and

AI were much more concentrated near the axis of the discharge. Similar, but less marked, radial distributions were found with oxygen and neon. An unexpected advantage of use of a.c. was that there was less tendency for the oxygen to move away from the middle section of the length of the tube than with d.c.; this may be an electrophoretic effect. It was again noticed that the line could sometimes be obtained more brilliantly after the tube had been open to the air, and only torched before admitting gas, than when it had been degassed rigorously, possibly because imperfect degassing leaves surface films on the glass which hinder recombination of oxygen atoms. The red lines were also obtained, but less consistently, probably because the long life of the ^{1}D state (see table) makes it necessary to operate within a restricted range of conditions in which the metastable atoms are not too rapidly destroyed by collisions with electrons or molecules; they were not observed preferentially from the periphery of the discharge in the same way as the green line. The transauroral line was obtained without difficulty, although not with high intensity; the measured wavelength was 2972·32 Å (Sayers and Emeléus 1950). When the auroral lines were excited in argon–oxygen discharges, a patch of continuous spectrum usually appeared between about 6 400 and 6 550 Å. It was always present when the red lines were obtained. Its origin is unknown.

§3. INTENSITY OF THE GREEN AURORAL LINE AND OTHER SPECTRA

If emission of a line occurs spontaneously, the rate E of radiation of energy of that wavelength per cm^3 of the discharge tube will be $NA\boldsymbol{h}\nu$ erg/sec, where N is the concentration of excited atoms, ν the frequency and A the transition probability. If E can be measured and A is known, N can be calculated, neglecting self-absorption in the discharge, which is usually permissible. This provides the most direct method at present available for finding concentrations of excited atoms. It has been used for part of the green spectrum from argon–oxygen discharges by comparing the intensity of the radiation received at the slit of a Hilger constant deviation spectroscope with that received from a calibrated hot-filament lamp. One half of the length of the slit was illuminated by light from the middle of the discharge tube, viewed laterally, and the other half by light from the standard lamp, both being brought to the slit by nearly identical optical systems. The intensity of the green light from the two sources was generally matched visually, but in a few cases the spectra were photographed and microphotometered. It was found convenient for visual observation to use a slit 0·3 mm wide. The lamp then gave a brighter illumination than the discharge, and the light from the former was therefore reduced by ground-glass plates calibrated for absorption. Since the discharge was intermittent, and inhomogeneous radially, more accurate photometric measurements were not warranted.

Some results are given in figs. 1 (*a*) and 1 (*b*). Before making each measurement a fresh charge of gas was admitted. Fig. 1 (*a*) shows on a logarithmic scale the number of quanta I emitted per cm^3/sec, as a function of tube current i, for a tube 4 cm in diameter containing 0·4 mm oxygen and 3·0 mm argon. The lines 1, 2, 3 in the figure are for the auroral line (5 577 Å), the unresolved permitted OI multiplet at 5 329 Å (3^5P-5^5D, excitation potential 13·0 v), and for a region of 20 Å centred on 5 530 Å of the continuous background which appears from this

source (Emeléus, Sloane and Cathcart 1939). Allowance has been made for the continuum in calculating the intensities of the lines. The three curves are nearly parallel. For the larger currents $I \propto i^2$. Kvifte and Vegard (1947), using mixtures ot oxygen and neon, found that $I \propto i^{1\cdot67}$ for the auroral line and the permitted line at 5 555 Å ($3^3P - 7^3S$, excitation potential 13·2 v).

Fig. 1 (*b*) shows I for the same spectra as a function of partial pressure p of oxygen, in mm Hg, for the same tube passing an r.m.s. current of 0·10 amp at a total pressure of 4·0 mm of oxygen and argon. For $p < 1\cdot7$ mm $I \propto p^{1\cdot1}$, and for $p > 1\cdot7$ mm $I \propto p^{-3\cdot1}$. The change in slope is connected with a change in type of the positive column; over the whole pressure range there was marked radial constriction of the discharge, but above 1·7 mm this increased more rapidly with increase of pressure than below 1·7 mm.

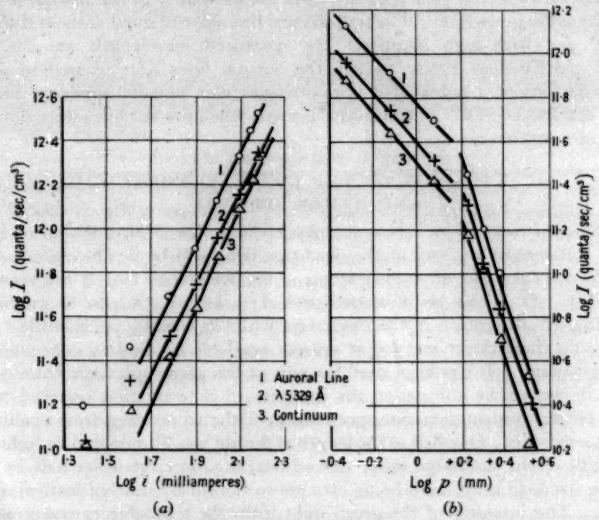

Fig. 1. (*a*) Mean rate of emission of quanta I plotted against current i. (*b*) Mean rate of emission of quanta I plotted against pressure of oxygen p.

The greatest value of N obtained for the ^1S state was $1\cdot5 \times 10^{12}/cm^3$. The corresponding concentration of oxygen atoms in the discharge, assuming all the oxygen was dissociated, was $4 \times 10^{17}/cm^3$. This is so much in excess of the number of excited atoms that the results, even allowing for very incomplete dissociation, are consistent with spontaneous emission of the auroral line. A previous estimate made by comparison of the intensities of the auroral line and an A I line gave a concentration of excited atoms of $2\cdot5 \times 10^{12}/cm^3$ under similar conditions (Emeléus, Sloane and Cathcart 1939). The concentrations of oxygen atoms in the 5^5D states are of the order of 10^{-7} or 10^{-8} times smaller, as the intensities of the lines at 5 577 Å and 5 329 Å are comparable, and the values of A for the permitted lines are of the order of $10^7 - 10^8$ sec^{-1}. No information can be deduced about the emitter of the continuum, whose origin is uncertain.

Analysis of the data shown in fig. 1, to find the probability of de-activation of excited oxygen atoms on collision with oxygen molecules and inert gas atoms, by a method developed by Kvifte and Vegard (1947) for neon, gave negative values for the probabilities. This might be due to regeneration of excited oxygen atoms occurring in argon by some process not operative in neon. We think it is more probably due to the constriction of the discharge in argon, which we found to be greater than in neon, making invalid Kvifte and Vegard's assumption that the current density is uniform over the cross section, and the consequences of this. A quantitative diffusion theory similar to Kvifte and Vegard's could be developed for the region between the core of the positive column and the wall, with a solution differing mainly from Kvifte and Vegard's in introducing Bessel functions of both kinds. There is, however, no point in doing this, as the boundary conditions at the edge of the core, which is itself diffuse, are uncertain. Caution is also necessary in using Kvifte and Vegard's results for the de-activation coefficients of the ^1S state of O in O_2–Ne mixtures, as similar results could be obtained if de-activating collisions occurred with high efficiency, with impurities, or ozone, present in minute quantities.

§4. HIGH PRESSURE SOURCES

Although the discharge changes from a glow to a spark as the pressure is increased from a low value to atmospheric, it has been shown by Janin (1946) that it may be a good source of forbidden spectra. Vegard and Kvifte (1948) and Jenkins, Bowtell and Strong (1949) have found that the afterglow of Tesla discharges at or near atmospheric pressure through a mixture of argon, or argon and nitrogen, with a trace of oxygen of the order of one part in 10^5, is a good source of the green auroral line, which is accompanied by diffuse bands and a continuum. This gas-filling is used for certain commercial incandescent lamps. We have made some studies of this interesting source, using 300 and 500 watt Osram bulbs and the tube shown in fig. 2 with nickel rod electrodes. The general features of

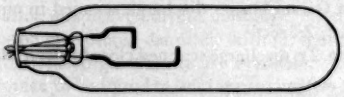

Fig. 2. High pressure discharge tube. Length 21 cm.

the discharges were the same in all cases. Near the point of entry to the gas, from the metal electrode or through the glass, there is a local spark, which branches at greater distances, and is surrounded by a green aureole a few millimetres in diameter. Green clouds move upwards from the spark, presumably on account of thermal convection of excited gas. These spread and, if the discharge is stopped, mingle with a general green afterglow which has been detected visually for more than 5 seconds. The spectrum of the spark contains nitrogen bands; these are weak or absent from the spectra of the aureole around the spark and from such afterglows as we have examined. Cyanogen bands also appear erratically, usually with feeble intensity. The main feature of the spectrum of the aureoles and the afterglows is the green auroral line. The continuum and bands near 5577 Å were most marked in the spectra of the aureoles, and less strong, if present at all, in the spectra of the sparks. A microphotometer

trace of the spectrum of an aureole is shown in fig. 3. The peaks of intensity at 5584, 5570, 5550, 5530, 5490 and 5455 Å can be attributed to an unstable AO molecule (Herman, Weniger and Herman 1951).

The decay of the green light from the afterglow has been followed by a photomultiplier, the current from which was amplified and shown on a cathode-ray oscillograph. For about the first 0·2 sec after the exciting discharge was discontinued the decay of light from any selected part of the tube was irregular, in some instances actually increasing with time for short intervals. After about

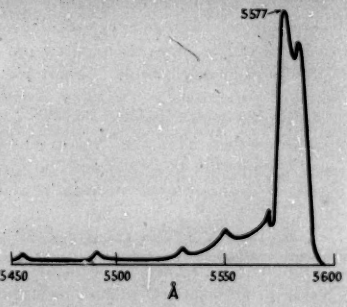

Fig. 3. Microphotometer trace of auroral line and associated band for high pressure source.

0·2 sec until about 1·5 sec, after which the light was too feeble to be recorded in this way, the decay was exponential. The values of the decay constant were in the neighbourhood of 2 to 3 sec^{-1}, depending on the tube used and the part studied. The following data show the trend of the values of the decay constant and the consistency obtained.

(i) First 300 watt Osram lamp: discharge scanned in middle of bulb; decay constants, 2·5, 2·6, 2·3, 2·9, 2·9 sec^{-1}.

(ii) Second 300 watt Osram lamp: discharge scanned in middle of bulb; decay constants, 2·4, 2·2, 2·2 sec^{-1}.

(iii) Electrode tube (fig. 2): discharge scanned close to electrodes; decay constants, 3·3, 3·5 sec^{-1}.

(iv) Electrode tube (fig. 2): discharge scanned at end remote from electrodes; decay constants, 2·6, 2·4, 2·7, 2·6, 2·9 sec^{-1}.

The decay constant was usually greatest close to the exciting discharge. Further away it usually diminished, but was not found to fall below about 2·0 sec^{-1} in these experiments.

At least four processes may be responsible for the decay: (*a*) convection of the luminous gas; (*b*) diffusion to the wall of excited atoms in the ^1S state and of the associated excited AO molecules; (*c*) emission of radiation from the same atoms and molecules; (*d*) de-activation of the excited atoms and molecules in collisions of the second kind. It is not possible to distinguish certainly between them. It has been shown that (*b*) can lead to about the observed rate after the effects of initial irregularities due to localization of the discharge and convection have died down (Emeléus, Sayers and Bailey 1950). On the other hand, the least value found for the decay constant is close to the *A* coefficient for the green

line (see table). More recently, however, L. Herman (private communication) has found values of the decay constant of $1{\cdot}5\,\text{sec}^{-1}$. If the value of A given in the table is accurate, this indicates, as he points out, that regeneration of oxygen atoms in the ^1S state may be taking place.

§5. DISCUSSION

The experimental problem of finding sources of the forbidden spectra coming from transitions between low terms of O I (and similar spectra of other light neutral atoms and molecules) is now largely solved. New methods for producing the necessary concentrations of metastable atoms have been developed, using gas at high pressure, which supplement the original methods employing gas at low pressure, and the original low pressure sources have been further developed. However, there is not yet available a satisfactory detailed description of the condition of the gas in any of the sources, for the criteria for a discharge, to serve as a good spectroscopic source for this purpose and to be amenable to electrical analysis, remain incompatible. The experiments made since our earlier analysis (Emeléus, Sloane and Cathcart 1939) have apparently all been carried out with discharges that were energized by an alternating or intermittent voltage. In some experiments, such as those at low pressure described in the present paper, a.c. has been used deliberately. With gas at high pressure it is probable that the discharge is inherently intermittent, wandering from one part of the gas to another if it is not interrupted in a single locality. The new experiments at low pressures, and the experiments which have been done at high pressure, do nevertheless confirm our earlier conclusions that forbidden transitions are likely to be produced in most isolation in feeble discharges and in the aureoles round heavy discharges or in afterglows, i.e. under conditions generally similar to those in the upper air, and that the metastable atoms may be produced by more than one process.

It is still uncertain if forbidden lines can be produced with appreciable intensity from the plasma of a heavy current discharge. Relations such as those shown in fig. 1 cannot be interpreted definitely without more detailed knowledge of the condition of the ionized gas than is yet available. It is not unusual for simple empirical formulae to be found to hold approximately for discharges under circumstances which indicate that the apparent simplicity is due to mutual compensation of a number of complex conflicting processes. The irregular moving striations present in the tubes with d.c. supply, which automatically introduce afterglows, might be suppressed by building an anode with a negative anode drop in potential (Pupp 1933), if this would operate steadily with oxygen present. Irregular low-frequency fluctuations may however occur even in the absence of moving striations (Cobine and Gallagher 1947), so that elimination of moving striations would not necessarily leave the discharge steady. The existence of striations and fluctuations, and even the use of 50 c/s a.c., does not nevertheless completely invalidate the application of the quantitative theory of de-activation developed by Kvifte and Vegard (1947), since the lifetime of the metastable atoms is much greater than the reciprocal frequency of the greater part of the electrical noise spectrum. The comparison of de-activation times with lifetimes of metastable atoms is simpler in afterglows where applied electric

fields are absent than when a current is passing, but even with afterglows regeneration of metastable atoms may add to the complexity of the processes (§4), whilst, as with sustained discharges, the determination of the degree of molecular dissociation and of the concentration of free radicles presents difficult problems not yet satisfactorily solved.

ACKNOWLEDGMENTS

The authors wish to thank the Research Laboratories of the General Electric Company, Limited, for gifts of the calibrated lamp and electrode tube, Miss M. E. J. West, Dr. D. Greene and Dr. O. White for building the low-pressure discharge tubes, Dr. R. A. Bailey for assistance with the photomultiplier experiments, and Dr. R. Herman and Dr. L. Herman for much helpful discussion.

REFERENCES

COBINE, J. D., and GALLAGHER, C. J., 1947, *J. Appl. Phys.*, **18**, 110.
EMELÉUS, K. G., SAYERS, N. D., and BAILEY, R. A., 1950, *Nature, Lond.*, **166**, 656.
EMELÉUS, K. G., SLOANE, R. H., and CATHCART, E. B., 1939, *Proc. Phys. Soc.*, **51**, 978.
HERMAN, L., and HERMAN, R., 1944, *Ann. Geophys.*, **1**, 165.
HERMAN, R., WENIGER, C., and HERMAN, L., 1951, *Phys. Rev.*, **82**, 751.
HOPFIELD, J. J., 1931, *Phys. Rev.*, **37**, 160.
JANIN, J., 1946, *Thesis* (Paris).
JENKINS, H. G., BOWTELL, J. N., and STRONG, R. W., 1949, *Nature, Lond.*, **163**, 401.
KVIFTE, G., and VEGARD, L., 1947, *Geofys. Publ.*, **17**, No. 1.
PASTERNACK, S., 1940, *Astrophys. J.*, **92**, 129.
PUPP, W., 1933, *Phys. Z.*, **34**, 756.
SAYERS, N. D., and EMELÉUS, K. G., 1950, *Phys. Rev.*, **79**, 166.
SLOANE, R. H., and MINNIS, C. M., 1935, *Proc. Phys. Soc.*, **47**, 1019.
VEGARD, L., and KVIFTE, G., 1948, *Nature, Lond.*, **162**, 967.

LETTERS TO THE EDITOR

Helium II Transfer on Metal Surfaces

The experiments of Mendelssohn and White (1950 a, b) on the transfer rate of the He II film had shown that, whereas clean glass surfaces yielded values almost identical with the earlier work (Daunt and Mendelssohn 1939), metal surfaces always showed much higher transfer rates. These results were confirmed by the observations of Dash and Boorse (1951). Two explanations of this phenomenon seemed feasible, either that the different transfer rates may be due to the chemical nature of the substrate, or that there may be only *one* transfer rate (that exhibited by the glass surfaces) and any higher rates would be due to the micro-structure of the substrate. For a number of reasons we had preferred the second explanation, and in particular considered that narrow surface cracks of the order of magnitude of the film thickness or somewhat larger might be filled up with liquid helium and thereby produce a much greater transport of liquid.

An opportunity to test this hypothesis arose when the Metrology Division of the National Physical Laboratory offered to prepare for us stainless steel beakers of a much better finish than any metal surface that had been previously used for helium transfer. The transfer rate obtained on two beakers of this kind in dependence on temperature is shown in the accompanying figure. As can be seen, the results for both beakers are identical, and the transfer rate is practically the same as that for a baked-out glass surface. Subsequently, one of the beakers was brought to red heat, thus destroying the smooth

surface finish, and it was then lightly polished with cotton wool to remove any deposit of oxide. Examination under a low power microscope did now show cracks and draw-marks. A transfer experiment on this beaker showed indeed that the flow rate had changed considerably, being now more than three times the original value.

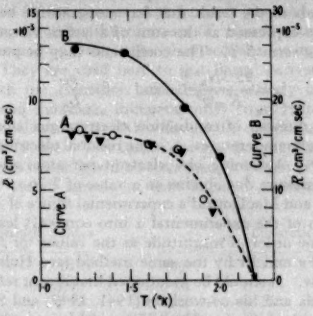

Transfer rates of the helium II film on two highly-polished stainless steel beakers (○ and ▼), and on one of these beakers (○) after destruction of the surface finish by heating (●). The broken curve is that obtained for baked-out glass by Mendelssohn and White.

In conjunction with other flow experiments and observations on the formation of the helium film which will be reported in detail later, we conclude that the present experiments show that the high transfer rates observed are in fact due to the micro-structure of the substrate.

We wish to thank Messrs. F. H. Rolt, V. W. Stanley and S. Woodhouse of the Metrology Division, National Physical Laboratory, for their helpful co-operation.

The Clarendon Laboratory,
Oxford.
21st December 1951.

B. S. Chandrasekhar.
K. Mendelssohn.

Dash, J. G., and Boorse, H. A., 1951, *Phys. Rev.*, **82**, 851.
Daunt, J. G., and Mendelssohn, K., 1939, *Proc. Roy. Soc.* A, **170**, 423, 439.
Mendelssohn, K., and White, G. K., 1950 a, *Nature, Lond.*, **166**, 27 ; 1950 b, *Proc. Phys. Soc.* A, **63**, 1328.

Anomalous Thermal Conductivity of Pure Metals at Low Temperatures

In a recent paper on the thermal and electrical conductivities of sodium at low temperatures, Berman and Macdonald (1951) have drawn attention to two types of discrepancy between their experimental data and the behaviour predicted by the electron theory of metals. They observe firstly that the thermal conductivity fails to pass through a theoretically predicted minimum at a temperature in the neighbourhood of $0{\cdot}25\,\Theta$, where Θ is the Debye temperature, and secondly that, although the experimental Lorentz number $K/\sigma T$ (where K and σ are the thermal and electrical conductivities respectively) exhibits a minimum at low temperatures, in accord with theory, the location and shape of the minimum deviate considerably from the theoretical results of Makinson (1938). The purpose of this letter is to point out that the discrepancy for sodium at the lowest temperatures ($< 0{\cdot}1\,\Theta$) is essentially of the same type as that already well known for ten other metals studied by Grüneisen and Goens (1927), de Haas and Rademakers (1940),

Hulm (1950) and Webber, Andrews and Spohr (1951), and originates in the fact that the observed coefficient of the T^2 term in the electronic thermal resistivity is nearly an order of magnitude lower than the theoretical value. A placing of special emphasis on the Lorenz number for sodium tends to obscure the fact that it is in the thermal resistivity rather than in the electrical resistivity that the main discrepancy occurs.

Makinson's theory leads to the result that for temperatures below $0{\cdot}1\Theta$ the electronic thermal resistivity may be expressed as the sum of a lattice vibration scattering term αT^2 and an impurity scattering term β/T. The coefficients may be put into the form

$$\alpha = \frac{95{\cdot}3N_a^{2/3}}{K_\infty \Theta^2} \quad \text{and} \quad \beta = \frac{\rho_0}{L_0}, \qquad \ldots\ldots (1)$$

where N_a is the effective number of conduction electrons per atom, K_∞ is the electronic thermal conductivity at high temperatures, ρ_0 is the residual electrical resistivity and L_0 is the Lorenz constant $\frac{1}{3}(\pi k/e)^2$. Assuming one electron per atom and substituting the other appropriate constants for sodium one obtains an α value of $2{\cdot}26 \times 10^{-3}$ watt/cm/deg^3, which is about six times Berman and MacDonald's experimental figure of $3{\cdot}8 \times 10^{-4}$ watt/cm/deg^3. Alternatively, substitution of the experimental α into eqns. (1) leads to a value for N_a of 0·069, which is of the same order of magnitude as the values for N_a obtained for Sn, Hg, Pb, In, Cu, Au, Al, W, Fe and Pt by the same method (see Hulm 1950, table 2), and is undoubtedly much too low. It should be mentioned that recent refinements of Makinson's theory proposed by Umeda and his co-workers (1941, 1949) and Sondheimer (1950) have decreased the theoretical value of α by about 25%, which is, however, far from sufficient to remove the disagreement with experiment.

While anomalous heat conduction in metals at temperatures above $0{\cdot}1\Theta$ may in part be due to deviations of the phonon spectrum from a Debye pattern, as Berman and MacDonald have stated, the quantitative discrepancy in the lattice vibration scattering term of the electronic thermal resistivity below $0{\cdot}1\Theta$ evidently involves a direct breakdown of the free-electron theory. The situation that an 'ideal' metal such as sodium gives a departure from theory which is of the same order of magnitude as those for more complex metals such as Sn, Pb, W, Fe and Pt suggests that this breakdown is of a rather fundamental nature.

J. K. Hulm.

Institute for the Study of Metals,
The University of Chicago.
12th December 1951.

Berman, R., and MacDonald, D. K. C., 1951, *Proc. Roy. Soc.* A, **209**, 368.
Grüneisen, E., and Goens, E., 1927, *Z. Phys.*, **44**, 614, **46**, 151.
de Haas, W. J., and Rademakers, A., 1940, *Physica*, **7**, 992.
Hulm, J. K., 1950, *Proc. Roy. Soc.* A, **204**, 98.
Makinson, R. E. B., 1938, *Proc. Camb. Phil. Soc.*, **34**, 474.
Sondheimer, E. H., 1950, *Proc. Roy. Soc.* A, **203**, 75.
Toya, T., Kroll, W., and Umeda, K., 1941, *Sci. Pap. Inst. Phys. Chem. Res., Tokyo*, **39**, 42.
Umeda, K., and Toya, T., 1949, *J. Fac. Sci., Hokkaido Univ.*, **3**, 257.
Umeda, K., and Yamamoto, T., 1949, *J. Fac. Sci., Hokkaido Univ.*, **3**, 249.
Webber, R. T., Andrews, F. A., and Spohr, D. A., 1951, *Phys. Rev.*, **82**, 328.

Transition Probabilities of some Band Systems of Nitrogen

With a view to understanding the processes in the upper atmospheric sources of the First Positive, Second Positive and Negative band systems of nitrogen, Bates (1949) derived the relative probabilities of transitions between the various vibrational levels by computing the square of the overlap integral containing the normalized vibrational wave functions,

$$\left| \int R(n', v'/r) R(n'', v''/r) r^2 \, dr \right|^2.$$

Using Morse's potential-energy expression, Bates solved the relevant differential equation in terms of Laguerre polynomials.

In verifying his theoretical predictions for the Second Positive system, Bates used the extensive data derived by Tawde (1934) from laboratory measurements of peak intensities. He pointed out the limitations of these data (due to wide differences between values from one condition of excitation to the other) and the importance of accurate quantitative intensity measurements. It would appear, however, that he was unaware of Tawde and Patankar's (1943) precise experimental intensity observations, the first to be computed from the areas under the contours of intensity curves. These observations should give a better approach to reality since they account for any variations in the overall intensities in a band. They are used here to test Bates' derivations, which, at the same time, are compared with the transition probabilities already computed (by Langstroth (1935) and by Tawde and Patankar, independently) from Hutchisson's (1930) intensity integral and with those calculated by Nicholls (1950) using the method of Gaydon and Pearse (1939) and Pillow (1949). The results for the Second Positive system are collected in the following table, from which it will be seen that Tawde and Patankar's revised observations show much better overall agreement with Bates' derivations than do Tawde's earlier data.

Band	Experimental values		Theoretical values			
v', v''	(1)	(2)	(3)	(4)	(5)	(6)
0, 0	0·40	0·43	0·48	0·53	0·48	0·46
0, 1	0·36	0·32	0·32	0·27	0·38	$0·38_8$
0, 2	0·17	$0·15_7$	0·14	0·12	0·12	$0·12_8$
0, 3	$0·05_8$	0·07	$0·04_8$	0·05	$0·01_8$	0·02
1, 0	0·49	$0·44_7$	0·39	0·43	0·32	$0·32_9$
1, 1	$0·02_6$	$0·02_9$	$0·03_8$	0·04	$0·03_8$	$0·02_7$
1, 2	0·16	$0·16_7$	0·22	0·21	0·34	$0·32_9$
1, 3	0·20	$0·20_8$	0·19	0·12	$0·23_7$	$0·24_8$
2, 0	0·29	$0·22_8$	0·12	0·21	$0·15_5$	$0·21_9$
2, 1	0·33	$0·49_8$	0·37	0·39	$0·25_4$	0·30
2, 2	0·03	$0·03_7$	$0·00_9$	0·01	0·02	0·04
2, 3	$0·05_9$	$0·06_6$	$0·09_4$	0·10	$0·22_6$	0·25
2, 4	0·14	$0·17_2$	—	0·08	0·34	0·32

(1) Tawde (mean values); (2) Tawde and Patankar; (3) Bates; (4) Nicholls; (5) Tawde and Patankar (Hutchisson's method); (6) Langstroth (Hutchisson's method).

As a consequence of a number of simplifying assumptions, as well as the different values of molecular parameters used in the calculations, there is a variation amongst the different sets of theoretical values. The sensitiveness of values of transition probabilities to a slight change in molecular constants has been demonstrated by McKellar and Tawde (1951). Proper comparison would require theoretical calculations from the same molecular constants; with the limitations of the available data, however, the following broad features become apparent.

Bates' and Nicholls' values do not differ widely, except for the (1,3) and (2,0) bands. The two sets of values derived from Hutchisson's theory are in a class by themselves, comparable with one another and departing about equally from Bates' or Nicholls' results. This is to be expected since they follow from the same theoretical expression, true only for a harmonic oscillator; the small differences between the two arise from the use of different molecular constants in the two sets of calculations. All four sets of theoretical results agree fairly well amongst themselves for bands associated with lower quanta.

In view of the errors and uncertainties in photographic photometry and the limitations of theoretical results, there is remarkable agreement of experimental observations (particularly those of Tawde and Patankar) for many bands, even bands of higher quanta, with Bates' or Nicholls' values. This relatively closer agreement over the entire region is attributable to the fact that, in different ways, both take account of anharmonicity: Bates directly uses the experimentally justified Morse potential-energy expression and normalized wave functions in the integration, while Nicholls starts with the parabolic curve of a harmonic oscillator and distorts it to fit the Morse expression. As Hutchisson's theory is based on a harmonic oscillator only, it is at higher quanta, e.g. in the (0, 3), (2, 3) and (2, 4) bands, that the values in the last two columns of the table show greater disagreement with Bates', Nicholls' and the experimental values.

More work on these aspects of theories of transition probabilities in relation to experiment is in progress.

We are grateful to Dr. N. R. Tawde for suggesting this study and for very helpful discussion in the preparation of this note and to Dr. W. Jevons in England for kindly revising the manuscript to the size of a "Letter".

Spectroscopic Laboratories,
Institute of Science,
Bombay, India.
28th November 1951.

D. D. Desai.
K. S. Korgaokar.
B. B. Laud.

Bates, D. R., 1949, *Proc. Roy. Soc.* A, **196**, 217.
Gaydon, A. G., and Pearse, R. W. B., 1939, *Proc. Roy. Soc.* A, **173**, 37.
Hutchisson, E., 1930, *Phys. Rev.*, **36**, 410.
Langstroth, G. O., 1935, *Proc. Roy. Soc.* A, **150**, 371.
McKellar, A., and Tawde, N. R., 1951, *Astrophys. J.*, **113**, 440.
Nicholls, R. W., 1950, *Phys. Rev.*, **77**, 421.
Pillow, M. E., 1949, *Proc. Phys. Soc.* A, **62**, 237.
Tawde, N. R., 1934, *Proc. Phys. Soc.*, **46**, 324.
Tawde, N. R., and Patankar, V. S., 1943, *Proc. Phys. Soc.*, **55**, 396.

CONTENTS FOR SECTION B

PAGE

Mr. J. S. Greenhow. Characteristics of Radio Echoes from Meteor Trails: III—The Behaviour of the Electron Trails after Formation 169

Dr. L. E. Lawley. The Propagation of Sound through Gases contained in Narrow Tubes 181

Dr. G. Liebmann. The Magnetic Electron Microscope Objective Lens of Lowest Chromatic Aberration 188

Dr. D. F. Gibbons. Effect of Strain Ageing upon the Distribution of Glide Bands in Cadmium Crystals 193

Dr. A. F. Gibson. Single Contact Lead Telluride Photocells 196

Dr. A. F. Gibson. Lead Sulphide Rectifier Photocells 214

Dr. E. Billig. A Note on the Structure of Selenium 216

Dr. B. R. Coles. Electronic Structures and Physical Properties in the Alloy Systems Nickel–Copper and Palladium–Silver 221

Dr. K. Hoselitz and Dr. M. McCaig. Torque Curves and other Properties of Permanent Magnet Alloys 229

Letters to the Editor:

Mr. P. C. Banbury. Double Surface Lead Sulphide Transistor 236

Miss T. J. Dillon. Photosensitive Neon–Argon Discharge Tubes in Photometry 236

Reviews of Books 238

Contents for Section A 246

Abstracts for Section A 247

ABSTRACTS FOR SECTION B

Characteristics of Radio Echoes from Meteor Trails: III—The Behaviour of the Electron Trails after Formation, by J. S. GREENHOW.

ABSTRACT. This paper deals with the durations and amplitudes of the radio echoes reflected from meteor trails. For wavelengths of 4·2 and 8·4 m the durations of most echoes are shown to be very nearly proportional to the square of the wavelength, as predicted by simple diffusion theory. It is suggested that long duration meteor echoes are due to total reflection from trails of very high electron density, and it is shown that the amplitudes of these echoes would only be of the same order as the amplitudes of the short duration echoes from trails of low electron density discussed in an earlier paper. Further evidence is given to show that the amplitude fluctuations in the radio echoes are caused by distortion of the column of ionization, relative motion of several reflecting centres due to wind turbulence producing changing interference conditions. Turbulent winds of the order of 20 m/sec are inferred at altitudes of 80 to 100 km.

The Propagation of Sound through Gases contained in Narrow Tubes, by L. E. LAWLEY.

ABSTRACT. A comprehensive investigation is made into the validity of the Helmholtz–Kirchhoff equations for the absorption and velocity of sound in a gas contained in a narrow tube. Results are given for air, oxygen, nitrogen and hydrogen contained in tubes of radii between 0·15 mm and 1·17 mm at frequencies between 60 and 150 kc/s. The form of both the velocity and absorption equations is confirmed, but the viscosity–thermal conductivity constant is found experimentally to be about 5% above the theoretical value. A method is outlined in which the free space absorption can be calculated from measurements in a tube at varying pressures, and results are given in the case of oxygen.

The Magnetic Electron Microscope Objective Lens of Lowest Chromatic Aberration, by G. LIEBMANN.

ABSTRACT. The shortest focal length f and smallest chromatic aberration constant C_c of an objective lens is directly proportional to the square root of the (corrected) accelerating voltage V_r and inversely proportional to the maximum magnetic field strength H_p in the parallel part of the pole-piece gap. For given values of V_r and H_p both f and C_c fall monotonically with the relative pole-piece separation S/D, although the reduction is insignificant for $S/D>2$. For each lens geometry there exists an optimum set of lens dimensions.

Effect of Strain Ageing upon the Distribution of Glide Bands in Cadmium Crystals, by D. F. GIBBONS.

ABSTRACT. It is shown that there is a marked difference in the distribution of visible glide bands, after plastic deformation, between cadmium crystals containing small amounts of nitrogen and those relatively free from nitrogen. The distribution of glide bands in the crystals containing nitrogen is compared with Lüders bands in strain-aged mild steel.

Single Contact Lead Telluride Photocells, by A. F. GIBSON.

ABSTRACT. In a recent paper the photoconductivity of lead sulphide films was discussed in terms of a barrier mechanism. Large single crystals of lead telluride have now been grown and, with these, single barrier photocells can be prepared. The simplest barrier is formed at a metal–semiconductor contact. Such barriers, as exhibited in rectifiers, have been mainly studied. It is found that the photosensitivity and time constant of such cells is determined by the total current at the contact point, as expected from barrier theory. The variation in barrier height with temperature and time has also been determined.

Lead Sulphide Rectifier Photocells, by A. F. GIBSON.

ABSTRACT. Following the study of lead telluride rectifier photocells described in a contemporary paper, similar properties have been found for lead sulphide.

A Note on the Structure of Selenium, by E. BILLIG.

ABSTRACT. The recently established identity of the width of the (optical) energy gap, 2·05 ev, for both amorphous and crystalline selenium, suggests that the chain structure of crystalline selenium is maintained also in the amorphous phase. The low electrical conductivity of amorphous selenium is ascribed to potential barriers existing between individual chains.

Electronic Structures and Physical Properties in the Alloy Systems Nickel–Copper and Palladium–Silver, by B. R. COLES.

ABSTRACT. A comparison is made of the magnetic, electrical and thermo-electric properties of alloys in the two systems, and the lattice spacings, optical properties, electronic specific heat, and x-ray spectroscopy of the nickel–copper alloys are also considered. Palladium–silver alloys show the behaviour expected of them on the band theory of metals, but nickel–copper alloys show well-marked and consistent deviations. It is concluded that unoccupied d-electron levels exist in the copper-rich alloys, whereas such levels do not exist in the silver-rich palladium–silver alloys. From theoretical considerations it seems unlikely that the unoccupied levels form part of a collective d-band, and alternative models are discussed. That the two systems differ so markedly is surprising, but a tentative explanation of the differences is sought in the differing proportions of the atomic volume occupied by the ions in copper and in silver.

Torque Curves and other Properties of Permanent Magnet Alloys, by K. HOSELITZ and M. MCCAIG.

ABSTRACT. Further investigations of Alcomax III and related alloys have been made using a torque magnetometer. Samples with both columnar and random crystals have been used. Torque curves have been obtained after various sequences of heat treatment designed to throw light on the changes that occur in these alloys, and the magnitude and direction of the magnetic field applied during cooling has been varied. A method of deriving three independent constants of crystal anisotropy without using single crystals has been devised.